International Science Group
ISG-KONF.COM

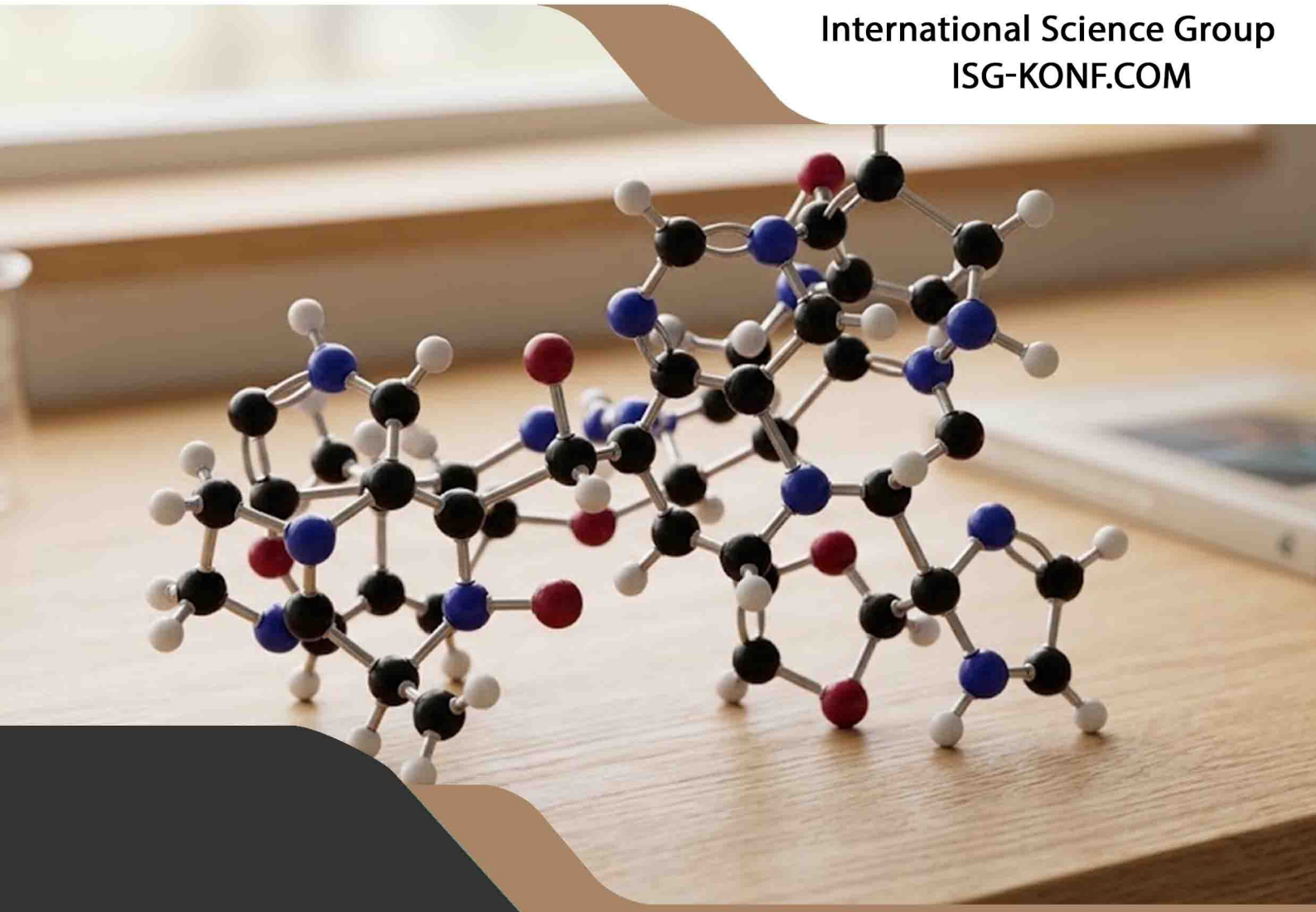

PROCESSING OF SECONDARY RAW MATERIALS FOR THE RECOVERY OF VALUABLE COMPONENTS

ISBN – 979-8-90671-558-6
DOI – 10.46299/979-8-90671-558-6

Sknar Yu., Hrydnieva T., Sknar I., Butyrina T.

PROCESSING OF SECONDARY RAW MATERIALS FOR THE RECOVERY OF VALUABLE COMPONENTS

Monograph

2026

UDC 678.046.361:541.64

Authors:

Sknar Yuri – Doctor of Chemical Sciences, Professor, Head of the Department of Processes, Apparatuses and General Chemical Technology, Ukrainian State University of Science and Technology, ORCID: 0000-0002-1188-3684.

Hrydnieva Tetiana – Ph.D., Associate Professor of the Department of Processes, Apparatuses and General Chemical Technology, Ukrainian State University of Science and Technology, ORCID: 0000-0002-0214-4636.

Sknar Iryna – Ph.D., Associate Professor of the Department of Processes, Apparatuses and General Chemical Technology, Ukrainian State University of Science and Technology, ORCID: 0000-0001-8433-1285.

Butyrina Tetiana – Ph.D., Associate Professor of the Department of of Inorganic Substances Technology and Ecology, Ukrainian State University of Science and Technology, ORCID: 0000-0002-0619-6783.

Reviewer:

Frolova Liliya – Doctor of Technical Sciences, Professor, Professor of the Department of Inorganic Substances Technology and Ecology, Ukrainian State University of Science and Technology, ORCID: 0000-0001-7970-2264.

Sknar Yu., Hrydnieva T., Sknar I., Butyrina T. Processing of Secondary Raw Materials for the Recovery of Valuable Components. Monograph. Primedia eLaunch, Boston, USA, 2026. 128 p.

Library of Congress Cataloging-in-Publication Data

ISBN – 979-8-90671-558-6
DOI – 10.46299/979-8-90671-558-6

UDC 678.046.361:541.64

ISBN – 979-8-90671-558-6

ABSTRACT

The monograph “Processing of Secondary Raw Materials for the Recovery of Valuable Components” is devoted to the development of scientific basis and the technology for obtaining amorphous silicon (IV) oxide of high purification requirement from the rice husk that allow to solve the important applied scientific problem of providing various industries with amorphous silicon(IV) oxide. The amorphous silicon (IV) oxide is widely used in such industries as electronics, cosmetology (toothpastes, creams), medicine (medicine filler), paint and varnish industry; in the production of building materials, glass, rubber, refractory materials and in food industry.

The estimation of the present state of research in the branch of obtaining amorphous silicon (IV) oxide from different raw materials was given. It is shown that amorphous silicon (IV) oxide is obtained from quartz or natural silicates by chemical deposition from the gas phase and by other methods. These processes are multi-stage, energy-intensive, require sophisticated equipment and are accompanied by harmful emissions into the environment. It has been found that by using rice husk (RH) as raw material it is possible to solve most problems inherent to the traditional technologies as well as to create waste-free, economically profitable production of multipurpose amorphous silicon(IV) oxide.

This study investigates combined processes involving physicochemical and thermal treatment for the production of amorphous silicon (IV) oxide of varying degrees of purity.

The rice husk composition as a raw material for the process of obtaining amorphous silicon (IV) oxide was investigated. According to the elemental composition of the rice husk and gas environment, the estimation of the thermodynamic probability of the heat treatment process of the rice husk is given. The results of thermodynamic analysis of the thermal decomposition of the rice husk in the range of 300−2000 K at the pressure of 0.01 −1 MPa in the different gas environments (in pyrolysis gases, water vapor) were shown. The gas phase-to- raw material ratio was

varied in the calculations, the rice husk composition being as follows, (% wt.): SiO_2 – 22.24; C – 35.77; O – 36.59; H – 5.05; N−0.32; S–0.03.

The influence of pressure, temperature and gas environment on the equilibrium state of the systems formed in the process of the rice husk heat treatment has been studied. The high thermodynamic probability of obtaining amorphous silicon (IV) oxide by heat treatment of the rice husk in the temperature range of 550−850 K was shown. The equilibrium compositions in the different gas environments differ only in the gas phase components.

The regularities of the process for obtaining amorphous silicon (IV) oxide of different purity levels by the method of thermal treatment in the air environment are deduced from experiments. It is shown that the temperature of the heat treatment process should be 923 K and duration 35−40 min. It is established that in these conditions the content of carbon in solid residue is 23.00−25.51% wt and that of silicon (IV) oxide is 20.90−22.00 % wt.

The obtained results indicate that using only thermal extraction of the silicon (IV) oxide allows getting the technical qualification product.

The possibility of obtaining amorphous silicon (IV) oxide of higher purity level by decreasing lignin and cellulose content in the rice husk by the physicochemical methods is deduced from experiments and in theory.

The hypothesis for the process mechanism is formulated and the equations that describe the lignin and cellulose extraction from the rice husk are received. The research of the obtained models has shown that by using the rice husk fractions 40−150 μm in size the maximum degree of lignin extraction by the mixture of ethanol and hydrochloric acid (3% by weight) at the temperature of 80°C and process duration of 6 hours accounts for 33% wt. During the process of cellulose extraction by 15% water solution of sulfuric acid the maximum degree of extraction is achieved at the temperature of 100°C for 6 hours and is 29.9 % wt.

The successive implementation these two stages allows to increase the degree of extraction of and thereby increase the content of the amorphous silicon(IV) oxide in the solid residue.

While making experimental studies on the extraction of carbon-containing components the process mechanism was determined. The kinetic parameters of lignin and cellulose extraction were calculated. The experimental research methods were worked out and the basic technological parameters for each stage of the process for obtaining high purity amorphous silicon (IV) oxide were found.

The processes of heat treatment of the rice husk after lignin and cellulose extraction in non-isothermal conditions were investigated. The kinetic parameters of the process are established as well. The installations for experimental studies of the process for obtaining various purpose amorphous silicon (IV) oxide by means of the rice husk thermal treatment and the extraction carbon-containing components were developed. The experimental implementation of the scheme which includes lignin and cellulose extraction, thermal decomposition of the solid residue in the air environment at the temperature of 885–913K allows to obtain high purity amorphous silicon(IV) oxide (with 99 % wt. of the product in the solid residue).

Physicochemical characteristics of the amorphous silicon(IV) oxide powder obtained by one-stage thermal decomposition and when using two-stage extraction and heat treatment (three-stage process) were established.

The chemical composition of the raw material and the finished product were determined using X-ray phase analysis which were performed on the DRON-3 diffractometer in Cu_{α} radiation. The phase identification was carried out with the help of X-ray card index. Besides, amorphous structure of silicon (IV) oxide powder was also confirmed.

The research show that using amorphous silicon (IV) oxide obtained from the rice husk appears to be promising in the manufacture of paint and varnish products.

Keywords: *rice husk, obtaining, powder, amorphous silicon (IV) oxide, thermal processing, extraction, carbon, lignin, cellulose, mechanism, kinetics, hypothesis, process flowchart.*

TABLE OF CONTENT

INTRODUCTION

Amorphous silicon (IV) oxide is used in many industries.

It is widely used in electronics, cosmetology (toothpastes, creams), medicine (filler for medicines), in the production of building materials and glass, ceramics, abrasives, concrete products, in the production of rubber and silica refractories, in the production of solar cells, sound and heat insulation materials, catalysts and in many other industries [1-11]. In the food industry, silicon (IV) oxide is registered as an additive E551.

In each specific case, different requirements are imposed on amorphous silicon(IV) oxide, but the main ones are the amorphous structure, degree of purification and particle size.

In traditional technologies for obtaining amorphous silicon(IV) oxide, quartz or natural silicates are used as the starting material, which entails high costs for extraction, preparation and purification of raw materials from associated impurities, the content of which is constantly changing. These processes are characterized by multi-stage, complex equipment and energy consumption, pollute the environment and do not always satisfy consumers in terms of quality.

In the search for an alternative and renewable source of raw materials for industry, attention is drawn to the large-tonnage waste of rice processing plants - rice husk (RH), which currently has no practical application. Most of the problematic issues inherent in traditional technologies can be eliminated when using rice husk as the starting material.

Therefore, research aimed at developing the physicochemical foundations and technology for obtaining high-purity amorphous silicon(IV) oxide from rice husks is relevant and at the same time solves the problem of "green chemistry" - the utilization of rice husks.

1. ANALYTICAL REVIEW OF METHODS FOR OBTAINING SILICON (IV) OXIDE

1.1.Physicochemical properties of silicon(IV) oxide

1.1.1 Fields of application of silicon(IV) oxide

Silicon (IV) oxide is used in various industries: radio electronics, aircraft construction, rubber and paint and varnish industries, pharmaceutical and perfumery industries, non-ferrous metal enterprises, ceramic industry enterprises and other industries [1-11].

Silicon (IV) oxide in the form of sand is widely used in construction, for the manufacture of glass, cement, ceramics, abrasives. A special field of use of silicon (IV) oxide is due to the fact that it is able to deform under the influence of an electric field. This property of silicon (IV) oxide crystals is used in sound recording equipment and for the generation of ultrasonic vibrations. Silicon (IV) oxide is easily converted into quartz glass, which is chemically and thermally stable.

Synthetic silicon (IV) oxide is a raw material for the production of quartz glass, ceramics and quartz fibers. Quartz glass is used for the manufacture of chemical equipment and in optical instruments [1,12,13].

Natural silicon (IV) oxide is used in the production of silicate glass, porcelain and earthenware products, abrasives, concrete, silicate bricks, ceramics. Synthetic silicon(IV) oxide ("white carbon black") is a filler in the production of rubber (up to 70% of the obtained silicon (IV) oxide). Precipitated hydrated forms of silicon (IV) oxide are mainly used, with a specific surface area of 60-300 m^2/g, and anhydrous forms of silicon (IV) oxide, which are called - aerosil, are less widely used. Aerosil is used as an adsorbent in chromatography, a thickener of lubricants, adhesives, and paints. Single crystals of silicon (IV) oxide are used in radio engineering (piezoelectric frequency stabilizers, filters, resonators, etc.), in optical instrument making (prisms for spectrographs, monochromators, lenses for UV optics, etc.), in jewelry (transparent, beautifully colored varieties of silicon (IV) oxide are semi-precious stones). Silica gels

with an effective pore diameter of 2-15 nm are used as industrial sorbents and catalyst carriers [5-9].

1.1.2 Types, modifications and properties of silicon(IV) oxide

Silicon (IV) oxide (silica) is a colorless crystalline substance with high strength and hardness. Silicon (IV) oxide melts at 1713°C and boils at 2590°C. Silicon (IV) oxide (SiO_2) is the most common substance on Earth. Types of silicon (IV) oxide include silica, quartz, flint, agate, jasper and others. Quartz is a component of granite and gneiss. Ordinary sand is small grains of quartz [14-16].

By chemical nature, silicon (IV) oxide is an acidic oxide that reacts at high temperatures with many metal oxides, forming silicates. It occurs in an amorphous and crystalline state.

Crystalline silicon (IV) oxide has more than a dozen polymorphic modifications. It is widely distributed in nature in the form of transparent colorless or colored single crystals (rock crystal, amethyst, smoky quartz, tridymite, quartzite, rose quartz, agate, jasper, carnelian, flint, chalcedony) and in the form of clastic rocks (sea sand, gravel, pebbles, sandstone and conglomerate).

Amorphous silica is divided into three types:

1) quartz glass;

2) amorphous silica, which is obtained by irradiating amorphous or crystalline varieties of silica with fast neutrons. In this case, the density of the original amorphous silica increases, and the crystalline one decreases. Amorphous silica is thermally unstable and turns into quartz when heated to 930 °C for 16 hours. Its density is 2.26 g/cm^3 compared to 2.20 g/cm^3 for quartz glass or microamorphous varieties of silica.

3) Microamorphous silica, which includes sols, gels, powders and porous glass.

Amorphous silica is divided into anhydrous and hydrous. Anhydrous varieties of amorphous silica include quartz glass or fused quartz. In nature, quartz glass occurs in the form of the mineral lechatelierite. Artificial quartz glass is obtained by melting vein quartz or pure quartz sand in electronic furnaces at temperatures above 1728 °C [16].

Representatives of hydrous amorphous silica are its natural and artificial hydrates, consisting of SiO_2 and H_2O. Hydrous varieties of natural silica are found in diatomaceous sediments on the bottom of the seas and oceans (trepel, kieselguhr, diatomite, infusorite).

Artificial silica hydrates are powdery amorphous silicon(IV) oxide [15-17], including sols, gels, powders and glass, which has a porous structure. They consist of primary particles with a size of less than one micron or with a specific surface area of more than 3 m^2/g.

Dehydration of hydrous silica causes profound changes in physical properties. After prolonged drying, silica is not completely dehydrated, some water remains in it. Dried hydrous silica is a substance with a porous structure with a highly developed internal surface, which is called silica gel.

The properties of silicon(IV) oxide have been studied for about two hundred years, and for a long time various formulas were attributed to it. The final formula of silicon (IV) oxide was established by D. I. Mendeleev [18]. All modifications of silica consist of a group of $[SiO_4]^{4-}$ – tetrahedra, in the center of which there is a silicon atom, and at each vertex there is one oxygen atom. The bonds are made using sp^3 – silicon orbitals, and the bonds between silicon and oxygen are of an ionic-covalent nature. Modern ideas about the mechanism of formation of siloxane bonds, taking into account the physicochemical features of the Si-O-Si and Si-OH bonds, suggest that the bond between all silicon and oxygen atoms leads to the fact that silica exhibits the properties of a polymer molecule $(SiO_2)n$:

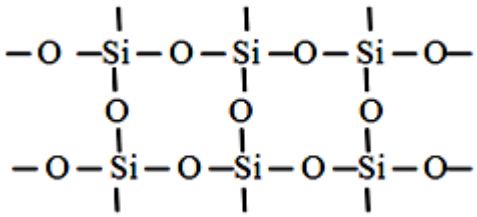

(1.1)

The diagram shows that silicon atoms are not directly bonded to each other, but are connected only by oxygen atoms, through the so-called siloxane bond:

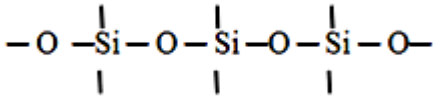

(1.2)

Silica, from a chemical point of view, is an extremely stable substance. Only hydrofluoric acid can dissolve silicon (IV) oxide, and upon interaction it forms silicon tetrafluoride or hydrofluorosilicic acid [18].

$$SiO_2 + 4HF = SiF_4 + 2\ H_2O \quad (1.3)$$

Silicon(IV) oxide is practically insoluble in water. When alloyed with alkalis, being an anhydride of silicic acid, silicon (IV) oxide easily converts into sodium silicate:

$$SiO_2 + 2NaOH = Na_2SiO_3 + H_2O \quad (1.4)$$

Similarly, it reacts when alloyed with alkali metal carbonates, releasing carbon(IV) oxide.

$$SiO_2 + Na_2CO_3 = Na_2SiO_3 + CO_2 \quad (1.5)$$

Amorphous silica dissolves slowly in aqueous alkali solutions, forming water-soluble alkali metal silicates. To a small extent, silicon (IV) oxide dissolves when reacted with methanol at elevated temperature and pressure in the presence of sodium methylate:

$$SiO_2 + 4CH_3OH = Si(OCH_3)_4 + 2H_2O \quad (1.6)$$

1.1.3 Laboratory methods for obtaining silicon (IV) oxide

Under laboratory conditions, synthetic silicon(IV) oxide can be obtained by the action of acids, even weak acetic, on soluble silicates [19-21]. For example:

$$Na_2SiO_3 + 2CH_3COOH = 2CH_3COONa + H_2SiO_3 \quad (1.7)$$

Silicic acid H_2SiO_3 immediately decomposes into water and SiO_2, which precipitates.

1.2 Industrial methods for obtaining silicon(IV) oxide

In the technology of obtaining silicon (IV) oxide, mineral raw materials (quartz, opal, tripoli, diatomite, etc.), silicon, colloidal silica, sodium silicate solutions, fluoride raw materials, organic substances are most often used as raw materials [18-22].

The production of silicon (IV) oxide is based on the following basic methods:

- Grinding, grinding or chemical treatment of natural silica materials without prior conversion of silicon into solution.

- Heating silicon to a temperature of 400-500°C in an oxygen atmosphere, while silicon is oxidized to silicon (IV) oxide;

- by the action of acids (H_2SO_4, HCl, H_2CO_3) on sodium silicate or other soluble silicates;

- vapor-phase decomposition (oxidation or hydrolysis) of volatile silicon compounds (pyrogenic method).

- chemical precipitation from the gas phase by burning $SiCl_4$ vapors in a mixture of H_2 and O_2 (aerosil, in the USA - cabosil).

- chemical precipitation from the gas phase by high-temperature combustion of previously purified $SiCl_4$ by rectification according to the reaction:

$$SiCl_4 + 2H_2O = SiO_2 + 4HCl \quad (1.8)$$

Particles of silicon (IV) oxide formed in an oxygen-hydrogen flame or plasma are precipitated, giving massive quartz glass;

- a sol-gel process that includes hydrolysis of organic silicon compounds, slow dehydration of the formed gel, and its moderate heating.

- production of silicon (IV) oxide and porous glass (type "Vycor") by heat treatment of borosilicate glass by acid leaching and washing of the silica framework.

When obtaining silicon(IV) oxide from natural silica materials, a number of natural minerals are most often used, including pumice, opal, diatomite, trepelle, infusorite, and others, the reserves of which in our country are practically inexhaustible. A technology for complex hydrothermal processing of amorphous rocks has been developed [15-17, 20-23], which allows obtaining silicate products for the

national economy and opens up prospects for the wide application of various rocks. Hydrothermal processing of amorphous rocks makes it possible to obtain more than 70 items of various products.

Silicon (IV) oxide can be obtained from quartz glass. Quartz glass, which is obtained by melting quartz sand, is ground in a ball mill to form a fine powder. As a result, 21% of particles with a size of less than 1 μm are obtained [24].

The listed methods for obtaining silicon (IV) oxide have a number of advantages: the ability to obtain various products for various purposes for industry (as additives in varnishes, paints, catalyst carriers, etc.); reserves of mineral raw materials are very large; absence of harmful emissions into the atmosphere.

However, the disadvantages of these methods are: the need for repeated grinding and mixing of the starting raw materials, resulting in contamination of the charge components with the material of the grinding bodies; materials obtained from natural raw materials have a low specific surface area; high energy intensity of the processes for obtaining silicon (IV) oxide.

Precipitated silicas can be obtained by mixing acids and sodium silicate in various ways [13,25].

In a sodium silicate solution with a ratio of SiO_2:Na_2O = 3.3:1, it turns out that the normality of sodium ions is 0.1C, where C is the concentration of silica, expressed in g/100 ml. These facts underlie many processes of silica precipitation. The sodium silicate solution is neutralized with acid in order for the colloidal silica particles to grow in a weakly alkaline medium and to be able to coagulate under the influence of sodium ions from a sodium salt solution.

In most precipitation processes, a simple partial neutralization of the sodium silicate solution in the presence of a soluble salt occurs in order to cause coagulation. The main stages in the formation of silicon (IV) oxide from silicates are:

1. Formation and growth of colloidal particles;

2. Coagulation of particles with the formation of aggregates, which leads to the production of precipitated silica.

3. Strengthening of aggregates.

When precipitating alkali metal silicate with acids or salts that are easily hydrolyzed, the nature and quality of the resulting product are greatly influenced by the precipitation temperature, pH of the medium, concentration of sodium silicate, concentration of salt and acid solutions, and intensity of stirring [27].

The main disadvantages of this technology for obtaining silicon (IV) oxide are that the processes of filtration and washing of raw materials containing silicon are long and laborious. But there are also advantages such as the simplicity of the process equipment, the use of affordable and cheap starting materials.

The pyrogenic method or the process that occurs in the vapor phase is one of the well-known industrial methods for obtaining anhydrous silicic acid - aerosils, carboxyls [28-30].

Pyrogenic silicon (IV) oxide was first obtained in Germany in 1941 by Klepfer (Degussa company) [28-31]. Pyrogenic silicon(IV) oxide is obtained in the process of synthesizing silicon tetrachloride in an oxygen-hydrogen flame according to the reaction [31]:

$$2H_2+O_2 \rightarrow 2H_2O \quad (1.9)$$

$$SiCl_4 + 2H_2O \rightarrow SiO_2 + 4HCl \quad (1.10)$$

$$2H_2 + O_2 + SiCl_4 \rightarrow SiO_2 + 4HCl \quad (1.11)$$

A homogeneous mixture of silicon tetrachloride vapor, hydrogen, and air is burned in an externally cooled combustion chamber. By changing the concentration of silicon tetrachloride vapor and inert gas in the mixture, the flame temperature, and the duration of the silicon (IV) oxide formed in the combustion chamber, it is possible to control the particle size and surface structure, and therefore the specific surface area of the resulting product. From the reaction chamber, the combustion products containing pure silicon (IV) oxide in the form of an aerosol are fed to the coagulation zone, where, under the action of a turbulent flow, silicon (IV) oxide precipitates in the form of flakes with a diameter of 1-200 μm. Then, to remove the combustion products containing

hydrogen chloride, they are centrifuged and filtered. The bulk density of freshly prepared silicon (IV) oxide after vacuum treatment is 60 kg/m^3 or 1250 kg/m^3 after compaction.

Aerosil is colloidal silicon (IV) oxide, a very light micronized powder with obvious adsorption properties. Aerosil is a trade name that was introduced by the German company Degussa (its new name is Evonik). They are used in the production of silicone rubbers, plastics, varnishes and paints. Among the CIS countries, the leading manufacturer of pyrogenic silicon (IV) oxide is Orysil LLC (Kalush), which produces various brands of Orysil: Orysil 100, Orysil 150, Orysil 175, Orysil 200, Orysil 300, Orysil 380, Orysil M130, Orysil M200, Orysil M300, Orysil MA300 [29-31].

Industrial production of aerosil is carried out in Germany, Belgium, Great Britain, and Ukraine. However, aerosil is a rather expensive product, its surface lacks hydroxyl groups OH–, the presence of which is associated with the high activity of the powder, and aerosil also has a low specific surface area.

1.3 Methods for obtaining silicon (IV) oxide from various raw materials

Analysis of scientific and technical information shows that over the past three decades, scientists from many countries of the world have been intensively searching for new methods for obtaining silicon (IV) oxide from various raw materials [32-34].

1.3.1 Methods for obtaining silicon (IV) oxide from soluble silicates

Methods for obtaining silicon (IV) oxide from soluble silicates using acid solutions have been studied [13,22,29,31,34-36]. One method for obtaining silicon (IV) oxide involves the interaction of silicate with acid in the presence of a coagulant, carboxymethylcellulose. The final product has a specific surface area of 25-800 m^2/g and a particle diameter of 0.2-50 μm. A method for obtaining silica hydrosol [22], which is used in paper production, in the composition of paints, etc., was proposed. The essence of the method for obtaining silicon (IV) oxide hydrosol includes ion-

exchange conversion of a sodium silicate solution into polysilicic acid, its stabilization with a solution containing sodium ions, and heat treatment of the obtained silicon (IV) oxide with hot steam at a temperature of up to 100°C and atmospheric pressure for 2.5-3 hours.

A method for obtaining silicon (IV) oxide was also proposed [36], which includes the precipitation of silicon (IV) oxide by adding solutions of sodium or potassium silicate to solutions of ammonium salts of sulfuric acid or hydrochloric, carbonic, nitric, formic, acetic acids at a ratio of the total amount of silicon (IV) oxide added with silicate to the total amount of ammonium salt ≤ 2 with subsequent treatment of the obtained silicon (IV) oxide. Precipitation conditions: temperature 35 – 95°C, precipitation rate 100 – 270 g SiO_2/l suspension per hour. After precipitation, additional treatment of the silicon (IV) oxide hydrogel is carried out with solutions of ammonium salts, which were selected from the series $(NH_4)_2SO_4$ or NH_4Cl, $(NH_4)_2CO_3$, NH_4HCO_3, NH_4NO_3 or NH_4HCO_2 , $NH_4CH_3CO_2$.

The main disadvantages of the above methods for obtaining silicon(IV) oxide from sodium silicate solutions are that the production is long, energy-intensive, expensive and labor-intensive.

1.3.2 Methods for obtaining silicon (IV) oxide from fluoride solutions

Methods [29] for obtaining silicon (IV) oxide from fluoride solutions have been studied.

According to one of the methods, silicon (IV) oxide is obtained from an aqueous solution of H_2SiF_6. In the precipitation zone, the aqueous solution of H_2SiF_6 is treated with MON or M_2CO_3, where M is an alkali metal. The reaction is carried out at the boiling point of the mixture and pH 7-9. Under these conditions, amorphous silicon (IV) oxide is precipitated. The liquid phase is a saturated solution of NaF_4. If crystalline NaF_4 begins to precipitate during the reaction, water is added to the mixture. The precipitate of amorphous silicon (IV) oxide is filtered through a filter with an average pore size of 15 μm, after which the filtrate is evaporated in the evaporation zone. As a

result of evaporation, a suspension of NaF_4 crystals in a saturated aqueous solution of this compound is obtained. The NaF_4 crystals are filtered off and the filtrate is treated with an Al compound, for example AlF_3. The precipitate is a sparingly soluble cryolite, which contains 50% of amorphous silicon(IV) oxide particles with a diameter of more than 15 microns.

A number of methods for the precipitation of silicon (IV) oxide in the presence of fluoride ions have been proposed [29]. The author introduced silicon tetrafluoride vapor into a hot sodium carbonate solution in order to obtain a finely dispersed silica residue. The author Svendsen proposed a method for the production of finely dispersed silica from silica residues by heating silica or silicates in the presence of ammonium fluoride to form products that hydrolyze in water. The product, which is only 2% water, has a density of 0.16-0.22 g/cm^3. Silicon (IV) oxide was characterized as α-silica. On the other hand, low-temperature hydrolysis in ammonia solution produced a substance containing 7% water at 110°C and 5% water at 250°C. Air-dried silicon (IV) oxide has a density of 0.48-0.64 g/cm^3.

A method for obtaining silicon (IV) oxide from a silicon-fluoride-containing solution was also considered [36], which includes the interaction of the silicon-fluoride-containing solution with ammonia water, aging of the resulting suspension, its filtration, washing of the silicon (IV) oxide precipitate and its drying. Ammonium silicon fluoride with a concentration of 3-25% by weight. heated at a temperature of 80–90°C, and the resulting suspension is kept for 50-60 minutes.

The advantages of these methods are a decrease in the synthesis temperature, the use of cheaper raw materials to obtain the product.

The main disadvantages of these methods are the use of aggressive solutions that require certain process conditions and expensive equipment.

1.3.3 Methods of silicon (IV) oxide precipitation

In [37], a method for obtaining amorphous silicon (IV) oxide by two-stage sulfuric acid treatment of raw materials containing nepheline was developed. This process

includes the decomposition of nepheline, the precipitation of silicon (IV) oxide and its subsequent extraction. The optimal conditions for sulfuric acid decomposition of nepheline concentrate (NC) are: acid concentration – 15%; mass ratio H_2SO_4/NC – 1; process duration – 20 min. In this case, the following degrees of component extraction (%) are ensured: Si – 82.4; Al – 84.8; K – 80.3; Na – 92.3. The structural and mechanical properties of silica gels formed from aluminosilicate systems at elevated temperatures or increased sulfuric acid content were established. It has been investigated that the sulfate acid precipitation of silica is technologically more acceptable. With an increase in the sulfuric acid content, the size and degree of polydispersity of silica particles decrease. It has been established that the method of silica precipitation affects its properties: dispersion, degree of hydration, residual content of solution components on the silica surface.

1.3.4 Methods for obtaining silicon (IV) oxide from silicon tetrachloride.

One of the methods for obtaining silicon (IV) oxide is the hydrolysis of $SiCl_4$ vapor [38]. Silicon (IV) oxide particles were obtained at room temperature by hydrolysis of $SiCl_4$ in a mixture of alcohol and water in a molar ratio of 1:3. $SiCl_4$ is a by-product of the industrial production of phosphate fertilizers.

In [39], a method for obtaining silicon (IV) oxide with a reduced specific surface area (30-95 m^2/g) and a butyl phthalate number (DBP number), which characterizes the degree of structuring (80 m of dibutyl phthalate per 100 m of SiO_2), containing aggregates with a size of 1000 nm, is proposed. The method consists in mixing silicon compounds (halides, organosilicon compounds, and others) in a vaporous state with oxygen and a combustible gas, and burning the mixture in a flame tube with the deposition of pure silicon (IV) oxide, which is used to regulate the rheology of liquids and to produce dispersions. Silicon (IV) oxide is obtained by mixing $SiCl_4$ with organic compounds with subsequent heating of the mixture and calcination [39]. To increase the purity of the target product and simplify the process of obtaining silicon (IV) oxide,

$SiCl_4$ is mixed with anhydrous formic acid. Then it is heated at a temperature of 30-60°C, $SiCl_4$ and formic acid are mixed in a molar ratio of 1:(4-4.25).

According to the following method, silicon (IV) oxide is obtained by oxidizing $SiCl_4$ in a low-temperature plasma flow of an electric arc discharge.

The disadvantages of the methods are the contamination of silicon (IV) oxide with erosion products of metal electrodes of electric arc type plasma generators and chlorine, which is formed during the combustion of tetrachloride. High process costs and energy consumption.

1.4 Rice husk – raw material for silicon(IV) oxide production

In traditional technologies for silicon(IV) oxide production, natural silicates, quartz, etc. are used as raw materials. However, these methods are associated with high costs for extraction, preparation and purification of raw materials. As a promising raw material source for the production of silicon(IV) oxide, waste from rice processing plants – rice husk (RH) can become. Currently, the potential of RH does not find industrial application. From time to time, RH is used for packaging, for the manufacture of abrasives, thermal and sound insulators, sorbents for water and air purification from dust, for improving soil structure, filler for plastics, resins, building materials, additives in animal and bird feed.

A wide group of scientists from many countries of the world are intensively searching for ways to use RH more rationally by obtaining silicon (IV) oxide from it [3-5,13,15,26,30,32-34,40-46].

A method for obtaining ultradisperse amorphous or nanocrystalline silicon (IV) oxide has been proposed [16]. Which includes sieving the husk, washing with water, acid treatment, pressing the husk, washing with water, distilling water by centrifugation, drying in an electromagnetic field of the microwave range, preliminary firing at 520-570°C and oxidative combustion. To obtain ultra-dispersed amorphous silicon (IV) oxide powder, heat treatment is carried out in a dynamic mode in a turbulent air flow formed by counter-tangential air flows, and to obtain nanocrystalline

powder with particles in the form of elongated crystals, oxidative combustion is carried out in a stationary mode in a laminar air flow with a stationary powder layer. This method allows obtaining silicon (IV) oxide with particle sizes of 20-100 nm and a purity of 99.0%.

The disadvantages of this method are cyclicity, multi-stage nature, the need to use various technical means and various special equipment for almost all operations. The creation of a laminar flow of oxidizing gas is difficult to ensure in practice.

The work on obtaining silicon (IV) oxide from rice husks suitable for the manufacture of solar cells is of great interest [43]. The RH is washed with water, treated with acetic acid solution at a volume ratio of acid: water = 1:10, for no more than 24 hours, dried at a temperature of up to 120°C, pyrolysis is carried out at 340-500°C, the mass ratio of carbon: silicon (IV) oxide in the obtained black ash is adjusted to 2:1, the ash is treated at 40°C for 24 hours with a 10% wt. H_2O_2 solution or with acetic acid solution at a volume ratio of acid: water = 1:(1–10). Carbothermal reduction is carried out in a nitrogen atmosphere at 1300-1500°C for 4-6 hours. The obtained silicon (IV) nitride is subjected to heat treatment for 4-8 hours in a vacuum at 1600-1800°C or in an argon atmosphere at 1800-2200°C.

This technology allows solving the problem of recycling rice production waste. In addition, environmental pollution during the synthesis of monohylan is many times less compared to the standard technology using chlorine compounds. The process has not gained wide application due to the complexity of the hardware and technological design.

In [44], a technology for obtaining high-purity amorphous silicon (IV) oxide and carbon from rice husks is described. The essence of the invention is that rice husk is subjected to acid treatment, washed with water, dried, pre-heated in a closed reactor with smoke suction and amorphous carbon capture, grinding and oxidative combustion sequentially in a stream of air or oxygen, smoke suction is carried out through a cooled labyrinth filter and water or zeolite or other adsorbent. Oxidative combustion is carried out first in a stream of air until the visible combustion process disappears, and then in

a stream of oxygen for 20-60 minutes with constant stirring. According to the invention, amorphous silicon (IV) oxide with a purity of 99.0% by mass is obtained.

There are known methods for obtaining silicon (IV) oxide [42,45] with a purity of 99.9%. The process includes sieving rice husk, washing in cold water, treatment in 0.01-0.1 normal hot sulfuric acid solution, washing in hot water, drying at 105-120°C, preliminary combustion at 200-500°C, grinding and oxidative combustion at a temperature of 700-780°C with air or oxygen supply. In this case, the temperature rise rate should not exceed 25 K/min, and the duration of oxidative burning is 0.5-2 hours. As a result, high-purity amorphous silicon(IV) oxide is obtained, but the process is accompanied by uncontrolled, unregulated smoke emissions.

The disadvantages of the above methods are the complexity of the technological process, high energy consumption and the need for constant monitoring of the filters so that there is no excess carbon in the final product. Known methods require the use of pure oxygen, which makes the processes expensive and energy-intensive. In addition, the duration of oxidative firing (0.5-2 hours) is implemented in periodic modes, which reduces the productivity of the processes and their environmental friendliness.

A method for obtaining silicon (IV) oxide from rice husks [46], which includes loading the husks into the reactor, supplying air, conducting heat treatment in an air stream at a temperature of 500-850°C with the addition of water vapor or carbon dioxide and unloading the product. Before feeding the rice husk into the reactor, it is treated with an aqueous solution of mineral acid to reduce the mass of the initial husk by at least 10%, using percolation hydrolysis, then washed with water and dried to a residual moisture content of 7%. The husk is loaded into the reactor together with silicon (IV) oxide. This process of obtaining silicon (IV) oxide is associated with additional special equipment for obtaining carbon dioxide and water vapor, as well as the use of control devices.

The main disadvantage is that in addition to rice husk, silicon (IV) oxide must be added to the reaction zone, which in turn complicates the process and its hardware

design. The high carbon content in the initial rice husk necessitates the additional use of water vapor.

In the dissertation [30], a method for a combined process for obtaining thermal energy and silicon (IV) oxide is proposed. This work presents the results of thermodynamic studies in air, nitrogen and oxygen environments. The influence of pressure, composition of the gas environment and the ratio of the flow rate of the HR to the gas environment on the concentrations of silicon (IV) oxide and carbon, which are in a condensed state, was determined. Thermogravimetric analysis in the air environment showed that the transformation of RH into SiO_2 occurs at a temperature of 950 - 1123 K and does not allow obtaining SiO_2 in pure form. According to this method, the silicon (IV) oxide powder obtained from RH was a highly dispersed black powdery material with the properties given in Table 1.1.

Table 1.1

Physicochemical properties of silicon (IV) oxide from RH

Parameter	Parameter value
1	2
SiO_2 mass percentage, %wt.	73 ± 0, 05
Carbon mass percentage, %wt.	17,9 ± 0, 05
pH of the water extract	8,6 ± 0, 1
Bulk density, kg/m^3	400 ± 3
Dibutyl phthalate adsorption, cm3/100 g	73,0 ± 0, 05
Moisture mass percentage, %wt.	1,67 ± 0, 1

This technology of the combined process of obtaining thermal energy and silicon(IV) oxide includes the following main stages:

- washing of the initial RH with distilled water and its drying;

- grinding of the washed and dried RH;

- thermal treatment of RH with the production of thermal energy and silicon (IV) oxide;

- utilization of thermal energy released during the heat treatment of HR.

The developed installation allowed to obtain hot water and samples of silicon (IV) oxide. It was established that as a result of the combustion of 1000 kg of RH, $10.75 \cdot 10^3$

MJ of energy can be usefully utilized, in the process of recovery of which 21.4 tons of water with a temperature from 20 to 80°C can be heated, or 2.5 tons of steam with a temperature of 120°C and a pressure of 0.2 MPa can be obtained.

The main disadvantage is that the silicon (IV) oxide samples have a high carbon content.

Existing methods for obtaining silicon (IV) oxide from RH have many disadvantages, namely the complexity of the technological process, high energy consumption. Some methods require a long thermal decomposition process (0.5-2 hours), as well as the use of pure oxygen, which makes the processes expensive and energy-intensive.

The production of amorphous silicon (IV) oxide from quartz or natural silicates is characterized by multi-stage, complex equipment and energy consumption, and these processes pollute the environment and do not always satisfy consumers in terms of quality.

Analysis of literature data showed that a promising direction is the use of rice production waste as a raw material for the process of obtaining silicon (IV) oxide in comparison with the raw materials currently used (quartz, silicates, $SiCl_4$ or SiF_4 vapors and esters).

When using rice husk, most of the problematic issues inherent in traditional technologies can be eliminated, and the product meets all production requirements.

2. CHARACTERISTICS OF RAW MATERIALS AND RESEARCH METHODS

In the process of fulfilling the research tasks, the following starting materials and research methods were used.

When performing experimental studies, the following reagents were used:

1. concentrated sulfuric acid H_2SO_4, chemical purity; concentration 93% by weight.

2. hydrochloric acid HCl, chemical purity; concentration 33% by weight.

3. ethyl alcohol hydrolyzed chda, concentration 96% by weight.

The starting materials are: rice husk.

2.1 Use of rice production waste to obtain silicon (IV) oxide

Rice is the most common crop in the world. It is sown in more than 100 countries of the world on areas occupying about 150 million hectares, and its production is about half a billion tons per year. It is rightfully considered one of the most important crops on our planet, because it is the main food product for most of the population of the earth. And although it is not a leading crop in our country and does not occupy a major position in the diet of Ukrainians, the rice industry, along with others, remains necessary for the agriculture of Ukraine.

Despite the fact that rice cultivation in our country has only been around for a few decades, domestic rice can successfully compete with the best world samples. In terms of quality indicators, it is not inferior to foreign varieties, and in terms of taste and nutritional properties it exceeds them, which is confirmed by the constant steady demand from the country's population.

The main rice systems are located in the Kherson region 17.8 thousand hectares Odessa region - 13.0 thousand hectares.

In Ukraine, the gross rice harvest in 2011 was 148 thousand tons, in 2012 - 160.1 thousand tons, in 2013 - 69 thousand tons, in 2014 - 49.5 thousand tons, in 2015 - 53.6 thousand tons [30].

Rice grain is in a shell, which scientists call the floral scales, and producers - the husk or husk. In the fall, grain from the fields is brought to grain mills, where it is cleaned of the shell, and the straw remains in the field [28].

The husked grain is yellow, and to obtain the white color familiar to the consumer, rice is polished, removing the upper layer. Thus, in the process of obtaining white milled rice groats, three types of waste are formed: straw, flower scales (husk, husk) and bran. The amount of waste at the enterprise when obtaining rice groats is up to 30 percent of the mass of dry grain. The main method of processing raw rice into groats at domestic rice mills is grinding, while depending on its varietal characteristics and processing technology, 18-30% husk and 10-12% bran are formed [29]. Therefore, a large amount of valuable plant raw materials accumulates annually, which has not yet found effective use.

Straw is used for agricultural needs, but most often it is simply burned in the fields, polluting the environment. Bran, as a rule, goes to animal feed. Recently, the literature has reported on the production of pharmaceutical and food products from it.

Bran has a wider range of applications. It is used for packaging, for the manufacture of abrasives, thermal and sound insulators, sorbents for water and air purification from dust, for improving soil structure, as a filler for plastics, resins, building materials, an additive to animal and bird feed.

From 1 ton of rice by-products, the following products can be obtained: 140–230 kg of silicon (IV) oxide (with a purity of 90.00 − 99.99% by weight); furfural (from straw and husk) - up to 50 kg; xylitol - up to 80 kg; up to 320 kg of raw material for bleached cellulose (from straw and husk); rice oil (from bran) - up to 180 kg; phytin - up to 40 kg; and other organic compounds, the yield of which is not less than 4% [28,29].

However, by-products and wastes of rice production have a low level of processing and utilization, so a fairly large amount of research is needed to develop

technological schemes for the complex processing of rice production wastes to obtain useful raw materials.

2.2. Physicochemical properties of rice husk and its components

The structure and composition of rice husk are considered in the works [40,47]. The composition of rice husk is not constant, this is explained by varietal characteristics, as well as the influence of climatic conditions. The husk content was within 16.3-26% [47] of the rice-grain mass. The positive correlation of the ratio of grain length to its width was 0.186. This confirms the fact that in longer and thinner grains the floral scales constitute a greater mass than in short and thick grains.

Rice husk includes an organic and inorganic component, the average composition of which is given in Table 2.1.

Table 2.1.

Average composition of rice husk

Substance	Substance content, wt. %.
1	2
Water	2,4 – 11,35
Protein	1,7 – 7,26
Fat	0,38 – 2,98
Fiber	31,71 – 49,92
Ash	13,6 – 29,04
Pentosans	16,94 – 21,95
Cellulose	34,34 – 43,8
Lignin	21,4 – 46,97

In 1871, Wolff [48] included rice husk among the agricultural products subject to analysis in order to determine their value as feed and fertilizer. Fluctuations in the chemical composition of rice husk are explained by varietal characteristics, climatic conditions in the year of harvest, sampling methods, and analysis methods. Rice husk contains a high content of crude fiber, lignin, and ash. These components reduce the nutritional value of the husk. Inorganic components are contained in the ash, which

makes up from 16 to 29% of the husk mass [49]. The main component of rice husk ash is silicon (IV) oxide, which makes up 90-99% of the mass, and all other elements are contained in rice husk ash at the impurity level. Fluctuations in the parameters are explained by the different composition of pure rice husk and the different purity of the samples, as well as the accuracy of the analysis methods. The ash of husks, which were burned in a thick layer of raw materials with insufficient air access, has a pink color with a lilac tint. If the husks are burned with sufficient air access (complete combustion of carbon), the ash is white. Incompletely burned carbon gives the ash a gray or black color [49].

All experimental studies were carried out with RH, the characteristics of which are given in Tables. 2.2 and 2.3.

Table 2.2.

Technical analysis and elemental composition of rice husk (RH)

Name of indicators	Analysis method	Symbol, unit of measurement	Actual value
1	2	3	4
Moisture analytical	ISO 589-81	W^a,%	1,90
Ash content per dry matter	ISO 1171-97	A^d,%	20,90
Mass fraction of total sulfur	ISO 334-92	St^d,%	0,001
Volatile yield	ISO 562-81	V^{daf},%	75,00
Mass fraction of carbon	ISO 625-96	C^d,%	35,51
Mass fraction of hydrogen		H^d,%	5,70
Mass fraction of nitrogen	ISO 333-83	N^d,%	0,31
Mass fraction of oxygen	ISO 1994-76	O^dd,%	37,54

Table 2.3.

The content of components that make up the mineral part (ash) RH

Name of indicators	Analysis method	Symbol, unit of measurement	Actual value
1	2	3	4
silicon (IV) oxide	ISO 23380	SiO_2,%	91,96
aluminum (III) oxide		Al_2O_3,%	0,67
iron (III) oxide		Fe_2O_3,%	4,15
magnesium (II) oxide		MgO,%	0,14
calcium (II) oxide		CaO,%	1,09
sodium (I) oxide		Na_2O,%	0,20
potassium (I) oxide		K_2O,%	1,61
sulfur (VI) oxide		SO_3,%	0,18

2.3 Theoretical and experimental methods for studying the properties of raw materials and obtained silicon (IV) oxide powders

Thermodynamic data for the Si–C–O–H–N system are given in [31]. Thermodynamic calculations were performed on a personal computer using the standard ASTRA 4.0 software package, which determines equilibrium compositions based on finding the maximum entropy of the system. Calculations were performed in the temperature range of 300–1500 K at pressures of 0.01; 0.1; 1 MPa and different ratios of mass flow rates of RH: medium.

The kinetics of the thermal treatment of RH was studied using complex methods, including thermogravimetric, X-ray phase and spectral analyses.

Complex thermal analysis was performed on a Q-1500D derivatograph of the Paulik, Paulik, Erdey system in the temperature range of 20-1000°C at a temperature rise rate of 10°C/min.

The microstructure of silicon (IV) oxide powders was studied by electron microscopy using scanning electron microscopy (SEM) using a scanning electron microscope "REMMA-106I".

The chemical composition of the raw material and the finished product was determined by atomic absorption spectrometry, volumetric and gravimetric analysis methods.

X-ray phase analysis was performed on a DRON-3 diffractometer in the range of reflection angles $2\theta = 10–800$ in Cu-Kα radiation using standard methods.

Phase identification was performed using an X-ray file and reference data. Spectroscopic studies were carried out using the infrared spectroscopy method (IR spectroscopy) using an IR spectrometer "Specord M-80" in the optical range $\nu = 800\text{-}3500$ cm^{-1}

The specific surface area of the powders was determined by the nitrogen thermal desorption method (BET). The essence of the method is to determine the amount of nitrogen adsorbed on the surface of the adsorbent from a flow of a nitrogen-helium mixture of a given concentration, at the temperature of liquid nitrogen and its subsequent desorption into the same mixture when the temperature is increased to 20 ± 5ºC.

The decrease and increase in the concentration of the adsorbing gas was recorded using a catharometer. The action of the catharometer is based on the dependence of the heat transfer of sensitive elements located in the comparative and measuring cells on the composition of the gas mixture. Therefore, a change in the composition of the gas mixture, and, accordingly, its thermal conductivity, causes an imbalance of the bridge and leads to the corresponding recording of the signal on the digital integrator display. The installation is designed to determine Sp of powder materials from 0.1 to 500 m^2/g by thermal desorption of nitrogen.

Experimental data processing was carried out on a computer using methods of mathematical statistics and data analysis using the programs "Statgraphics Plus 5.1" and "MathCAD 14".

3. THERMODYNAMIC ANALYSIS OF THE PROCESS OF OBTAINING SILICA (IV) OXIDE FROM THE RICE HUSK

The high rates of development of modern directions in engineering and technology require a sharp reduction in the development time of production processes. Reducing the time for creating new technological processes is impossible without the use of reliable calculation and technological methods, which are more rational than expensive, slow methods of experimental selection of technology parameters, which are based on the experience and intuition of developers.

Thermodynamic calculation and theoretical methods of system equilibrium, first of all, allow you to find conditions that ensure the maximum yield of the target product per unit mass of the working fluid, as well as to identify the possibility of obtaining certain quantities of a substance. Determine the content of by-products and impurities. In the calculations of thermodynamic multi-component equilibrium systems, the variable parameters are: temperature, pressure, ratio of initial components. By changing the initial conditions of a thermodynamic multicomponent system, it is possible to find the optimal conditions of the technological process for various parameters: the yield of target products, the minimum content of undesirable impurities, the specific consumption of raw materials, energy, etc.

The general basis of chemical processes is thermodynamic analysis, which indicates the direction of transformations in the reacting working medium from the initial content to the state in which the system is at the end of the process. Therefore, the task of thermodynamic calculation is to establish the relationship between all the characteristics of the system and determine the values of all dependent quantities. The solution of this problem is important in the case of complex multicomponent heterogeneous systems that have individual gaseous chemical substances in an electrically neutral and ionized state, as well as condensed substances and their compounds.

The purpose of this work is to calculate the equilibrium states of multicomponent thermodynamic systems and determine the optimal conditions for conducting the

thermal process of obtaining silicon (IV) oxide from rice husk. As a result of the calculation, the influence of temperature, the ratio of input flows of raw materials and coolant, as well as the influence of the environment on the equilibrium content of each multicomponent thermodynamic system at a pressure of 0.1 MPa were revealed. Specific energy consumption per unit of the target product was determined depending on the process conditions.

3.1 Calculation Method

A large number of methods for calculating equilibrium compositions of multicomponent heterogeneous thermodynamic systems and means for solving thermodynamic equilibrium equations are used in various branches of science and technology. The works [31,49] describe various methods of thermodynamic calculation based on the second law of thermodynamics. We have chosen a method using primary quantities in calculations, i.e. the first variational principle of chemical thermodynamics, which contains additional initial information - equilibrium constants, values of thermodynamic potentials or their combination. From a mathematical point of view, the method based on the first principle of thermodynamics has a number of advantages:

- Simplicity and clarity of the initial assumptions used in the construction of the method.

- High degree of universality and uniformity of the resulting system of equations, which is suitable without any changes for calculations of other types.

- Reduction of the necessary information related to the thermodynamic properties of the components.

- The possibility of creating a calculation algorithm that considers a thermodynamic system as a set of simple individual substances.

Chemical reactions, their direction, and intensity in the theory of chemical processes are usually investigated by the magnitude of the change in the isobaric-isothermal potential ΔG_p . The answer to the question of whether a given

thermodynamic system is in equilibrium can be obtained from the conditions of the minimum of the characteristic function. The calculation method we have chosen is that we need to find the equilibrium composition from the conditions of the experimentality of the characteristic function. The isobaric-isothermal potential ΔGp is used as the characteristic function, the minimum of which determines the equilibrium of a multicomponent thermodynamic system. The subscript "p" in the value of the isobaric-isothermal potential shows that it includes the energy of the bonds of atoms in the molecule. In order to show the state of a multicomponent thermodynamic system, the values of one “mechanical” (P – pressure) and one “thermal” (T – temperature) parameters were set, as well as the content of chemical elements in the working medium.

It is not possible to carry out an absolutely clear calculation of the equilibrium of a multicomponent thermodynamic system, which would correspond to the true extremum (minimum) of the isobaric-isothermal potential, due to the large number of calculations. Therefore, the calculation is carried out with a number of assumptions.

Individual substances that form a thermodynamic system in equilibrium and have the properties of an ideal gas are considered as components.

During all transformations of the working medium, the gas phase obeys the equation of state of ideal gases. We neglect the pressure of Brownian motion and the volume of condensed particles of the thermodynamic system. We consider the boundary of the phase distribution of the chemical system to be flat, therefore we do not take into account the surface tension energy and its contribution to the thermodynamic characteristics of the function. Thus, the thermodynamic system is considered isolated from the environment, which is expressed in the form of the law of conservation of mass and energy.

When performing calculations to determine the equilibrium composition, the necessary data are:

- The initial content of the working fluid, which is determined by the mass of chemical elements contained in it

$$[el] = \frac{m_{\text{syst.}}}{A_j} \cdot g_j \quad (3.1)$$

where $g_j = \frac{m_{el.j.}}{m_{\text{syst.}}}$ – mass fraction j – of that element in the system;

Aj – atomic mass of that element;

m $_{el.j}$ – mass j – of that element in the system;

m $_{akt}$ – mass of the working body;

- Thermodynamic properties of individual substances of the working fluid: heat capacity Cp, heat of formation ΔHт°, absolute entropy Sт. Instead of absolute enthalpy H, which cannot be determined, another complete thermodynamic function is used - total enthalpy J_f. The value of total enthalpy is determined by the following equation:

$$J_{f.j} = \Delta H_0° + H_т - H_0° = \Delta H_{298}° + (H_T° - H_0°) - \Delta H_{298}° - H_o° \quad (3.2)$$

where $H_0°$ – the heat of formation of an individual substance from elements at standard temperature;

$H_T = (H_T° - H_0°)$ – change in enthalpy of a substance in the temperature range from 0 K to T K.

The result of the thermodynamic calculation is the determination of the equilibrium composition of a chemically reacting system, which is expressed in terms of the number of moles Mi, partial pressures Pi, and volume fractions ri, which are related to each other as follows:

$$M_i = M \cdot P_i/P = \overline{Z}P_i \quad (3.3)$$

$$P_i = M_i \cdot P/M = ZM_i \quad (3.4)$$

$$r_i = P_i/P = M_i/M \quad (3.5)$$

where P is the total pressure in the system, which is equal to $\sum_{i=1}^{k} P_i$

M is the number of moles of all components in 1 kg of the working fluid

$\overline{Z} = M/P; Z = P/M$ - auxiliary quantities.

When finding the extremum of the characteristic function, auxiliary conditions for the existence of the system are imposed, which limit the range of changes in the number of moles of components:

- When the equilibrium state of the system is reached, the law of conservation of mass of all chemical elements is observed.

$$-[El_j] + \sum_{i=1}^{k} M_i n_{ji} = 0 \quad (3.6)$$

where $[El_j]$ is the number of moles of the jth element per unit mass of the working fluid;

n_{ji} is the number of atoms of the jth element in the corresponding individual component substance of the system;

- During transformations of the working fluid, the law of conservation of electric charge (conditions of electroneutrality) is observed.

$$\sum_{i=1}^{k} M_i n_{ei} = 0 \quad (3.7)$$

where nei – determines the sign and multiplicity of ionization of the component.

- During all transformations of the working fluid, the gas phase of the system obeys Dalton's law.

$$P = \sum_{i=1}^{k} P_i \quad (3.8)$$

For the existence of condensed components, the following conditions are met:

$$P_i < P_s \quad (3.9)$$

When $P_i < P_s \qquad M_i = 0 \qquad P_i \geq P_s \,.\, M_i > 0$

where M_i is the number of moles of the i-th component in the condensed phase.

For one mole of a component, the full isobaric-isothermal potential Gp of the thermodynamic system depends on the type of component, temperature, and partial pressure:

$$G_{ni} = \Delta H_0^0 + H_T - H_0^0 - TS_{T,i}^p \quad (3.10)$$

where $S_{T,i}^p$ – entropy of the component at partial pressure P_i;

$$S_{T,i}^p = S_{T,i}^0 - R_o \ln(P_i/P) \quad (3.11)$$

where Sot and is the standard entropy of the component at temperature T and partial pressure 0.1 MPa Pi;

Ro is the universal gas constant.

After substituting expressions (3.3), (3.4) and (3.5) into equation (3.11), we obtain:

$$S^{p}_{т,i} = S^{0}_{т,i} - R_o \ln(ZMi) \quad (3.12)$$

Then the equation of the full isobaric-isothermal potential for 1 mole of the component has the form:

$$G_{pi} = G^{0}_{p} - R_o \ln(ZMi) \quad (3.13)$$

where G^{0}_{p} and is the standard full isobaric-isothermal potential.

Since in thermodynamic calculations T≠0, the full isobaric-isothermal potential is used.

$$G^{*}_{p} = \frac{G_p}{T} = \frac{J_f}{T} - S^{0}_{т} = \frac{\Delta H^{0}_{0}}{T} - \frac{H_T - H^{0}_{0}}{T} - S^{0}_{т} = \frac{\Delta H^{0}_{0}}{T} - G^{*}_{f} \quad (3.14)$$

G^{*}_{f} – the total induced isobaric-isothermal potential.

For a multicomponent thermodynamic system consisting of k-components, the total induced isobaric-isothermal potential is determined by the following equation:

$$G_p = \sum_{i=1}^{k} M_i G_{pi} = \sum_{i=1}^{k} \left(G^{0}_{p} - R_o \ln ZMi \cdot Mi\right) \quad (3.15)$$

$$G^{*}_{p} = \frac{G_p}{T} = \sum_{i=1}^{k} \left(G^{*}_{pi} + \frac{R_o}{T} \ln ZMi\right) \cdot Mi \quad (3.16)$$

In accordance with the first variational principle of chemical thermodynamics, the composition of the chemically reacting system obtained as a result of the calculation must ensure the achievement of the minimum value of the isobaric-isothermal potential.

$$G^{*}_{p} \rightarrow \left(G^{*}_{p}\right)_{min} \quad (3.17)$$

Thermodynamic calculations and the subsequent analysis of the results allow us to study the conditions for the formation of the maximum amount of silicon(IV) oxide

in the equilibrium state and to determine the optimal intervals of the values of the main technological parameters of the process.

Thermodynamic calculations were performed using the standard ASTRA 4.0 software package, which determines equilibrium compositions based on finding the maximum entropy of the system [31].

Based on scientific and technical information and the results of previous own research [31,49], we identified the main directions of an effective method of processing RH to obtain silicon (IV) oxide.

3.2 Thermodynamic studies of the process of obtaining silicon (IV) oxide from the initial rice husk

Thermodynamic studies of the system were carried out in the temperature range of 300–2000 K at a pressure of 0.01 – 1 MPa.

In the calculations, condensed substances were considered as separate phases. The gas phase was a mixture of ideal gases.

The following were taken into account:

- in the condensed state:

SiO_2; C; SiC; Si;

- in the gas phase:

H_2O; C; CO; CO_2; CH_4; O_2; N_2; H; H_2; SiO_2; OH; SiH; SiH_2; Si_2C; SiC_2; HCN; NO; NO_2; N_2O; NH_3.

The concentrations of substances were expressed in moles per kilogram of the working mixture.

3.2.1 Thermodynamic analysis of the process of obtaining silicon (IV) oxide by pyrolysis from the initial rice husk

The initial RH has the following elemental composition, wt%: SiO_2–22.24; C – 35.77; O–36.59; H–5.05; N–0.32; S–0.03.

The heterogeneous system Si – O – C – H – N – S was studied in the temperature range of 300–2000 K at a pressure of 0.01–1 MPa in the process of RH pyrolysis.

Fig. 3.1 and 3.2 show the temperature dependences of the equilibrium compositions of pyrolysis products at normal pressure (0.1 MPa) and 0.01 MPa, respectively.

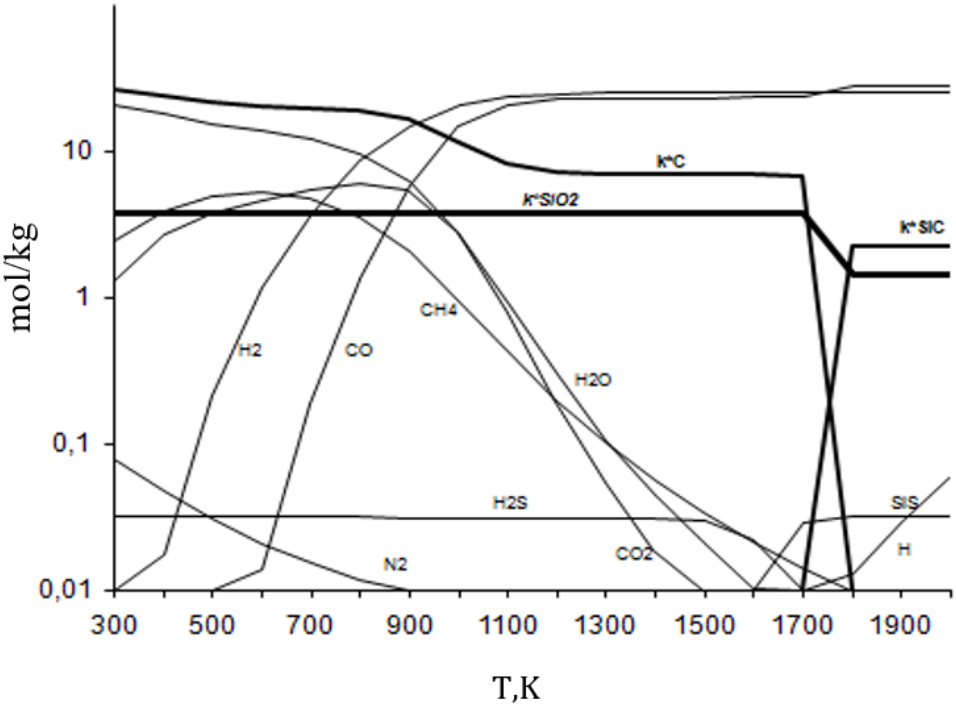

Figure 3.1. Dependence of equilibrium compositions of pyrolysis products at normal pressure (0.1 MPa).

Source of the figure: author's development

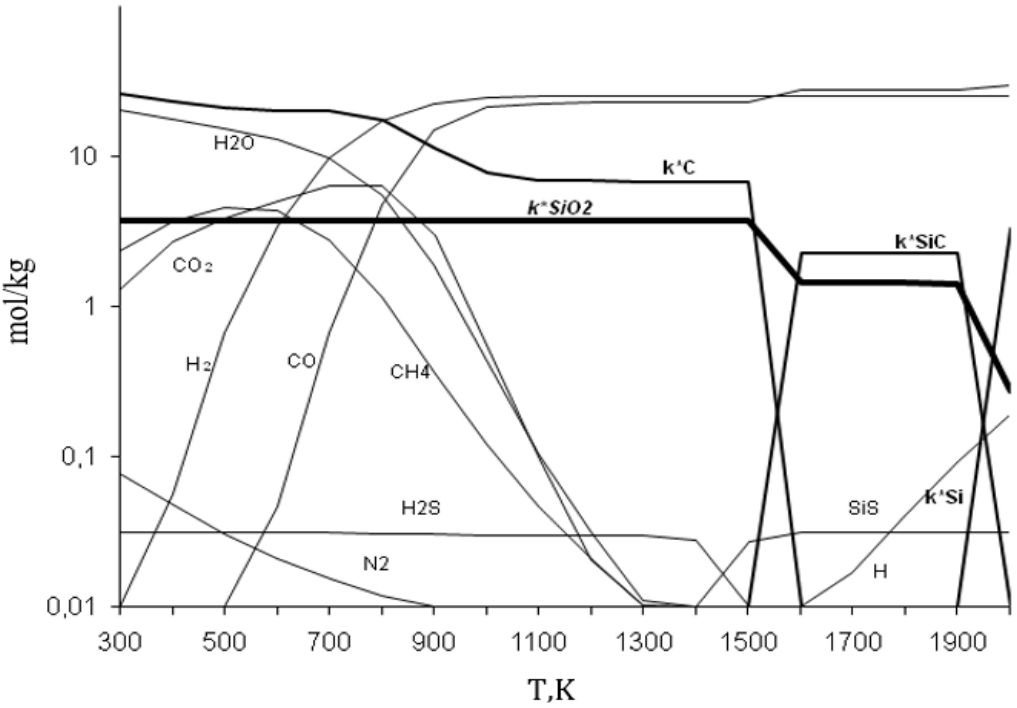

Figure 3.2. Dependence of equilibrium compositions of pyrolysis products at a pressure of 0.01 MPa in the environment of pyrolysis gases

Source of the figure: author's development

As can be seen from Fig. 3.1, carbon gasification occurs only due to the formation of CO_2 and CH_4 at temperatures above 300 K and CO at temperatures above 500 K. Thermodynamic analysis (Fig. 3.1) of RH pyrolysis showed that up to a temperature of about 1700 K, the content of condensed silicon (IV) oxide and carbon in the solid phase is preserved and pyrolysis and gasification of carbon-containing structures are completed. After that, the interaction of silicon (IV) oxide and carbon leads to the formation of silicon(IV) carbon. Thus, pyrolysis does not allow the extraction of silicon (IV) oxide in its pure form. As can be seen from Fig. 3.2, the condensed phase, which corresponds to the maximum content of silicon(IV) oxide, is in the temperature range of 300–1600 K. After 1500 K, silicon (IV) carbon is formed, so the content of silicon (IV) oxide decreases. The condensed phases contain silicon (IV) oxide, carbon and silicon(IV) carbon. Condensed carbon exists in the temperature range 300-1600 K.

A similar thermodynamic analysis was performed at an elevated pressure of 1MPa. Similar equilibrium compositions of pyrolysis products were obtained. The

difference is that with rarefaction, the equilibrium shifts towards low temperatures by 200 K, and with increasing pressure – towards high temperatures by 200 K, which does not change the general conclusion.

Thus, the gasification of carbon during pyrolysis, which is necessary to increase the content of silicon (IV) oxide, is not achieved at any temperatures and even under conditions of sufficiently deep vacuum.

3.2.2 Thermodynamic analysis of the process of obtaining silicon (IV) oxide from the initial rice husk in a water vapor environment

For a more complete extraction of carbon, a thermodynamic analysis was carried out in a water vapor environment.

The heterogeneous system Si–O–C–H–N–S was studied in the temperature range of 300-2000 K at normal pressure

Fig. 3.3 shows the temperature dependence of the equilibrium composition of the Si–O–C–H–N–S system on the temperature and the ratio of the mass flow rate of the RH to water vapor W = 1:1.

When conducting thermolysis with water vapor, the process intensification is observed from 400 K and above, and the composition of thermolysis products during steam-water conversion also changes, compared to pyrolysis. As can be seen from Fig. 3.3, in the temperature range of 400-700 K, silicon (IV) oxide and carbon are present in the condensed phases, and at temperatures above 700 K, the condensed phase is represented only by condensed silicon (IV) oxide. At temperatures up to 2000 K, the gas phase is represented by H_2O; CO; CO_2; CH_4, H_2. At temperatures above 1000 K, CH_4 disappears in the gas phase, and all other components are present.

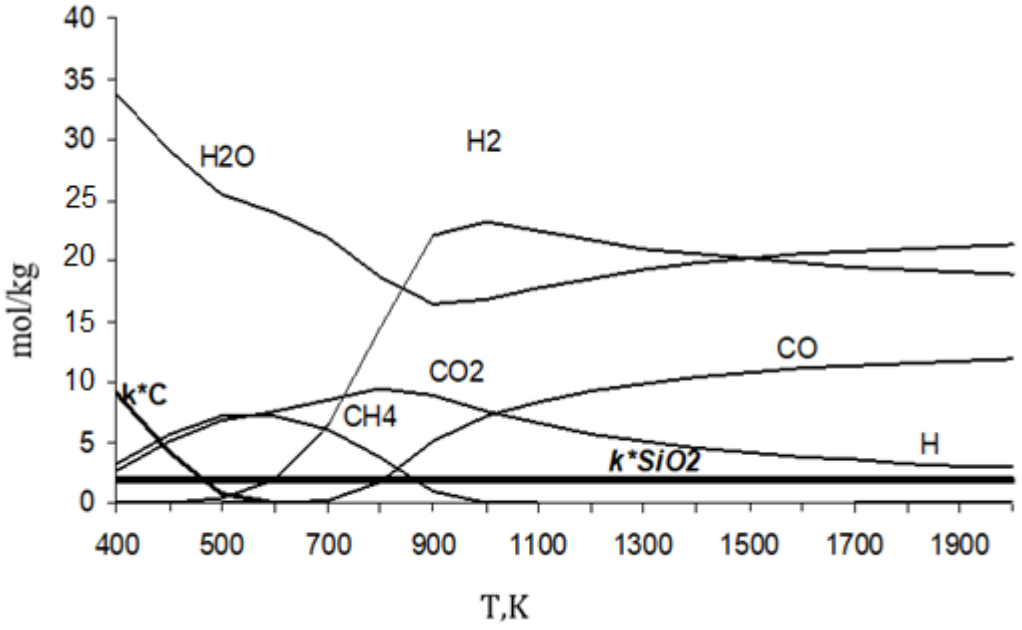

Figure 3.3. Temperature dependence of the equilibrium composition of the Si-C-O-H-N system on temperature and the ratio of the mass flow rate of RH to water vapor W = 1:1

Source of the figure: author's development

Based on the dependence of the products of thermolysis of RH steam-water conversion on temperature and the ratio of mass flow rates of RH to water vapor 1:1, probable reactions of carbon gasification and concomitant reactions of RH decomposition with the production of silicon (IV) oxide have been established.

The following reactions are most likely:

$$C + H_2O = CO + H_2 \quad (3.18)$$

$$C + 2H_2O = CO_2 + 2H_2 \quad (3.19)$$

$$2C + 2H_2O = CO_2 + CH_4 \quad (3.20)$$

$$C + CO_2 = 2CO \quad (3.21)$$

$$CO + H_2O = H_2 + CO_2 \quad (3.22)$$

$$CH_4 + H_2O = 3H_2 + CO \quad (3.23)$$

$$CH_4 + 2H_2O = CO_2 + 4H_2 \quad (3.24)$$

$$CH_4 + CO_2 = 2CO + 2H_2 \quad (3.25)$$

For each reaction (3.18) - (3.25) we calculated the thermodynamic characteristics, which are the Gibbs energy (DG), the enthalpy change (DH), the equilibrium constant Kp and the degree of transformation Xj, where j is the name of the substance. As a result, we obtained the dependences of the change in Gibbs energy, the enthalpy change, the equilibrium constant and the degree of transformation on temperature.

The dependence of the thermodynamic characteristics on temperature for the reaction $C+H_2O=CO+H_2$ is shown in Fig. 3.4.

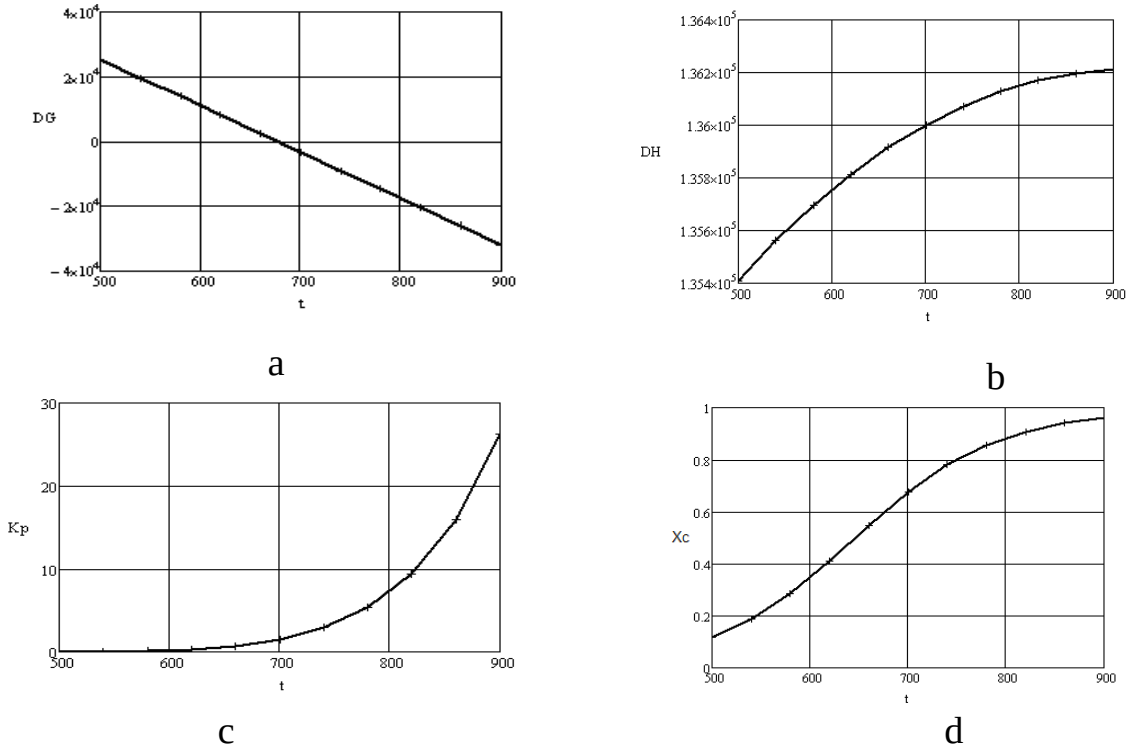

a – dependence of Gibbs energy (DG) on temperature; b – dependence of enthalpy change (DH) on temperature; c – dependence of equilibrium constant Kp on temperature; d – dependence of degree of conversion Xc on temperature.

Figure 3.4. Dependence of thermodynamic characteristics on temperature for the reaction $C+H_2O \leftrightarrow CO+H_2$

Source of the figure: author's development

From Fig. 3.4 it is clear that the reaction $C+H_2O \leftrightarrow CO+H_2$ becomes thermodynamically plausible at temperatures above 700°C. At the same time, in the temperature range 700-900°C, the equilibrium constant increases to 28 units (Fig. 3.4c). From the graph in Fig. 3.4b it is clear that the reaction is strongly endothermic, so that its course requires significant energy expenditure. From the graph in Fig. 3.4d it is clear that in the region 700-900°C the equilibrium degree of carbon conversion increases from 0.4-0.96.

The dependence of the thermodynamic characteristics on the temperature for the reaction $C+2H_2O=CO_2+2H_2$ is shown in Fig. 3.5.

From Fig. 3.5 it is seen that the reaction $C+2H_2O=CO_2+2H_2$ becomes thermodynamically plausible at temperatures above 650°C. At the same time, in the temperature range 650-900°C the equilibrium constant increases to 20 units (Fig. 3.5c). From the graph in Fig. 3.5b it is seen that the reaction is strongly endothermic, so that its course requires significant energy expenditure. From the graph in Fig. 3.5d it is seen that in the region 650-900°C the equilibrium degree of carbon conversion increases from 0.65-0.840.

The dependence of the thermodynamic characteristics on the temperature for the reaction $2C+2H_2O=CO_2+CH_4$ is shown in Fig. 3.6.

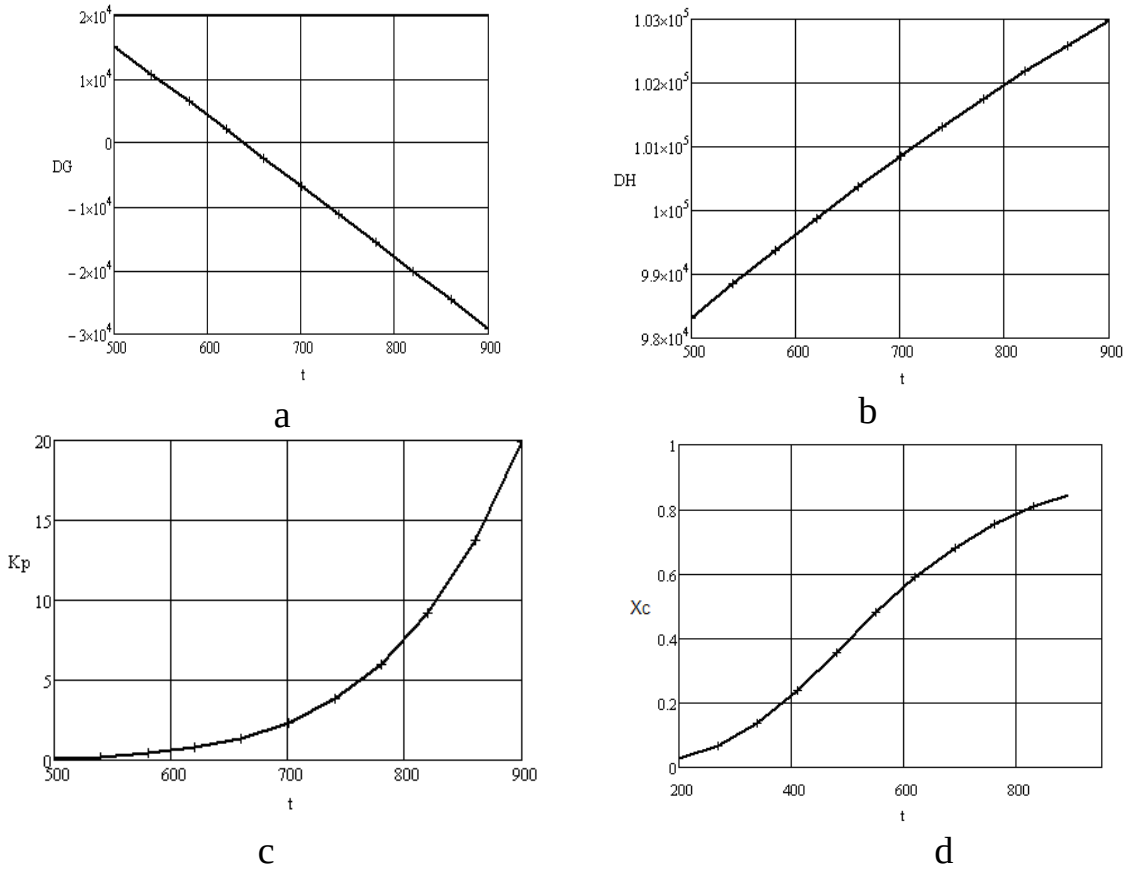

a – dependence of Gibbs energy (DG) on temperature; b – dependence of enthalpy change (DH) on temperature; c – dependence of equilibrium constant Kp on temperature; d – dependence of degree of conversion Xc on temperature.

Figure 3.5. Dependence of thermodynamic characteristics on temperature for the reaction $C+2H_2O=CO_2+2H_2$

Source of the figure: author's development

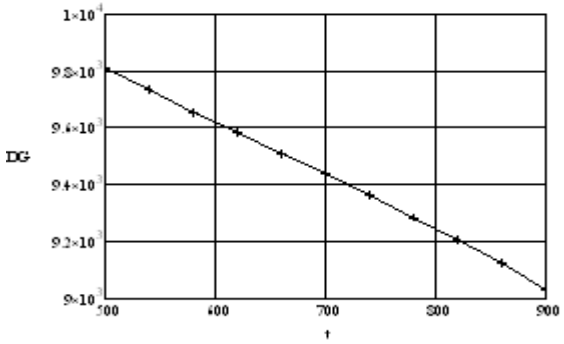

Figure 3.6. Gibbs free energy (DG) versus temperature for the reaction $2C+2H_2O=CO_2+CH_4$

Source of the figure: author's development

From Fig. 3.6 it is clear that the reaction $2C+2H_2O=CO_2+CH_4$ is thermodynamically improbable in the temperature range 500-900°C.

For the reaction $C + CO_2 \leftrightarrow 2CO$, the dependence of the thermodynamic characteristics on temperature is shown in Fig. 3.7.

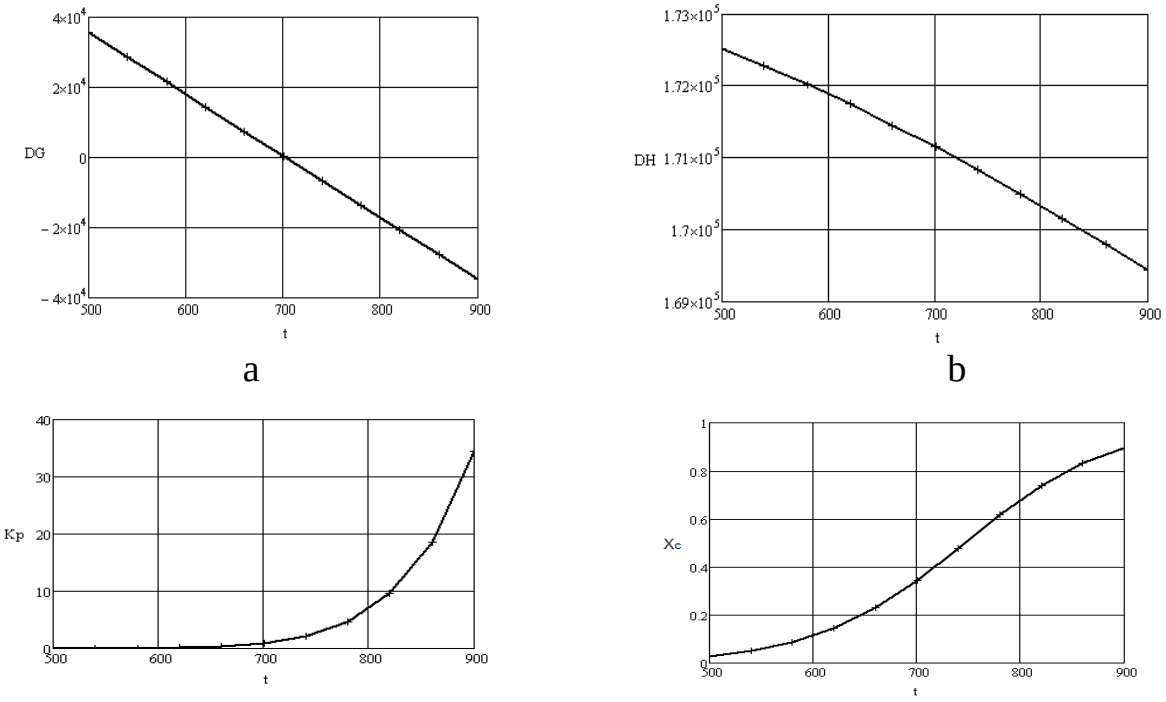

a – dependence of Gibbs energy (DG) on temperature; b – dependence of enthalpy change (DH) on temperature; c – dependence of equilibrium constant Kp on temperature; d – dependence of degree of conversion Xc on temperature.

Figure 3.7. Dependence of thermodynamic characteristics on temperature for the reaction $C + CO_2 \leftrightarrow 2CO$

Source of the figure: author's development

From Fig. 3.7 we can conclude that the reaction $C + CO_2 \leftrightarrow 2CO$ is thermodynamically probable at temperatures above 700°C.

At the same time, in the temperature range 700-900°C, the equilibrium constant increases to 35 units (Fig. 3.7c). The graph in Fig. 3.7b shows that the reaction is strongly endothermic, so that its occurrence requires significant energy expenditure.

The graph in Fig. 3.7g shows that in the region 700-900°C, the equilibrium degree of carbon conversion increases from 0.35-0.90.

From the data obtained for the reactions (3.18 - 3.21), we can conclude that with increasing temperature, the vapor pressure increases, which shifts the equilibrium and reduces the equilibrium degree of conversion. The increase in pressure is also affected by the increase in the volume of the reaction 3.19 and 3.20.

The dependence of thermodynamic characteristics on temperature for the reaction $CO+H_2O=H_2+CO_2$ is shown in Fig. 3.8.

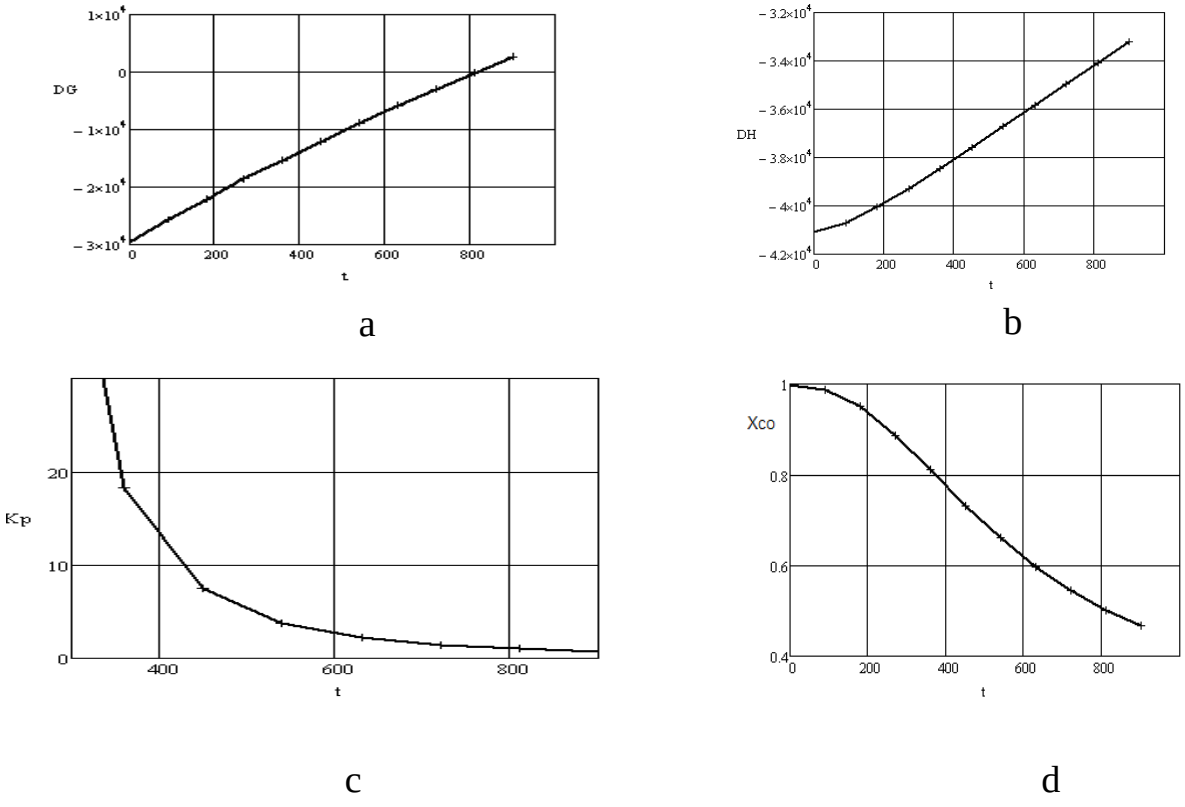

a b

c d

a – dependence of Gibbs free energy (DG) on temperature; b – dependence of enthalpy change (DH) on temperature; c – dependence of equilibrium constant Kp on temperature; d – dependence of degree of conversion Xco on temperature.

Figure 3.8. Dependence of thermodynamic characteristics on temperature for the reaction $CO+H_2O=H_2+CO_2$

Source of the figure: author's development

The reaction $CO+H_2O=H_2+CO_2$ is thermodynamically plausible at temperatures above 800°C. Fig. 3.8b shows that the reaction is strongly exothermic. For this reaction,

with increasing temperature, the equilibrium constant decreases to 2 units at a temperature of 800°C (Fig. 3.8c), which stimulates the reverse reaction. This leads to the fact that the equilibrium degree of CO conversion decreases intensively to 0.46 with increasing temperature Fig. 3.8d.

The dependence of the thermodynamic characteristics on the temperature for the reaction $CH_4+H_2O=3H_2+CO$ is shown in Fig. 3.9.

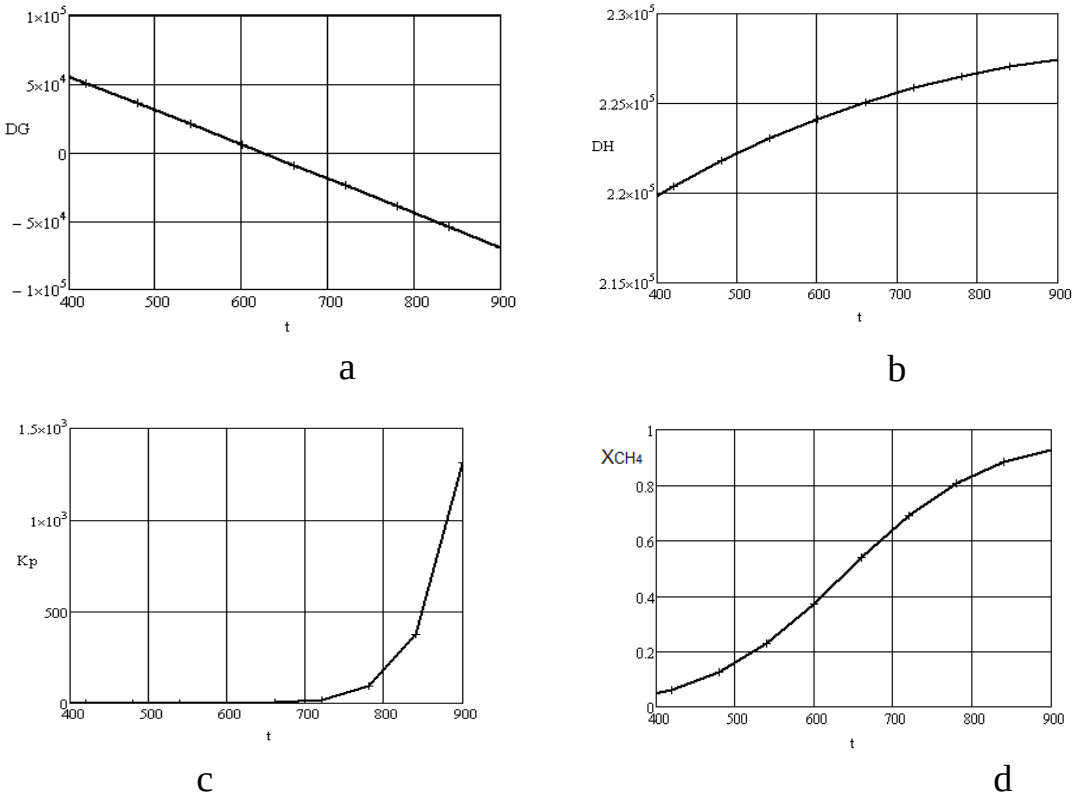

a – dependence of Gibbs free energy (DG) on temperature; b – dependence of enthalpy change (DH) on temperature; c – dependence of equilibrium constant Kp on temperature; d – dependence of degree of conversion of CH_4 on temperature.

Figure 3.9. Dependence of thermodynamic characteristics on temperature for the reaction $CH_4+H_2O=3H_2+CO$

Source of the figure: author's development

From Fig. 3.9 it is seen that the reaction $CH_4+H_2O=3H_2+CO$ is thermodynamically probable at temperatures above 630°C. At the same time, in the temperature range 630–900°C the equilibrium constant increases to 1300 units (Fig.

3.9 c). From Fig. 3.9 b it is seen that the reaction is strongly endothermic, so that its course requires significant energy expenditure. From the graph in Fig. 3.9 d it is seen that in the region 630-900°C the equilibrium degree of methane conversion increases from 0.40-0.93.

The dependence of the thermodynamic characteristics on the temperature for the reaction $CH_4+2H_2O=CO_2+4H_2$ is shown in Fig. 3.10.

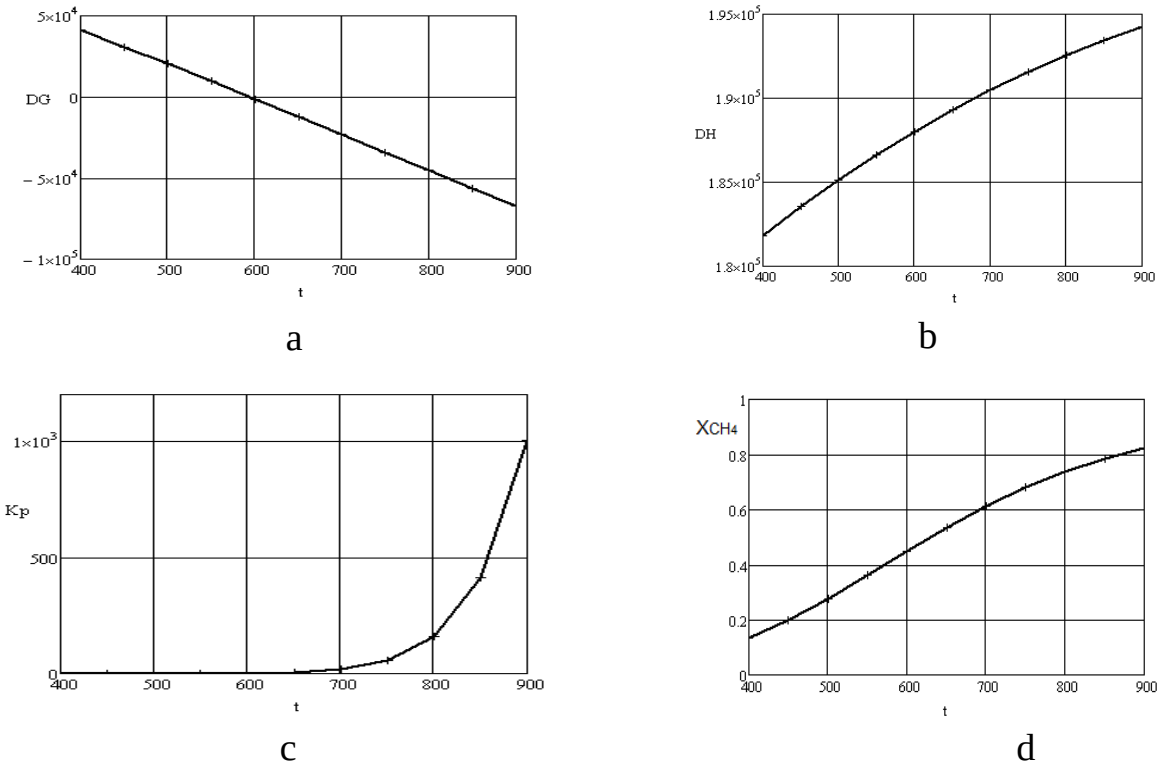

a – dependence of Gibbs free energy (DG) on temperature; b – dependence of enthalpy change (DH) on temperature; c – dependence of equilibrium constant Kp on temperature; d – dependence of degree of conversion of CH_4 on temperature.

Figure 3.10. Dependence of thermodynamic characteristics on temperature for the reaction reaction $CH_4+2H_2O=CO_2+4H_2$

Source of the figure: author's development

The reaction $CH_4+2H_2O=CO_2+4H_2$ is thermodynamically plausible at temperatures above 600°C. At the same time, in the temperature range 600-900°C, the equilibrium constant increases to 1000 units (Fig. 3.10 c). From Fig. 3.10 b it is clear

that the reaction is strongly endothermic, so that its course requires significant energy expenditure. From the graph in Fig. 3.10 g it is clear that in the region 600-900°C the equilibrium degree of methane conversion increases from 0.45-0.82.

The dependence of the thermodynamic characteristics on the temperature for the reaction $CH_4+CO_2=2CO+2H_2$ is shown in Fig. 3.11.

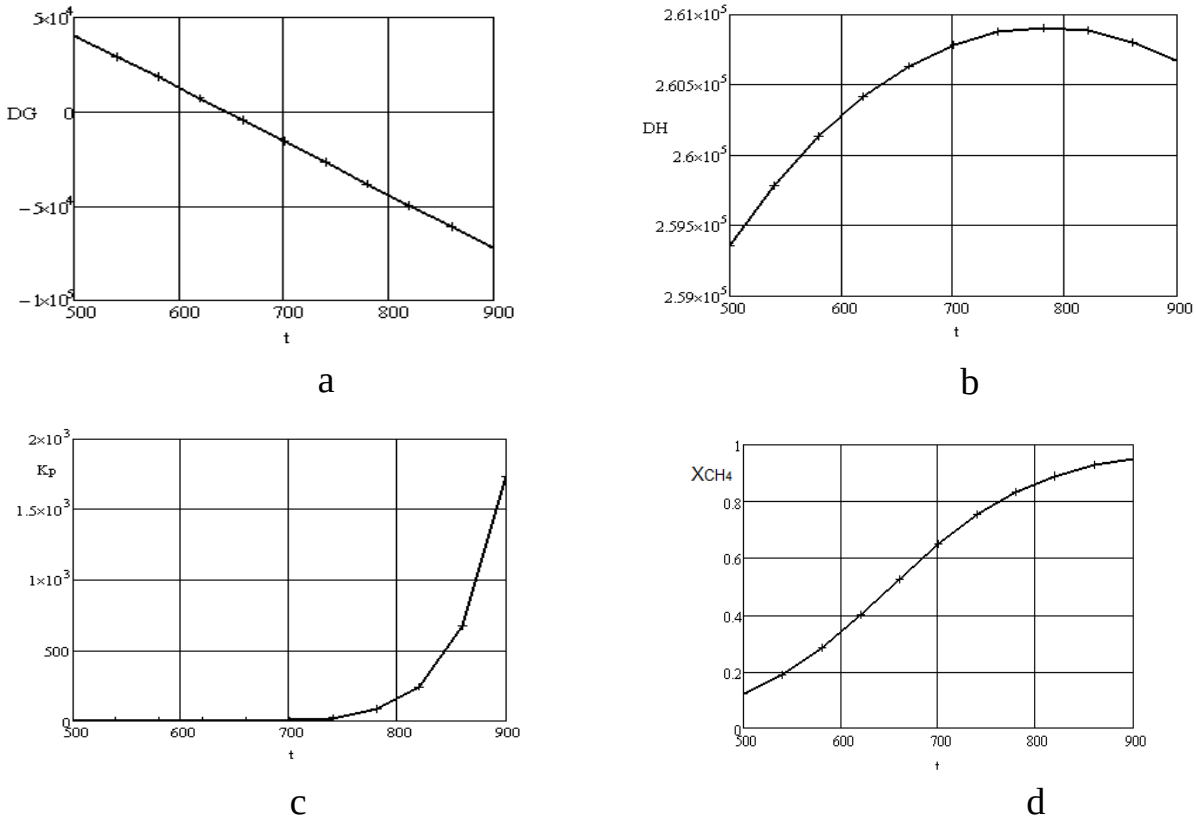

a – dependence of Gibbs free energy (DG) on temperature; b – dependence of enthalpy change (DH) on temperature; c – dependence of equilibrium constant Kp on temperature; d – dependence of degree of conversion of CH_4 on temperature.

Figure 3.11. Dependence of thermodynamic characteristics on temperature for the reaction $CH_4+CO_2=2CO+2H_2$

Source of the figure: author's development

The reaction $CH_4+CO_2=2CO+2H_2$ is thermodynamically plausible at temperatures above 640°C and endothermic (Fig. 3.11 b). In the temperature range 640-900°C, the equilibrium constant increases to 1700 units (Fig. 3.10 c). In the

temperature range 640-900°C, the equilibrium degree of methane conversion increases from 0.55-0.95.

Thus, the steam-water conversion of carbon according to reactions 3.18 - 3.19 allows increasing the degree of carbon gasification with increasing temperature, however, the water vapor pressure increases significantly and the equilibrium degree of conversion decreases. Reaction 3.20 is thermodynamically improbable. Reactions 3.22 - 3.24 are thermodynamically plausible and proceed with a high degree of conversion, which thereby leads to an increase in the non-target consumption of water vapor. Reaction 3.21, which contributes to the gasification of carbon, is highly endothermic and is not effective at increasing the pressure, which is established when using high-temperature water vapor.

Due to the combination of the noted features, as well as due to the high energy consumption of the process of steam-water conversion of carbon, it was decided to consider the possibility of using the extraction process at the previous stage of silicon(IV) oxide extraction. This process includes the extraction of carbon-containing compounds from the RH, which allows increasing the content of silicon(IV) oxide in solid residues.

4. INCREASING THE CONTENT OF AMORPHOUS SILICON(IV) OXIDE IN SOLID RICE HUSK RESIDUE BY PHYSICO-CHEMICAL METHODS

4.1 Mechanism of the process of extracting a component of a solid particle by a liquid extractant

In the general case, the process of extracting a certain component A from a solid material using a liquid extractant should be considered taking into account the features of the structural and chemical organization of the solid phase.

The structural organization of solid plant materials, as well as solid fossil fuels, which is the result of continuous transformation (metamorphism) of initial materials of plant origin, can be conditionally represented by the following three levels:

- microlevel - the state and properties of the material are determined by the movement of molecules of various organic and inorganic substances;

- macrolevel - the properties and state of the material determine complexes of molecules of various substances (macromolecules), bound by intermolecular interaction forces of different nature;

- solid particle level - the properties and state of the material determine the association of macromolecules, the connection between which is provided by various means of polyconnection (hydrogen bonds, Eda interactions, strong C-C bonds).

Taking this into account, the mechanism of transition of solid component A into a liquid state is as follows:

- liquid selective extractant penetrates into the pores of the solid particle and comes into contact with component A;

- as a result of the mutual influence of the electronic shells of the extractant molecules and component A, the ratio between the means of polyconjugation at the 3rd level and the forces of intermolecular interaction at the 2nd level of the structural and chemical organization of the solid particle changes;

- as a result of the weakening of the bonds between the elements of this structure, it collapses (transitions to the 2nd and even 1st levels of structural organization, which correspond to the liquid state of the substance) at the same energy consumption supplied from the outside (at the same temperature), at which it was completely resistant to the influence of the liquid extractant;

- with increasing concentration of the extractant, the degree of extraction of component A, which has passed into the liquid state, increases to the maximum possible value under the given conditions, while the new level of the process result depends not only on the concentration of the extractant, but also on the level already achieved.

The phenomena described above, occurring simultaneously at many points in the volume of a solid particle, facilitate mass transfer in the solid-liquid system, "loosening" the macrostructure of the particle and increasing the content of substances in it that were not extracted.

Within the framework of the presented hypothesis about the mechanism of the process of extracting a component of a solid particle by a liquid extractant, it is possible to formulate a number of practical recommendations on technological operations and factors of the technological regime, as well as to formulate as a process model an equation that establishes the relationship between the degree of extraction of component A and the main technological factors.

In particular, the mentioned operations should include:

1. Grinding of solid material with the formation of particles with the maximum total surface area;

2. Intensive mixing of phases for effective use of the surface of their contact;

3. Selection of a liquid phase with a low surface tension.

Technological factors include:

- process temperature;

- process time;

- extractant concentration.

To derive the equation that connects the degree of extraction of a solid component with these factors, we introduce the notation:

y – degree of extraction, %wt.

x – concentration of extractant %wt.

$\frac{dy}{dx}$ – change in degree of extraction in response to change in concentration of extractant (for simplicity, we will hereinafter call this ratio the extraction rate).

In accordance with the hypothesis about the mechanism of the process, we write the expression:

$$\frac{dy}{dx} = f(x, y), \tag{4.1}$$

which means that the extraction rate depends not only on the concentration of the extractant, but also on the already achieved degree of extraction.

As an exception, we consider the simplified equation (4.1) in the form:

$$\frac{dy}{dx} = f_1(y) \cdot f_2(x), \tag{4.2}$$

or

$$\frac{dy}{f_1(y)} = f_2(x)dx. \tag{4.3}$$

Integrating (4.3) gives the equation:

$$F_1(y) = F_2(x) \tag{4.4}$$

which defines the value of *y* as a function of *x*.

To move from general results to the specific process of extracting a solid component with a liquid extractant, we take into account the dependence of the extraction rate on the achieved extraction level and the still unextracted (residual) amount of the component, introducing the expression as a function f1

$$f_1(y) = y(y_{max} - y) \tag{4.5}$$

where ymax is the maximum possible degree of extraction.

Substituting (4.5) into (4.2), we obtain:

$$\frac{dy}{dx} = y(y_{max} - y) \cdot f_2(x), \tag{4.6}$$

or, after multiplying by y_{max}:

$$\frac{dlny}{dx} = \frac{dln(y_{max}-y)}{dx} = y_{max} \cdot f_2(x), \tag{4.7}$$

It can be shown that

$$\frac{y_{max}}{y(y_{max}-y)} = \frac{1}{y} + \frac{1}{y_{max}-y}. \tag{4.8}$$

Taking into account equation (4.7) and (4.8), we obtain:

$$\frac{dy}{ydx} + \frac{dy}{(y_{max} - y)dx} = y_{max} \cdot f_2(x). \tag{4.9}$$

Since

$$\frac{dy}{ydx} = \frac{dlny}{dx}, \tag{4.10}$$

and

$$\frac{dy}{(y_{max}-y)dx} = \frac{dln(y_{max}-y)}{dx}, \tag{4.11}$$

equation (4.9) is rewritten as:

$$\frac{dlny}{dx} - \frac{dln(y_{max}-y)}{dx} = y_{max} \cdot f_2(x) \tag{4.12}$$

or

$$dlny - dln(y_{max} - y) = y_{max} \cdot f_2(x) \cdot dx \tag{4.13}$$

Equation (4.13) is easily integrated (see equations (4.3) and (4.4)):

$$lny - ln(y_{max} - y) = y_{max} \cdot F_2(x) + c_1 \tag{4.14}$$

From (4.14), solved for y, we obtain:

$$y = \frac{y_{max}}{1+b \cdot e^{-y_{max} \cdot F_2(x)}}, \tag{4.15}$$

where $b = e^{-c_1}$, a is the constant of integration that can be found for a given value (x, y).

Let $f_2(x)$ be linear, i.e.

$$f_2(x) = bx. \tag{4.16}$$

Then

$$F_2(x) = b\int xdx = \frac{1}{2}bx^2. \quad (4.17)$$

Substituting (4.17) into (4.15) and taking

$$y_{max} = a \quad (4.18)$$

and

$$\frac{1}{2}\cdot y_{max}\cdot b = c \quad (4.19)$$

Finally, we find the dependence of the degree of extraction of the solid component on the concentration of the extractant in the form:

$$y = \frac{a}{1+b\cdot e^{-cx^2}}. \quad (4.20)$$

The parameters of equation (4.20) are found from experimental data, we assume:

- according to (4.18) a = ymax;

- at x=0 and $y_{x=0} \neq 0$ from (4.20) we get:

$$b = \frac{a}{y_{x=0}} - 1, \quad (4.21)$$

- for x=1 and $y_{x=1}$ from (4.20) we get:

$$c = -ln\frac{a - y_{x=1}}{b\cdot y_{x=1}}. \quad (4.22)$$

Thus, to determine the parameters a, b, and c, the experimental design should include experiments at x = 0, x = 1, and x at which ymax is achieved.

We can assume that a, b, and c are functions of temperature and process duration. In the case of establishing these functions, they can be included in equation (4.20) and then it will be transformed into a dependence of the degree of extraction simultaneously on all technological factors.

4.2 Research on the chemical preparation processes of rice husk

To conduct research on the chemical preparation processes, crushed rice husk was used as raw material.

The grinding was carried out on a plant material fine grinding unit [27], the schematic diagram of which is shown in Fig. 4.1.

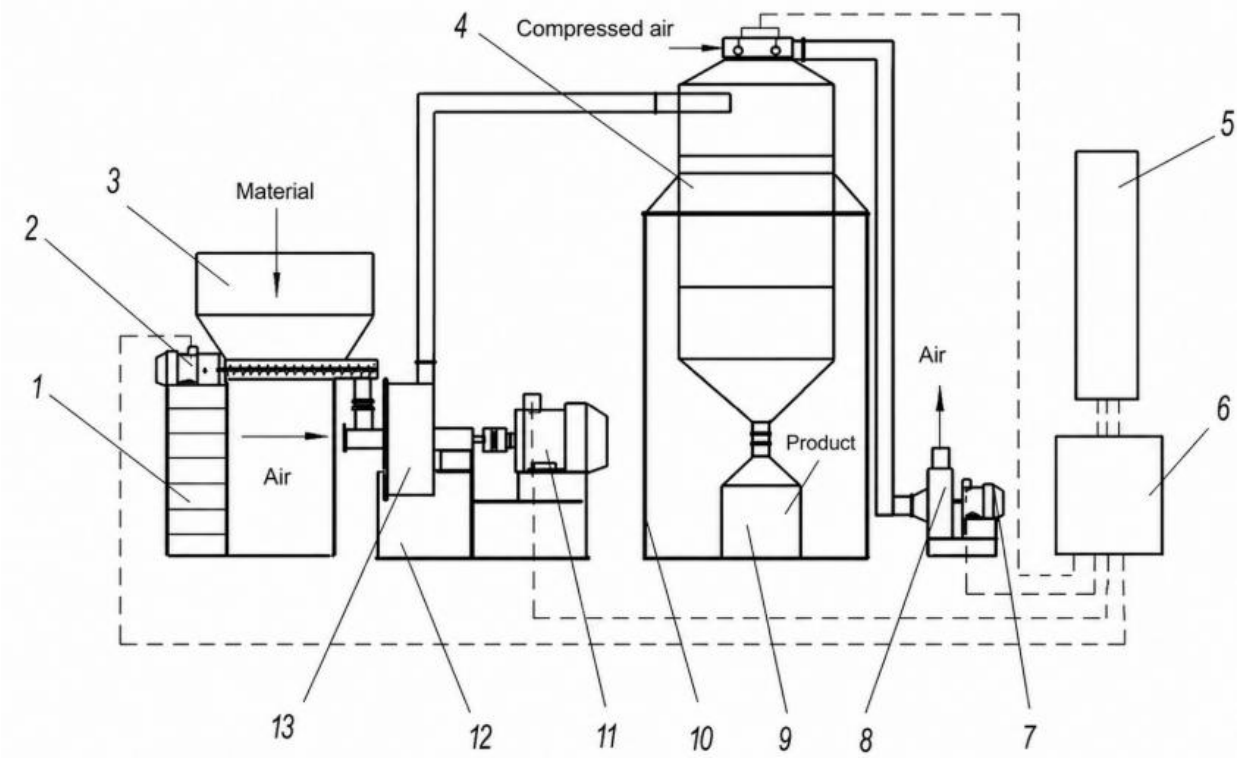

1, 10, 12 – frame, 2 – electric motor, 3 – feeder, 4 – filter - cyclone, 5 – power cabinet, 6 – control panel, 7 – fan electric motor, 8 – fan, 9 – container, 11 – mill electric motor, 13 – two-stage impact mill.

Figure 4.1. Schematic diagram of the plant material fine grinding installation

Source of the figure: author's development

After that, the rice husk was dispersed into fractions using sieves with the following hole diameters: 40, 60, 150, 200, 1000 μm.

The influence of the particle size of the crushed RH on the bulk density of the RL powder was studied.

Fig. 4.2 shows the dependence of the bulk density of compacted and non-compacted RH on the average particle size during grinding.

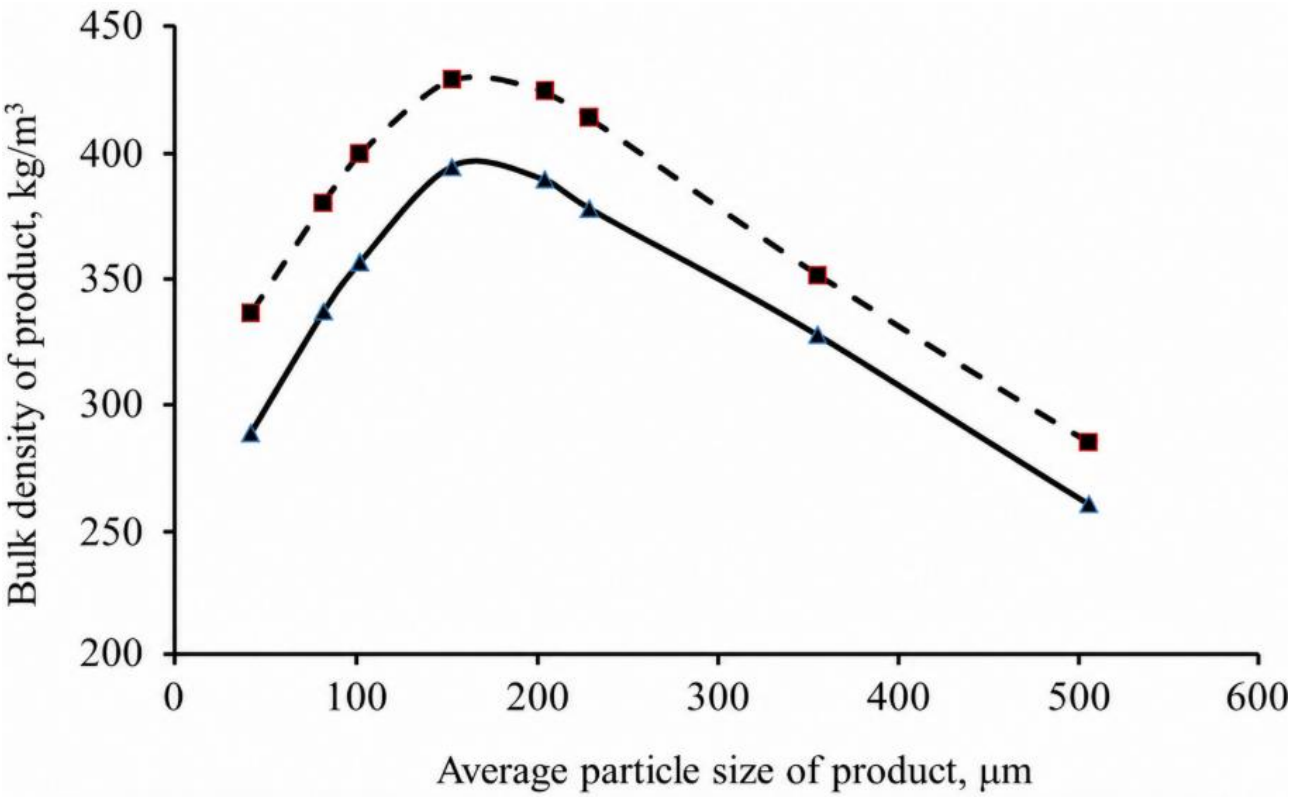

___ - bulk density of uncompacted rice husk particles, kg/m³ ;

---- - bulk density of compacted rice husk particles, kg/m³

Figure 4.2. Dependence of bulk density on the average particle size of crushed rice husk

Source of the figure: author's development

As can be seen from Fig. 4.2, the minimum bulk density is the fraction of uncompacted rice husk particles of 40 μm and is 280 kg/m³, and for compacted particles – it is 330 kg/m³. It can be assumed that this value of bulk density is associated with the removal of moisture from the RH (free and bound), as well as non-heat-resistant components during grinding and increasing porosity. Grinding of RL with a particle size of 40-100 μm occurs along the fibers and a further increase in bulk density occurs due to the destruction of RH fibers and a change in the shape of the particles from sharp-needle to cubic and prismatic [23].

A further increase in bulk density with increasing fraction size indicates a denser packing of the crushed RH when combining large and small particles. For a coarse

fraction of 500 μm and more, the bulk density naturally decreases due to a change in the shape of the particles from round-spherical to prismatic.

Direct thermolysis of RH allowed obtaining amorphous silicon (IV) oxide of technical qualification, due to the presence of carbon residues and metal oxide impurities in the final product [17].

Subsequent studies were aimed at developing methods for preliminary chemical preparation of RH in order to reduce its composition of inorganic metal impurities and carbon-containing components by removing lignin or cellulose, as well as by sequential removal of lignin and then cellulose [50-52].

4.2.1 Lignin extraction process

Lignin preparations removed from wood by different methods differ significantly in physical and physicochemical properties. The properties of lignin are also influenced by the type of wood [52].

It is known from literature that rice husk contains 40.02% crude and 24.1% purified by the Clason method lignin [52]. Gray lignin often contains significant amounts of cellulose and ash. According to Leonzio, the content of purified lignin ranges from 19.20 to 24.2%, with most of the ash being associated with crude lignin [52]. The results of lignin analysis depend strongly on the method of its extraction [50-52].

Natural lignin is colorless or very light in color (from yellow to brown). Lignin isolated by alcohol without the use of acid additives is a light cream powder. Acid lignins have a very dark color. The color is caused by chromophoric groups, for example, o-quinoids, which are formed during the isolation of lignin. The density of lignin preparations ranges from 1.25 g/cm^3 to 1.45 g/cm^3. The refractive index of a lignin solution is 1.6, which is typical for aromatic compounds [52].

X-ray studies, as well as studies of the thermoplastic properties of lignin, show that it is amorphous. Lignin, despite the presence of asymmetric carbohydrate atoms in it, is optically inactive. The bulk of natural lignin is insoluble in organic solvents. The

insolubility of lignin is explained by the existence of cross-linked chemical bonds in it with the formation of a three-dimensional structure. Lignins isolated under mild conditions are soluble in organic solvents, such as dioxane, pyridine, dimethyl sulfoxide. Lignin preparations are soluble only in those organic solvents that are able to overcome the energy of intermolecular hydrogen bonds (cohesion energy).

Lignin solutions at sufficiently low concentrations are true. However, the presence of hydroxyl, carbonyl, carboxyl groups in lignin molecules, capable of strong intermolecular interaction, leads to a high degree of association in lignin solutions.

Natural lignin and preparations of soluble lignins are thermoplastic, while preparations of insoluble lignins are usually infusible.

Lignin is a high-molecular compound. Different preparations of isolated lignins have different molecular weights.

Lignin is a mixture of irregular branched polymers of related structure, based on aromatic substances similar in structure. Lignin macromolecules are built from C6-C3 structural units, α- and β-structures are established (Fig. 4.3).

Rice husk lignin has the following chemical bonds: simple C-C-; C-H-; O-H-; C-O-C- and aromatic C=C, C≡O, C=C.

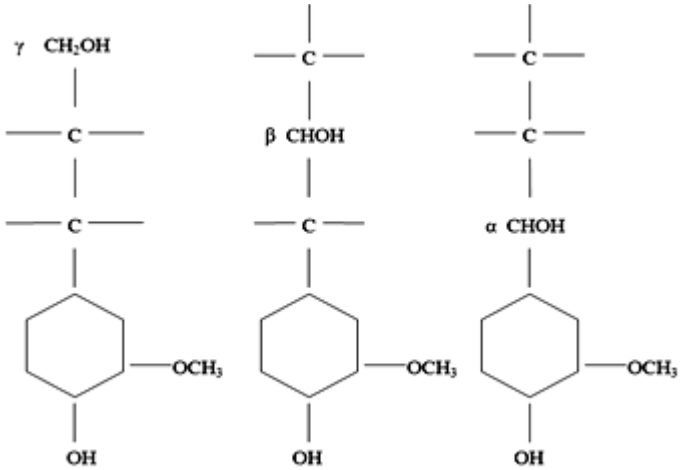

a) b) c)

a) γ-lignin; b) β-lignin; c) α-lignin.

Figure 4.3. Structural formula of lignin

Source of the figure: [52]

Lignin is chemically reactive. Lignin is also characterized by destruction reactions, which can occur with the rupture of simple ether bonds, and in some cases with the rupture of more stable carbohydrate-hydrocarbon bonds. A feature of chemical behavior is the chain crosslinking reaction, as well as condensation reactions with the formation of new carbohydrate-hydrocarbon bonds.

Methods for isolating lignin from wood can be divided into two groups: 1) methods based on the transfer of the carbohydrate part into solution and obtaining lignin as an insoluble residue; 2) methods based on the dissolution of lignin with its subsequent precipitation from the resulting solutions [52].

The most studied reactions for the extraction of lignin are those that occur when heated with aqueous dioxane in the presence of HCl (acidolysis) and with ethyl alcohol in the presence of HCl (ethanololysis).

Other alcohols (methyl, butyl, ethylene glycol) can also be used to isolate lignin. All of these lignin preparations are grouped into the group of alcohol lignins.

It is also possible to extract lignin from wood with glacial acetic acid when heated after previous infusion in 17-18% wt. hydrochloric acid in the cold [19].

The ethanolysis reaction was first used to study the structure of lignin by Hibbert, and the acidolysis reaction was first used by Adler, who also established the mechanism of these reactions [27].

The mechanism of cleavage of a simple ether bond in the main structure of lignin – the structure of β-aryl ether of arylglycerol Adler presents as follows: during ethanolysis, ethoxyl groups are introduced into lignin, protecting the benzyl alcohol groups formed during destruction from further condensation.

During acidolysis, simple ether bonds in lignin structures with free phenolic hydroxyl are more easily cleaved. The mechanism of the reaction of ethanolysis of lignin is shown in Fig. 4.4.

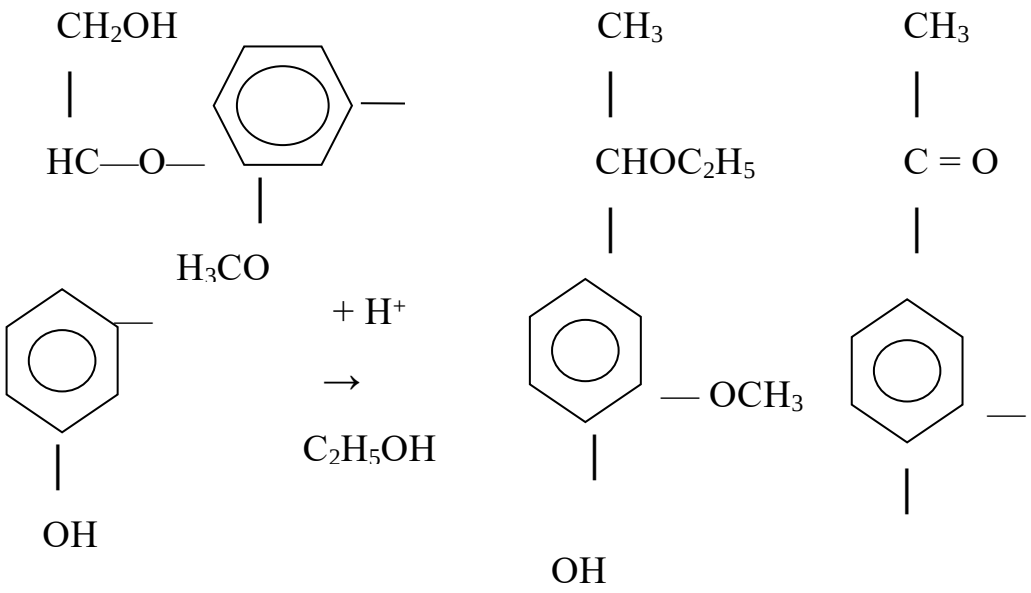

Figure 4.4. Mechanism of the lignin ethanolysis reaction

Source of the figure: [27]

The study of the process of lignin extraction from RH was carried out on a laboratory setup, which is shown in Fig. 4.5.

A sample of crushed RH weighing 5 g was placed in a thermostated reactor 1. 50 ml of extractant was added there. The temperature of the extraction process was maintained within the range from 20 to 80°C. The duration of the process was varied from 0.5 hours to 6 hours. The reaction mixture was intensively stirred using a propeller stirrer 5. After the end of the experiment, the insoluble residue was filtered, washed repeatedly with water until complete visual clarification. The washed residue was dried at a temperature of 90-95°C in air to a constant mass.

A sample of crushed RH weighing 5 g was placed in a thermostated reactor 1. 50 ml of extractant was added there. The temperature of the extraction process was maintained within the range from 20 to 80°C. The duration of the process was varied from 0.5 hours to 6 hours. The reaction mixture was intensively stirred using a propeller stirrer 5. After the end of the experiment, the insoluble residue was filtered, washed repeatedly with water until complete visual clarification. The washed residue was dried at a temperature of 90-95°C in air to a constant mass.

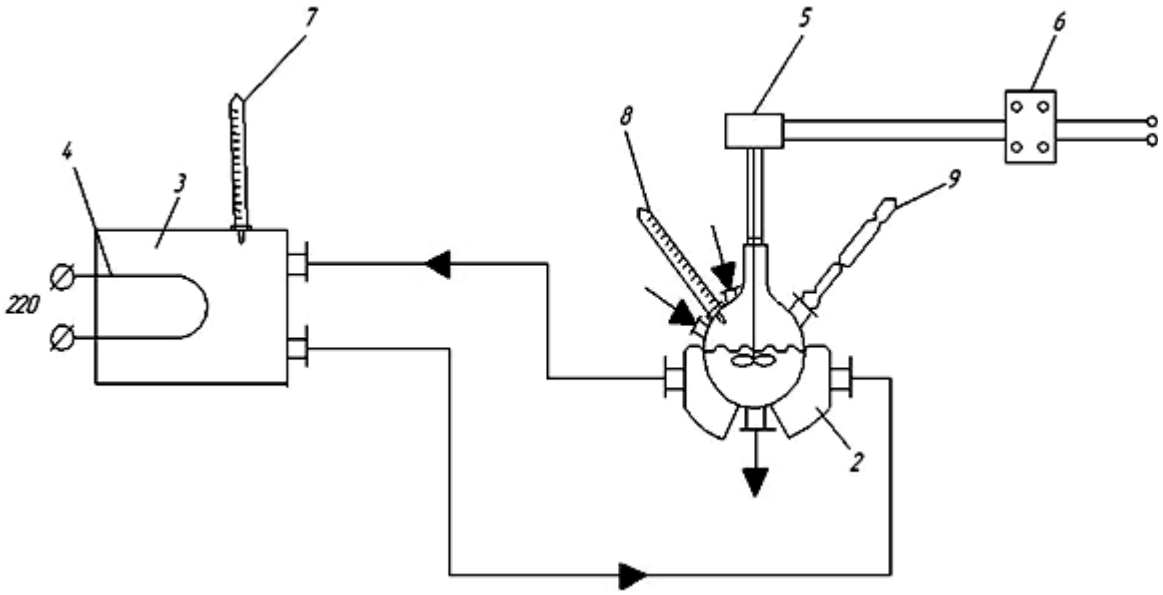

1 – thermostatic reactor; 2 – thermostatic jacket; 3 – tank; 4 – heating element; 5 – stirrer with electric motor; 6 – LATR; 7 – alcohol thermometer; 8 – contact thermometer; 9 – water cooler.

Figure 4.5. Scheme of a laboratory setup for studying the process of removing organic components from RH

Source of the figure: author's development

After that, the degree of lignin extraction from RH was determined according to the following dependence:

$$\alpha = \frac{G_{init} - G_{fin}}{G_{init}} \cdot 100\%, \quad (4.23)$$

where α – degree of extraction, % wt.

G_{init} – initial mass of the test sample, g;

G_{fin} – final mass of the sample after extraction, g.

The initial RH is covered with a protective film, the structure of which includes silicon (IV) oxide. This film prevents the penetration of the extractant into the organic component of the RH. To improve the extraction conditions, the RH was crushed according to the method described earlier and in works [19,27,52].

The study of the influence of the nature of the organic solvent on the degree of lignin extraction was carried out using the following solvents: pure dimethylformamide and dimethylformamide with the addition of hydrochloric acid, pure ethyl alcohol and

with the addition of hydrochloric acid, ethyl alcohol with the addition of acetic and sulfuric acids. The results obtained are graphically depicted in Fig. 4.6.

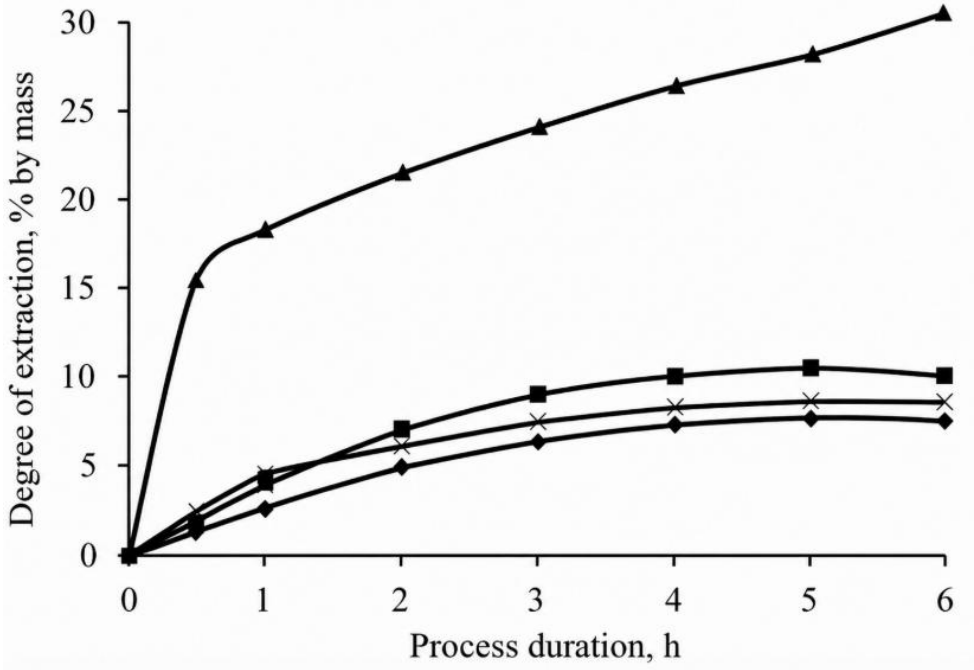

♦ – pure dimethylformamide; x – pure ethyl alcohol; ■ – dimethylformamide with the addition of hydrochloric acid (1.5% by weight); ▲ – ethyl alcohol with the addition of hydrochloric acid (1.5% by weight).

Figure 4.6. Dependence of the degree of lignin extraction from RH on the duration of the process for different organic solvents

Source of the figure: author's development

Fig. 4.6 shows the dependence of the degree of lignin extraction from RH on the duration of the process for the specified solvents. As can be seen from the figure, the process of lignin extraction from RH in pure dimethylformamide and dimethylformamide with the addition of hydrochloric acid is not very intensive - the degree of extraction is achieved 10 wt. %, which is significantly less than in ethyl alcohol with the addition of hydrochloric acid (the degree of extraction is 31 wt. %). In addition, the use of dimethylformamide is impractical because it has a high cost compared to ethyl alcohol.

From literature sources [19,27,52] it is known that lignin is well extracted by alcohols in the presence of mineral acid additives. When lignin is extracted from RH with ethyl alcohol, ethanolic lignin is obtained.

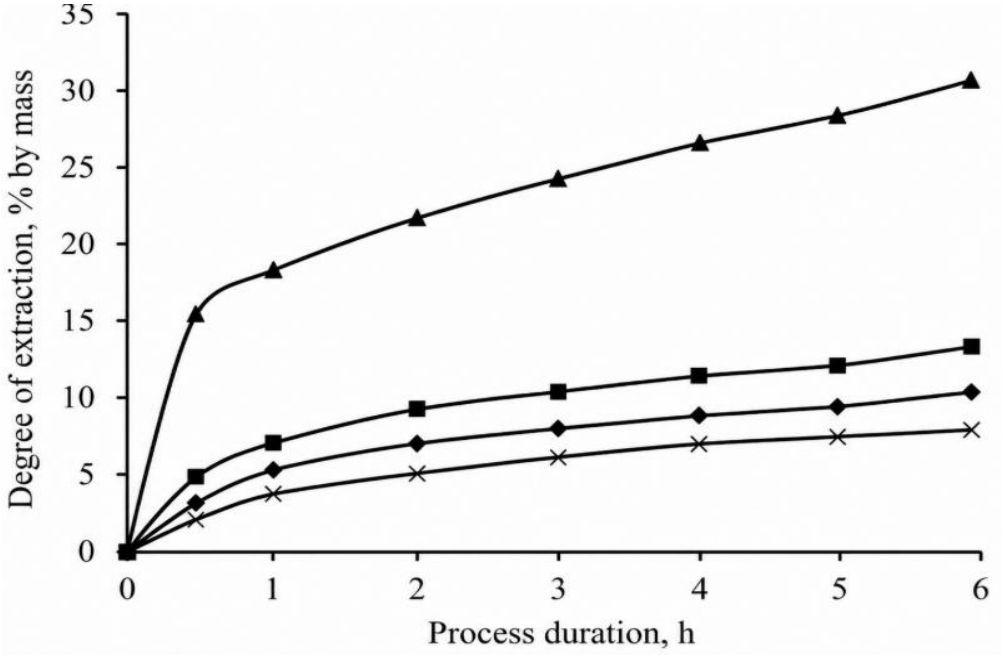

▲ – ethyl alcohol with the addition of hydrochloric acid (1.5%wt.);

■ – ethyl alcohol with the addition of sulfuric acid (1.5%wt.);

♦ – ethyl alcohol with the addition of acetic acid (1.5%wt.);

x – pure ethyl alcohol.

Figure 4.7. Dependence of the degree of lignin extraction from RH on the duration of the process for pure ethyl alcohol and with the addition of various acids

Source of the figure: author's development

Fig. 4.7 shows the dependence of the degree of lignin extraction from RH on the duration of the process for pure ethyl alcohol and with the addition of various acids. Studies of the degree of lignin extraction showed that when using pure ethyl alcohol, the degree of extraction does not exceed 9% by weight. When adding various solvents in the form of acids, an increase in the degree of lignin extraction is observed. This occurs due to the rupture of ligno-hydrocarbon bonds and allows to increase the degree of lignin extraction to 31% by weight when adding 1.5% by weight of hydrochloric acid to ethyl alcohol. When carrying out the extraction process with the addition of

sulfuric and acetic acid, a slight increase in the degree of lignin extraction was observed when adding sulfuric acid within the limits of up to 13.1 wt %, and acetic acid up to 13.1 wt %. In further studying the lignin extraction process, we will use ethyl alcohol with the addition of hydrochloric acid as the extractant.

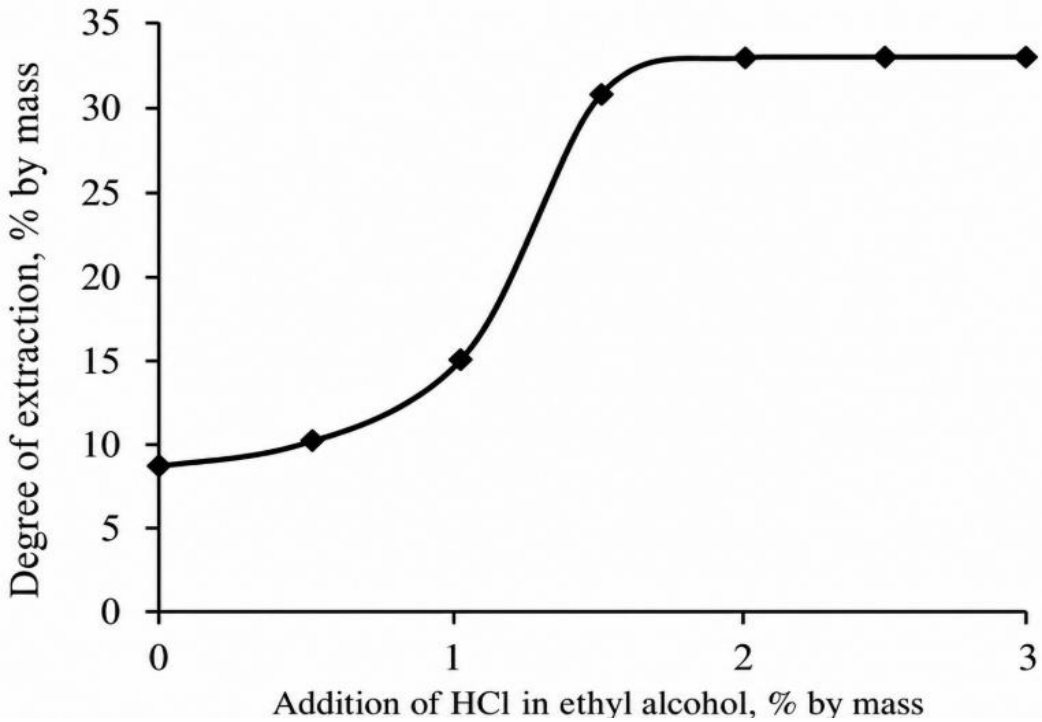

Figure 4.8. Dependence of the degree of lignin extraction from RH on the concentration of hydrochloric acid in ethyl alcohol at τ = 6 hours, temperature 80 °C

Source of the figure: author's development

Fig. 4.8 shows the dependence of the degree of lignin extraction from RH on the concentration of hydrochloric acid in ethyl alcohol at τ = 6 hours, temperature 80 °C.

Experimental studies have shown that when using pure ethyl alcohol, the degree of lignin extraction does not exceed 9 wt. % (Fig. 4.8) The introduction of a small amount of hydrochloric acid into the extractant composition contributed to the rupture of lignohydrocarbon bonds and allowed to increase the degree of lignin extraction. As can be seen from Fig. 4.8, with an increase in the concentration of hydrochloric acid in ethyl alcohol, the degree of lignin extraction increases.

The process of lignin extraction is intensified by adding 1-1.5 wt. % of hydrochloric acid to ethyl alcohol (α = 31%). In the range of hydrochloric acid

concentration of 2-3.5 wt. % (α = 33%), the increase in the degree of lignin extraction is very slow. The highest intensity of lignin extraction was observed when hydrochloric acid was added in the range of up to 3 wt %.

Thus, it can be concluded that the optimal content of hydrochloric acid in ethyl alcohol should be maintained within 1-2 wt %, since a further increase in the concentration of hydrochloric acid had practically no effect on the degree of lignin extraction from RH [19,27,52].

A study of the influence of the dispersion of pre-crushed RH on the rate of lignin extraction in an alcohol-acid extractant showed (Fig. 4.7) that the process speed increases with a decrease in the average particle size. When processing particles with an average size of 40 μm, the maximum speed value was observed 20 minutes after the start of the process. Then the extraction speed decreased exponentially. This is explained by the fact that in the initial period the extraction proceeds from the surface layer of the particles. With a decrease in the lignin content in the surface layers, the extraction speed decreases. The limiting stage of the process is the rate of diffusion of the extractant and reaction products inside the RH particles.

When using RH particles with an average size of 150 μm, the peak of the maximum speed is reached 30 minutes after the start of the process, and its value is 10–15% lower compared to the 40 μm fraction. But after 2.5 hours, the extraction speed values from both fractions are equalized. Under conditions when the process lasts 5–6 hours, almost the same degree of extraction is achieved. Therefore, in the following experiments, crushed RH in the range of average particle sizes of 40-150 μm was used.

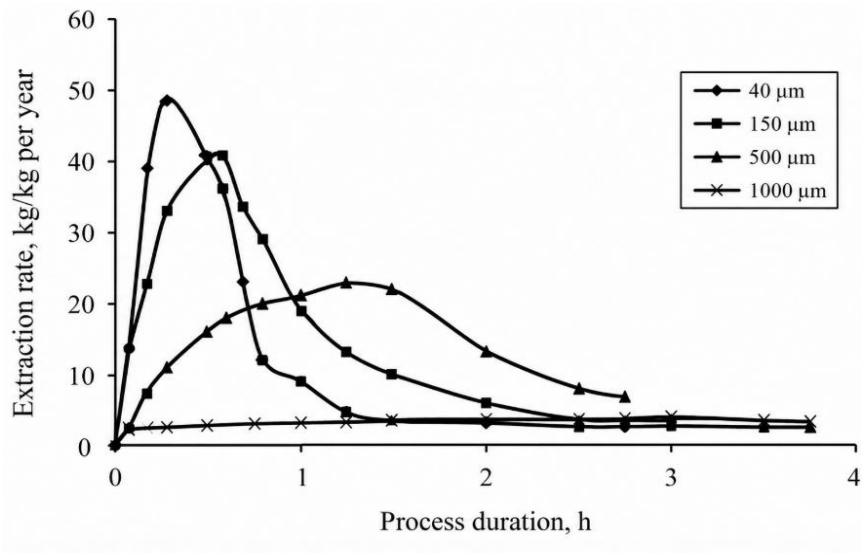

Figure 4.9. Effect of particle size of crushed RH on the rate of lignin extraction in an alcohol-acid solution

Source of the figure: author's development

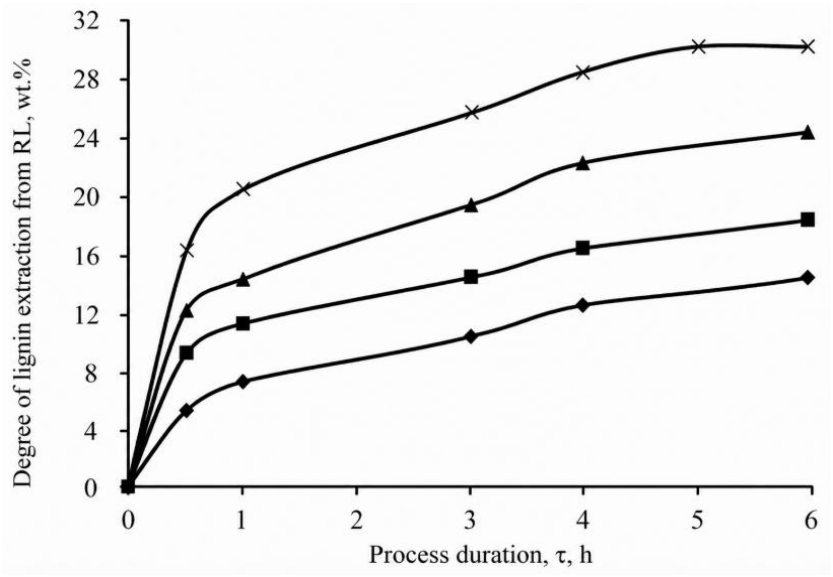

♦ -20°C; ■ – 40°C;▲ – 60°C; x – 80°C

Figure 4.10. Dependence of the degree of lignin extraction on temperature and process duration

Source of the figure: author's development

Fig. 4.10 shows the results of the study of the influence of temperature and duration of the process on the degree of lignin extraction from RH.

The maximum degree of lignin extraction from RH is achieved when the process duration is 6 hours and is 31% by weight. The temperature of 80 °C corresponds to the boiling point of an alcohol-acid mixture at atmospheric pressure. Increasing the duration of the process is impractical in terms of achieving a practically equilibrium state.

An increase in the temperature of the lignin extraction process from 20 to 80°C causes, respectively, an increase in the degree of lignin removal from 14 to 30% by weight, which corresponds to 43-87% by weight of the total amount of lignin in RH.

4.2.2 Cellulose extraction process

Cellulose, as the main component of wood cell walls, determines its structure and properties [50,52]. Cellulose is a significant component of RH in significant quantities of 34-42% [50]. Chemical processing of cellulose allows it to be converted into a soluble state and to obtain substances with new properties from it [50,52].

For cellulose, as a high-molecular compound, four types of reactions can be distinguished: 1) destruction; 2) redistribution of functional groups; 3) crosslinking of chains; 4) intramolecular rearrangements.

During destruction reactions, glycosidic bonds in cellulose chain macromolecules are broken with a decrease in its degree of polymerization, and in some cases, hydrocarbon bonds are broken. Destruction can occur under physical influence and under the influence of chemical agents.

Cellulose as a heterochain polymer with acetal bonds is particularly susceptible to oxidative destruction. Hydrolysis is a destruction under the action of water and aqueous solutions of acids, alkalis and salts, which is accompanied by the addition of water at the site of bond breakage. Acetal bonds in heterochain polymers are most sensitive to hydrolysis. Glucosidic bonds of cellulose and its derivatives are easily hydrolyzed. The reaction of hydrolytic destruction of cellulose is the basis of industrial hydrolysis of wood. Destruction of cellulose under the action of organic acids is possible - acidolysis.

Reactions of rearrangement of functional groups of cellulose have important practical application. As a result of such transformations, which occur with the participation of alcohol hydroxyl groups, new artificial polymers with valuable properties are obtained - various complex and ethers of cellulose.

Cellulose derivatives can be divided into three main classes: molecular (additive) compounds, substitution products and oxidation products. It should be noted that the mechanism of the above-mentioned cellulose reactions has not been fully studied, and therefore it has not been clarified which compounds the resulting products are - additive compounds or substitution products.

Substitution products are formed during a chemical reaction between cellulose hydroxyls and reagents with the replacement of hydrogen by the corresponding groups, for example -NO_2, -$COCH_3$, -C_2H_5 and others. These groups are bound to the hydroxyl oxygen by a covalent bond. Substitution products include cellulose esters and ethers, which are of great industrial importance.

As a result of oxidation, cellulose is destroyed with the formation of reaction products of variable composition. Cellulose, which is oxidized by NO_2, is used in the textile industry, in medicine, as a hemostatic agent [50, 52] and is a high-molecular organic compound of the polysaccharide type, the molecules of which are built from β-D-glucopyranose units connected by a 1-4 glycosidic bond. The empirical formula of cellulose is $(C_6H_{10}O_5)n$ or $(C_6H_7O_2(OH)_3)_n$. Its structural formula is presented in Fig. 4.11.

Cellulose includes the following chemical bonds and groups: simple C-C-; C-H-; C-C-; C-O-C- and CH_2OH group.

The structure of the cellulose molecule was established using chemical and physicochemical research methods [50,52]. As a result, it was found that the elementary link in the cellulose chain macromolecule is the β-D-glucose residue $C_6H_{10}O_5$.

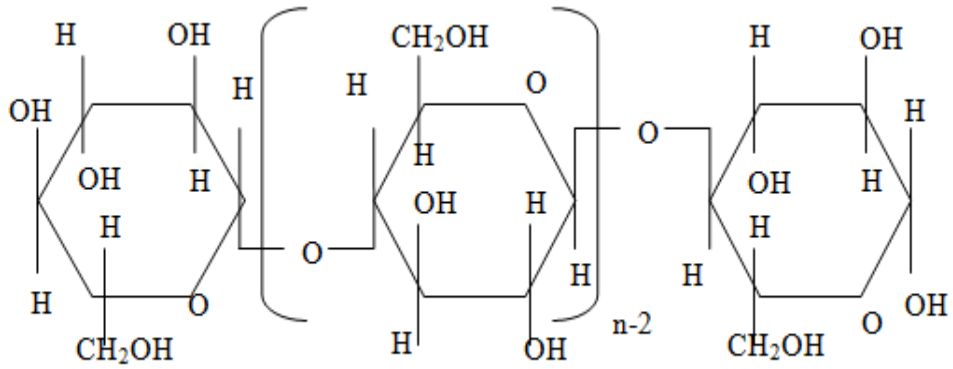

Figure 4.11. Structural formula of cellulose

Source of the figure: [52]

With complete hydrolysis of cellulose, the yield of D-glucose is 96-98% of the theoretical:

$$(C_6H_{10}O_5)_n + nH_2O = nC_6H_{12}O_6 \quad (4.24)$$

The study of the process of cellulose extraction from RH was carried out on a laboratory setup, which is presented in Fig. 4.5 using the same method. The difference was that an aqueous solution of sulfuric acid (concentrations of 5, 10, 15 wt.%) was used as the extractant [27]. The process temperature varied within 20-100°C. The duration of the process was controlled for 6 hours. The fraction of crushed RH with average particle sizes from 40 to 150 μm was processed. When cellulose is treated with concentrated acids, the formation of a jelly-like precipitate is observed, which is difficult to separate from the undissolved fraction of RH. Therefore, dilute hydrogen sulfuric acid solutions were used in the studies.

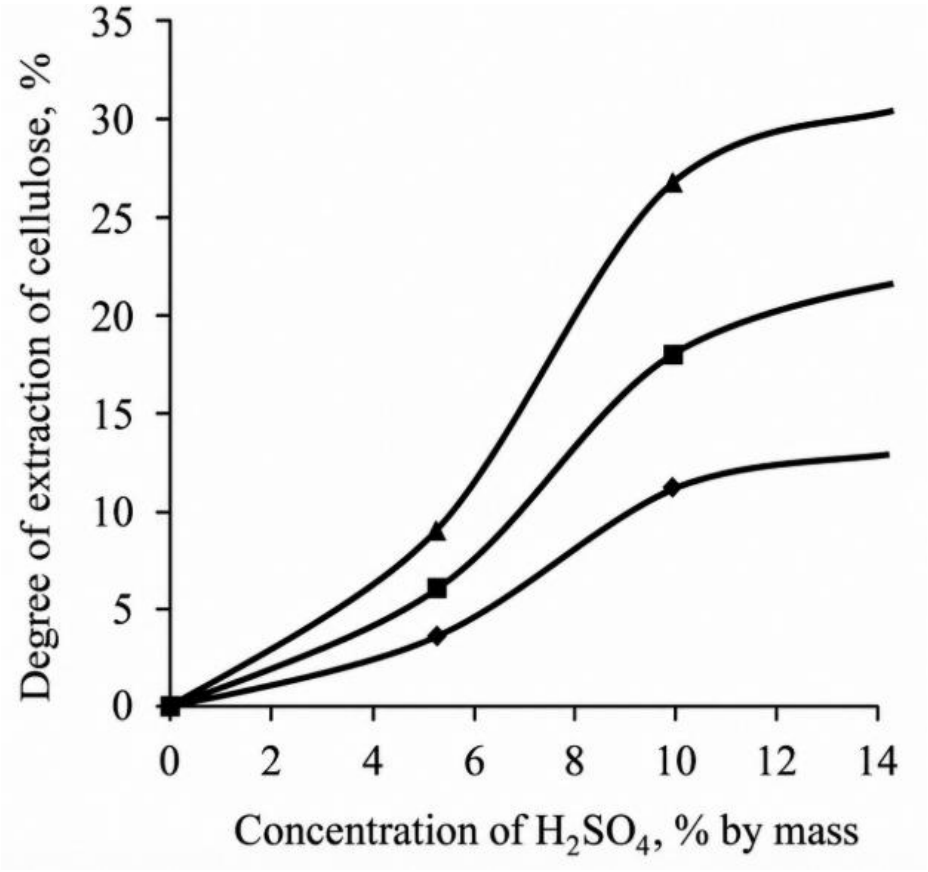

♦ – 20°C; ■ – 40°C; ▲ – 100°C.

Figure 4.12. Dependence of the degree of extraction from RH on the concentration of H_2SO_4 at different process temperatures, τ = 6 h

Source of the figure: author's development

Fig. 4.12 shows the dependence of the degree of cellulose extraction from RH on the concentration of an aqueous solution of sulfuric acid at different process temperatures. Fig. 4.13 presents the experimental dependences of the degree of cellulose extraction from RH with an aqueous solution of 15 wt. % sulfuric acid at different process temperatures. With an increase in the concentration of sulfuric acid, an increase in the degree of cellulose extraction is observed. The maximum value of the degree of cellulose extraction from RH (α = 30-32 wt. %, and in terms of the total amount of cellulose 73-75 wt. %) is achieved when treating the raw material with sulfuric acid with a concentration of 15 wt. % for 6 hours.

It was established that simultaneously with the extraction of cellulose, the removal of metal oxides from RH is observed.

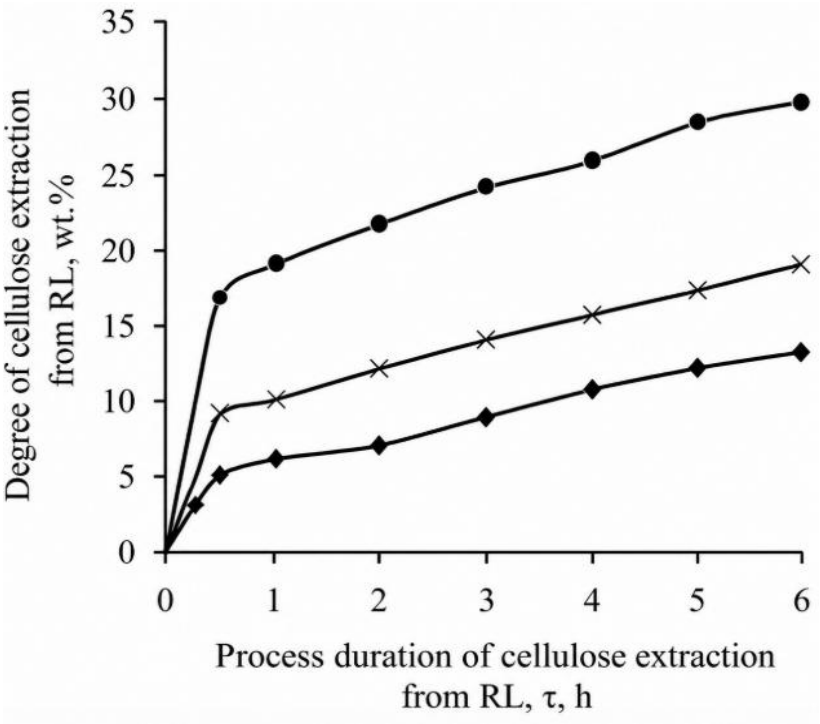

♦ –20°C; x – 40°C; ● – 100°C

Figure 4.13. Dependence of the degree of cellulose extraction on temperature with 15% H_2SO_4 solution at different process temperatures

Source of the figure: author's development

The results obtained gave reason to believe that for a more complete removal of components containing carbon, it is necessary to treat the solid residue after lignin extraction with an acid extractant (a two-stage process).

4.2.3 Study of the cellulose extraction process after preliminary lignin removal (double treatment)

In order to achieve a deeper additional removal of organic components from RH, the process of cellulose extraction from the intermediate raw material obtained after removing part of the lignin from it, i.e. a two-stage extraction process, was studied [27].

The raw material residue obtained after lignin extraction from it was subjected to repeated treatment with an aqueous-acid extractant in a laboratory setup, which is

presented in Fig. 4.5. The experimental conditions are similar to the process described in subsection 4.2.1.

Figures 4.14 and 4.15 show the results of the study of the cellulose extraction process after lignin removal (two-stage extraction). The maximum degree of cellulose extraction from the solid residue after lignin removal (α = 57 wt.%) corresponds to the condition in which the extractant is an aqueous solution of 15 wt.% sulfuric acid at a temperature of 100°C after 6 hours of raw material processing.

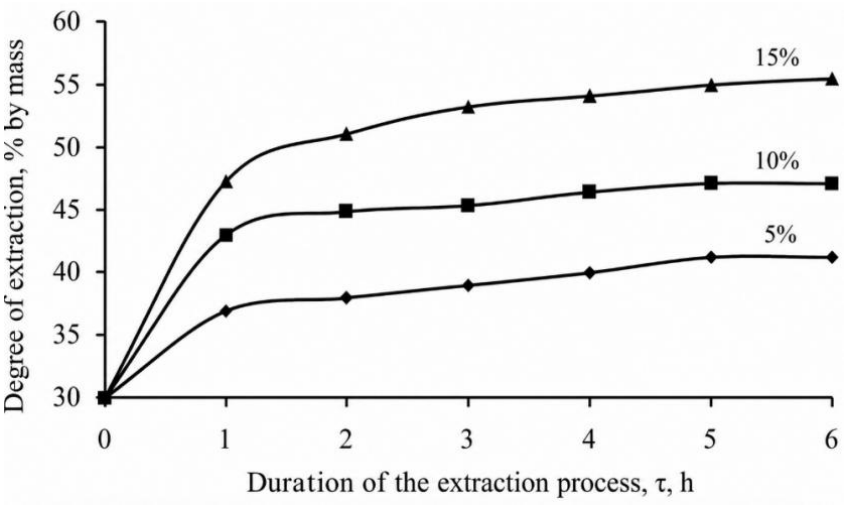

Figure 4.14. Dependence of the degree of cellulose extraction after lignin extraction on the concentration of sulfuric acid and the duration of the process at a temperature of 100°C

Source of the figure: author's development

Thus, effective extractants and characteristics of the extraction processes of organic components of RH (lignin and cellulose) were established, which allowed to ensure the removal of almost 30% by weight of lignin and the same amount of cellulose. With double processing, the total degree of extraction of organic carbon-containing compounds reaches 57% by weight, which is 84-87% by weight of the total amount of carbon-containing compounds.

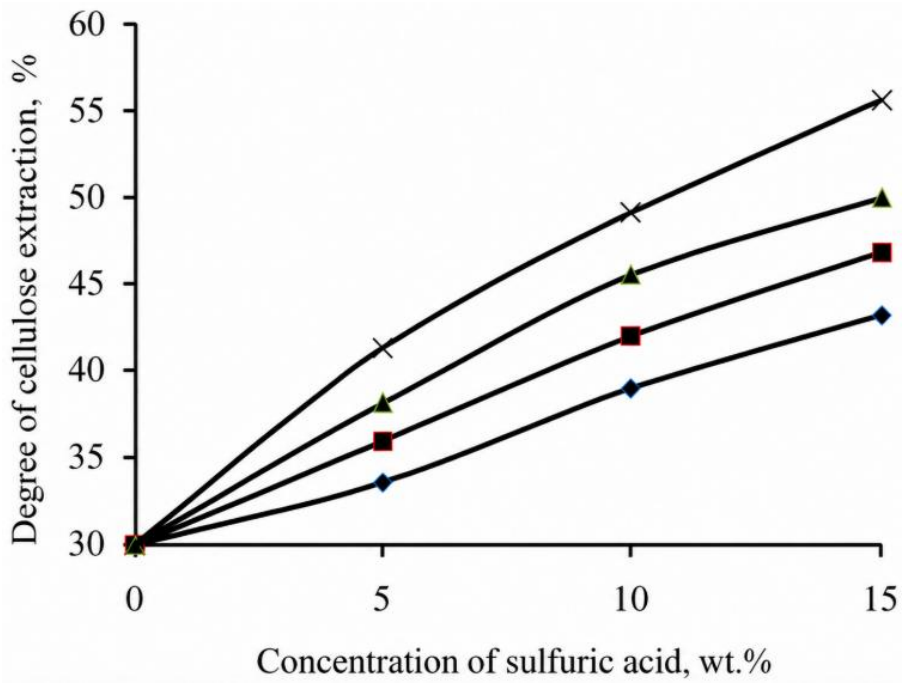

♦ – 20°C; ■ – 40°C; ▲ – 60°C; x – 100°C

Figure 4.15. Dependence of the degree of cellulose extraction on the concentration of the aqueous solution of H_2SO_4 and temperature with a process duration of 6 hours

Source of the figure: author's development

When processing RH with an aqueous-acid solution, undesirable impurities of metal oxides are simultaneously removed from the raw material.

4.2.4 Assessment of the accuracy of the accepted hypothesis about the mechanism of the studied processes of extraction of carbon-containing compounds

The assessment of the accuracy of the accepted hypothesis about the mechanism of the studied processes of extraction of lignin and cellulose was carried out on the basis of experimental data on the degree of extraction of lignin and cellulose from RH [19,27,50-52].

In Table 4.1 presents experimental data on the degree of lignin extraction from RH depending on the concentration of hydrochloric acid in ethyl alcohol, temperature and duration of the process.

Table 4.1

Experimental data on the degree of lignin extraction from RH

Concentration of hydrochloric acid, wt. %	The degree of lignin extraction from RH, α			
	20°C	40°C	60°C	80°C
Process duration 4 hours				
0	1,9	3,9	6,4	8,2
0,5	2,5	4,6	7,5	9,6
1	4,6	7,5	11	13,9
1,5	12,1	16	18,9	26,6
2	12,8	17	20,3	28,3
2,5	12,9	17,1	20,5	28,8
Process duration 6 hours				
0	2,1	5,3	7,5	8,5
0,5	2,6	5,9	8,2	10
1	5,8	8,5	12,5	15
1,5	14	18	22,6	31
2	14,7	21	25,4	33
2,5	14,7	21,2	25,6	33

Experimental data on the degree of cellulose extraction from RH depending on the concentration of sulfuric acid, temperature and duration of the process are given in Table 4.2.

Table 4.2.

Experimental data on the degree of cellulose extraction from RH

Concentration of aqueous sulfuric acid solution, wt.%	The degree of cellulose extraction from RH,α			
	20°C	40°C	60°C	100°C
Process duration 4 hours				
0	0	0	0	0
5	2	3,4	5,9	7,8
10	7,3	10,2	17,2	22
15	11,5	15,3	22	25,7
Process duration 6 hours				
0	0	0	0	0
5	2,5	3,8	6,4	8
10	10	15,2	21,1	26
15	14,2	18,9	25,2	29,9

In accordance with the hypothesis about the mechanism of the process of extraction of carbon-containing components from RH, the values of the parameters a, b, c of equation (4.20) were found according to the experimental results. These values for the processes of extraction of lignin and cellulose are presented in Tables 4.3 and 4.4, respectively.

Table 4.3.

Parameters of equation (4.20) for the lignin extraction process

Regime		Equation coefficients (4.20)		
t,^{0}C	τ, h	a	b	c
1	2	3	4	5
20	4	10,9707	51,7183	2,8635
	6	12,6000	38,43917	2,657247
40	4	13,1648	36,4083	2,6309
	6	15,8152	36,344	2,218453

Continuation of Table 4.3.

1	2	3	4	5
60	4	14,0248	19,224	2,24012
	6	17,9552	25,344	2,208191
80	4	20,3803	29,2457	2,4616
	6	24,5653	38,43917	2,657247

Table 4.4

Parameters of equation (4.20) for the cellulose extraction process

Regime		Equation coefficients (4.20)		
t,^{0}C	τ,ч	a	b	c
20	4	11,684	9,549091	0,690646
	6	14,28	10,22	0,797
40	4	15,6264	6,74975	0,635435
	6	18,952	9,544	0,908
60	4	22,176	5,5764	0,73607
	6	25,376	6,758	0,867
100	4	25,76853	5,225581	0,84892
	6	29,832	6,317073	0,933575

As an assessment of the accuracy of equation (4.20) when using the values of a, b, c, the values of the residual standard deviation are given in the last columns of Table 4.3 and Table 4.4.

Fig. 4.16 and Fig. 4.17 show curves showing the dependence of the degree of lignin and cellulose extraction on temperature and on the concentration, respectively, of hydrochloric acid in ethyl alcohol and sulfuric acid.

The closeness of the calculated (solid lines) and experimental (points) values indicates the adequacy of the model (4.20) and, as a consequence, the validity of the hypothesis about the mechanism of the process being developed.

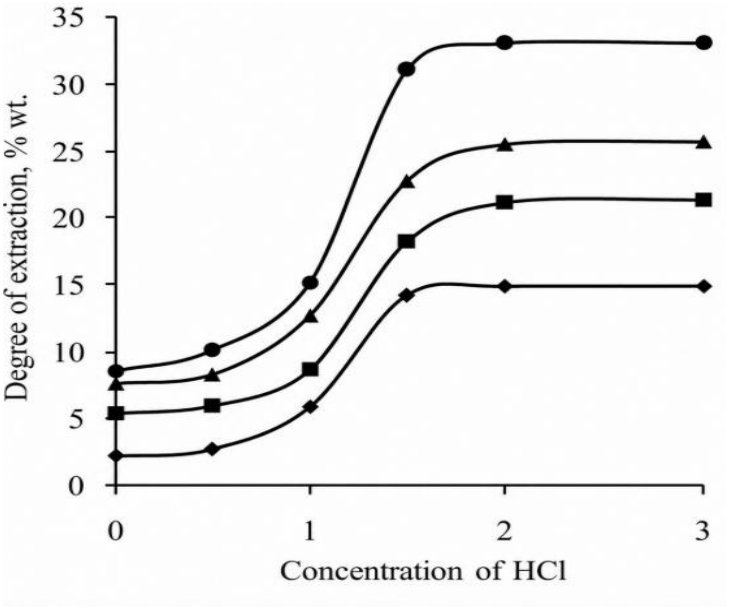

♦ – 20°C; ■ – 40°C; ▲ – 60°C; ● – 80°C.

Figure 4.16. Dependence of the degree of lignin extraction from RH on temperature and concentration of hydrochloric acid in ethyl alcohol at τ= 6 hours

Source of the figure: author's development

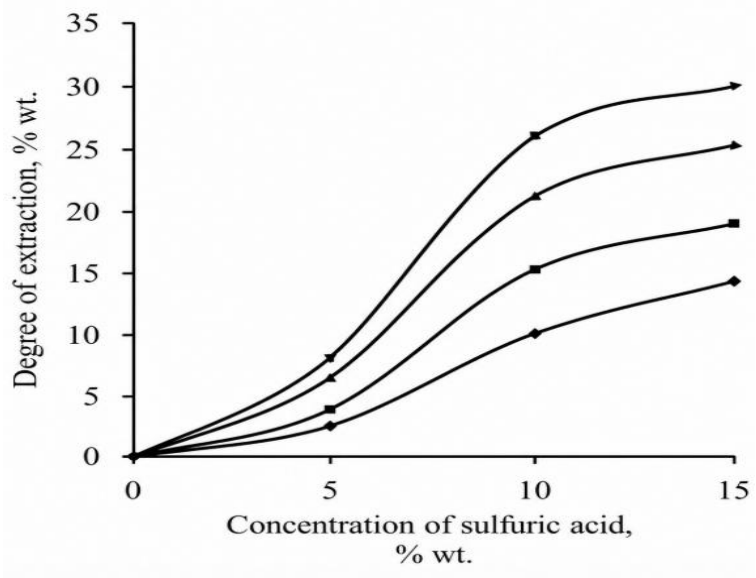

♦– 20°C; ■ – 40°C; ▲ – 60°C; ● – 100°C.

Figure 4.17. Dependence of the degree of cellulose extraction from RH on temperature and sulfuric acid concentration at τ= 6 hours

Source of the figure: author's development

Fig. 4.18 and Fig. 4.19 show data indicating the dependence of the coefficient a on temperature and process duration. This leads to the conclusion that the main role is assigned to temperature, the effect of changing which is 3-5 times greater than the effect of the process duration. At the same time, we conclude that additional experimental studies are necessary to describe the dependencies presented in Fig. 4.18 and Fig. 4.19.

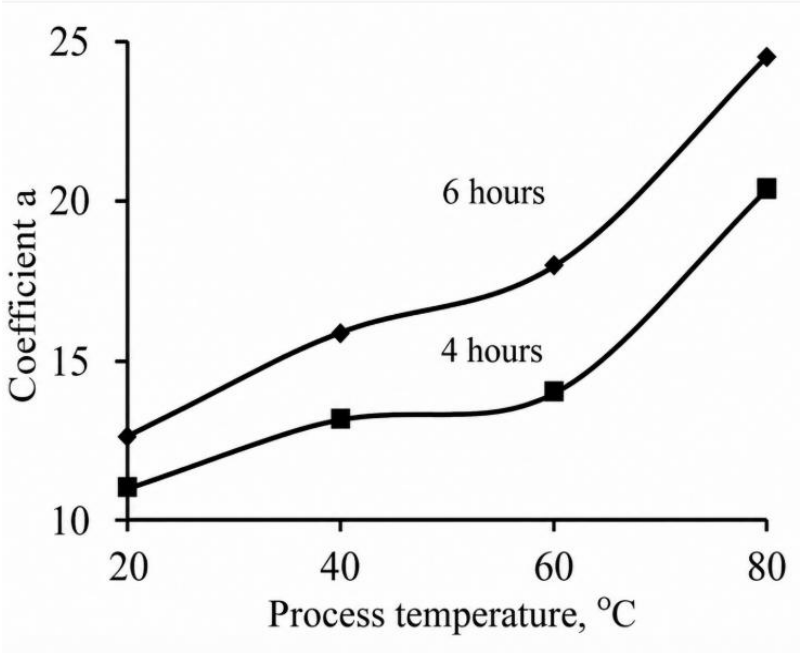

Figure 4.18. Dependences of the coefficient a on the temperature and duration of the process of lignin extraction from RH

Source of the figure: author's development

Experimental data on the total degree of lignin and cellulose extraction at different temperatures and process durations are given in Table 4.5.

The results obtained served as the basis for implementing the processes of lignin and cellulose extraction as successive stages of one process, which allowed increasing the degree of extraction to 57% (see Fig. 4.20).

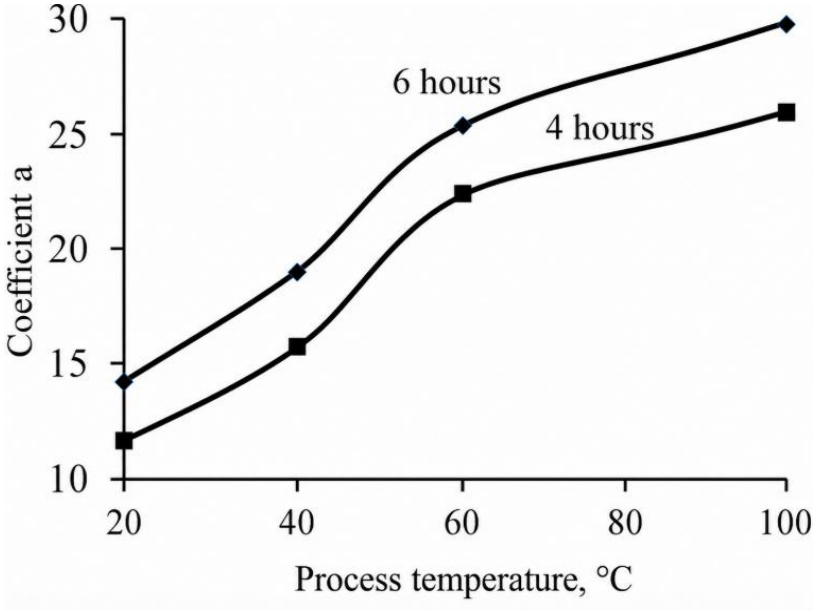

Figure 4.19. Dependences of the coefficient a on the temperature and duration of the cellulose extraction process from RH

Source of the figure: author's development

Table 4.5.

Experimental data on the degree of lignin and cellulose extraction (two-stage process)

Concentration of aqueous sulfuric acid solution, wt.%	The degree of lignin and cellulose extraction from RH,α			
	20°C	40°C	60°C	100°C
Process duration 4 hours				
0	30	30	30	30
5	32	34,3	35,5	40
10	36,4	39,1	42,1	48,1
15	41,4	44,5	47,8	54
Process duration 6 hours				
0	30	30	30	30
5	33,6	35,9	38,1	41,3
10	39	42	45,5	49,1
15	43,2	46,8	49,9	55,4

Based on the hypothesis that amorphous silicon (IV) oxide is practically not extracted from the carbon-containing components of the RH in the extract, we conclude that the content of silicon (IV) oxide in the solid residue as a result of the two-stage process increases almost to 42.71 wt.%.

When comparing the ash content of the initial RH and its solid residue after extraction, we see that a significant contribution to the increase in the content of silicon (IV) oxide (7.13% wt.) is achieved due to the selective extraction of all, except silicon (IV) oxide, components of the mineral part of the RH substance. This suggests that the mentioned components are distributed in lignin and cellulose, while silicon (IV) oxide is associated with more condensed structures containing carbon, which do not pass into the liquid state under the studied conditions.

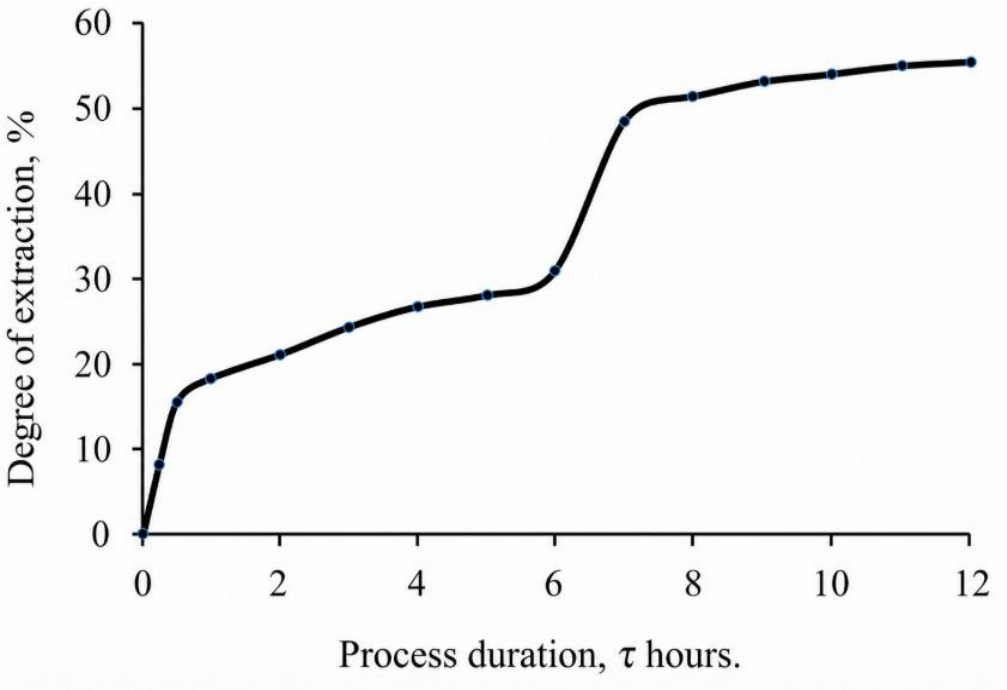

Figure 4.20. Dependence of the degree of lignin and cellulose extraction (two-stage process) on the duration of the process.

Source of the figure: author's development

In this regard, to obtain silicon (IV) oxide of high purity, the process includes a stage of burning the solid residue of the two-stage extraction of RH.

5. THERMAL DECOMPOSITION OF SOLID RESIDUES FOLLOWING EXTRACTION FOR THE PREPARATION OF HIGH-PURITY SILICON (IV) OXIDE

The thermodynamic computational-theoretical approach made it possible to establish the fundamental feasibility of producing silicon (IV) oxide from rice husk (RH).

However, the most comprehensive information required for the development of an actual technological process can only be obtained through a combination of thermodynamic, experimental, and kinetic studies [50]. Kinetic analysis makes it possible to determine the regularities governing the progress of chemical processes over time. Thus, quantitative time-dependent characteristics of the technological process can be obtained, and the dependence of changes in the composition of the reacting system on the process conditions can be established. Furthermore, chemical kinetics [50,53,54] enables the identification of the sequence of elementary reaction steps, thereby providing insight into the reaction mechanism.

In addition, knowledge of the spatial and temporal characteristics of the technological process makes it possible to determine the required dimensions of process equipment as well as the process duration. Therefore, chemical kinetics provides a basis for controlling and intensifying the process. Consequently, when designing a technological process, it is essential to consider the interaction between the thermodynamic equilibrium analysis of the system and its kinetic analysis.

5.1. Methodology for Determining the Kinetic Parameters of the Thermal Decomposition Process of Solid Residues after Extraction

The kinetics of thermal decomposition were investigated using the thermogravimetric analysis (TGA) method [55]. This technique makes it possible to continuously and accurately monitor the mass of a sample, thereby enabling the reaction mechanism to be inferred and the kinetic parameters to be determined under

laboratory conditions that simulate industrial processes. Such processes can be studied by thermogravimetric analysis under both isothermal [55] and non-isothermal [25] conditions.

In the present study, the non-isothermal approach was selected because it allows the application of a comprehensive methodology based on the simultaneous analysis of mass-loss (TG), differential mass-loss (DTG), and differential thermal analysis (DTA) curves obtained under a continuously increasing temperature.

Another advantage of this method is that it enables the entire temperature range of interest to be investigated within a single experiment or a limited number of experiments.

The thermal decomposition of rice husk (RH) belongs to the class of topochemical reactions [55] and can be described by the following general chemical equation:

$$A(\text{тв}) \rightarrow B(\text{тв}) + C\ (\text{газ}) \quad (5.1)$$

According to the Arrhenius law, the reaction rate and the temperature dependence of the rate constant can be expressed as follows [55]:

$$\frac{d\alpha}{d\tau} = -k \cdot \alpha^n \quad (5.2)$$

$$k_i = k_{0\,i}\, exp\left(-\frac{E_i}{RT_i}\right) \quad (5.3)$$

where **α** is the fraction of solid substance **A** remaining undecomposed at time **τ**, which is determined according to the following equation:

$$\alpha = \frac{W_{in} - W_\tau}{W_{in} - W_f} \quad (5.4)$$

where W0 is the initial mass of the sample, g;

W_{in} is the current mass of the sample at a given temperature, g;

W_f is the final mass of the sample, g;

ki is the reaction rate constant, s^{-1};

k0i is the pre-exponential factor, s^{-1};

Ei is the activation energy of the reaction, J/mol;

R is the universal gas constant, R=8.310 J/(mol·K);

Ti is the variable temperature, K.

Solving equations (5.2) and (5.3) together, we obtain:

$$\frac{d\alpha}{\alpha^n} = \frac{k_0}{g} exp\left(\frac{E}{RT}\right) d\tau \quad (5.5)$$

Let us determine the linear heating rate of the substance we are investigating: $g = \frac{dT}{d\tau}$

Then, for n = 1, equation (5.5) after some other transformations has the form:

$$\ell n\alpha = -\int_0^T \frac{k_0}{g} exp\left(-\frac{E}{RT}\right) d\tau \quad (5.6)$$

Since the thermal decomposition reaction takes place in a narrow temperature range, we choose the so-called temperature Ts (reference temperature) at which the rate of change in the mass of the sample is maximum:

$$\alpha_s = \frac{W_{in} - W_\tau}{W_{in} - W_f} \quad (5.7)$$

where α_s is the concentration at which the mass change curve breaks and determines the order of the reaction, according to the formula:

$$\alpha_s = n^{\frac{1}{1-n}} \quad (5.8)$$

The order of reaction in the calculations was taken equal to unity.

Instead of the variable T, the variable θ is introduced, which is determined by the formula: θ= T – Ts.

Using the approximate expression $\frac{1}{T} \approx \frac{\left(1-\frac{\theta}{Ts}\right)}{Ts}$, we integrate equation (5.6) and obtain:

$$\ell n\alpha = -\frac{k_0}{g} \cdot \frac{RT_s^2}{E} exp\left[-\frac{E}{RT_s}(1 - \frac{\theta}{T_s})\right] \quad (5.9)$$

Under the condition that θ = 0, and α = αs, then equation (5.9) has the form:

$$1 = \frac{k_0}{g} \cdot \frac{RTs^2}{E} \cdot exp\left(-\frac{E}{RTs}\right) \quad (5.10)$$

Substitute expression (5.10) into equation (5.9) and obtain:

$$W^* = \ell n \frac{W_o - W_f}{W_o - W_\tau} = \frac{E \cdot \theta}{RTs^2} \quad (5.11)$$

To construct the dependence $W^* = f(\theta)$, we divide the DTG curve on the derivative graph into n equal parts with parallel lines. The intersection points of these

parallel lines with the thermogravimetric curve allow us to determine the mass of the sample at a given time. The value of Ts is determined by the extremum point on the DTG curve.

From the angle of inclination of the linear dependence $W^* = \ell n \frac{W_o - W_f}{W_o - W_\tau}$ on θ, it is possible to determine the value of the activation energy of the thermal decomposition reaction of a substance:

$$E_i = tg\beta \cdot RTs^2 \quad (5.12)$$

where tg β is the tangent of the slope of the line constructed in the coordinates $W^* = f(\theta)$.

Having determined the reference temperature Ts and the activation energy of the reaction, we can determine k_0 – the pre-exponential factor from the equation:

$$k_{0i} = \frac{g \cdot E_i}{RTs^2 \, exp\left(-\frac{E_i}{RTs}\right)}, \quad (5.13)$$

which is obtained by rearranging Equation (5.10).

When modeling the thermal treatment process of rice husk (RH) for the production of silicon(IV) oxide using a computer, the sample temperature at each time instant was calculated according to the following equation [55]:

$$T = T_0 + u\tau, \quad (5.14)$$

where T_0 is the initial temperature of the sample, K;

u is the heating rate of the sample, $K \cdot s^{-1}$;

τ is the heating time of the sample, s.

The concentration of the *Ci* components was expressed in mole fractions and determined for the condensed phases:

$$C_i = \frac{n_i}{\sum_{i=1}^{i=p} n_i}, \quad (5.15)$$

where p is the number of components of the condensed phase;

ni is the number of moles of the i-th component of the condensed phase.

The initial number of moles of the RH was denoted by , and the rate constant of the i-th reaction was denoted by k_i.

Thermogravimetric studies of the thermal decomposition of rice husk (RH) samples were carried out under non-isothermal conditions in a dynamic air atmosphere. The thermograms were recorded using a Paulik F.–Paulik J.–Erdey L. derivatograph over the temperature range of 20-1000°C at a heating rate of 10°C/min (0.17 K/s). The objective of the present study was to model the kinetics of the thermal decomposition of RH samples for the production of silicon (IV) oxide. The kinetics of the thermal decomposition of untreated rice husk for the production of technical-grade silicon (IV) oxide have previously been investigated in Refs [25,50-55].

5.2. Investigation of the Kinetics of the Thermal Decomposition of Solid Residues after Extraction for the Production of Silicon (IV) Oxide

Thermogravimetric analysis (TGA) was employed to investigate the kinetics of the thermal decomposition process [25,51,55]. This method enables the simultaneous analysis of thermogravimetric (TG), derivative thermogravimetric (DTG), and differential thermal analysis (DTA) curves. Combined with other analytical techniques, such as chemical analysis, X-ray diffraction (XRD), and related methods, thermogravimetric analysis makes it possible to determine the chemical transformations occurring during the heating of solid residues after extraction and to calculate the activation energy, (E_i), and the pre-exponential factor, (k_{0i}), of the corresponding reactions.

5.2.1. Investigation of the Kinetics of the Thermal Decomposition of Solid Residues after Lignin Extraction

The sample investigated was the solid residue obtained after lignin extraction using an alcohol-acid extractant [27].

Fig. 5.1 presents the derivatogram of the thermal decomposition of the solid residue after lignin removal in an air atmosphere.

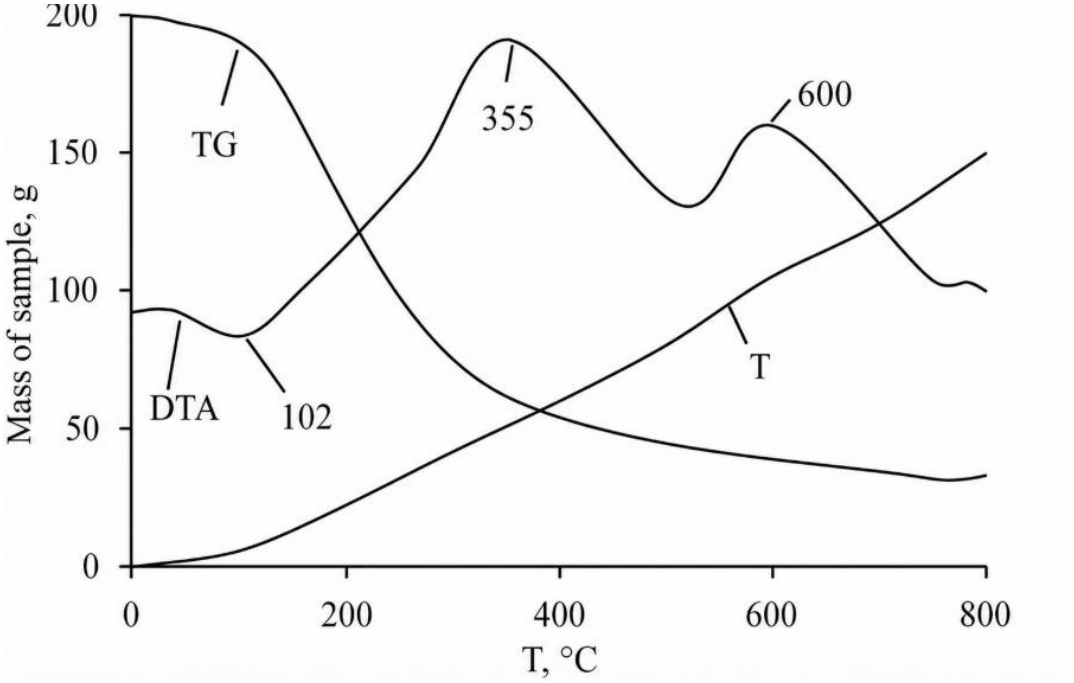

Figure 5.1. Derivatogram of the thermal decomposition of the solid residue after lignin removal in an air atmosphere.

Source of the figure: author's development

As shown in Fig. 5.1, three thermal effects are observed on the thermogram of the sample. The first is an endothermic peak at 102°C, while the two exothermic peaks occur at 355°C and 600°C. To determine the composition of the residue after lignin extraction and the intermediate products formed at the temperature extrema, chemical analysis, Fourier-transform infrared (FTIR) spectroscopy, and X-ray diffraction (XRD) analysis were employed [56].

The principal organic constituents of rice husk (RH) are cellulose and lignin, whose combustion temperatures are approximately 350°C and 500°C, respectively. Therefore, it can be concluded that the exothermic peaks observed on the derivatogram correspond to the combustion of cellulose and the fraction of lignin that remained in the rice husk after the extraction process. Thermal decomposition of the sample was completed at approximately 680°C.

The endothermic effect observed at 750°C is not accompanied by any measurable mass loss of the solid residue after lignin extraction. This phenomenon is attributed to

a structural transformation of SiO_2, namely the transition from the amorphous to the crystalline state [15,16].

To determine the structure of the silicon (IV) oxide samples obtained from the solid residues after lignin extraction, X-ray diffraction (XRD) analysis was performed.

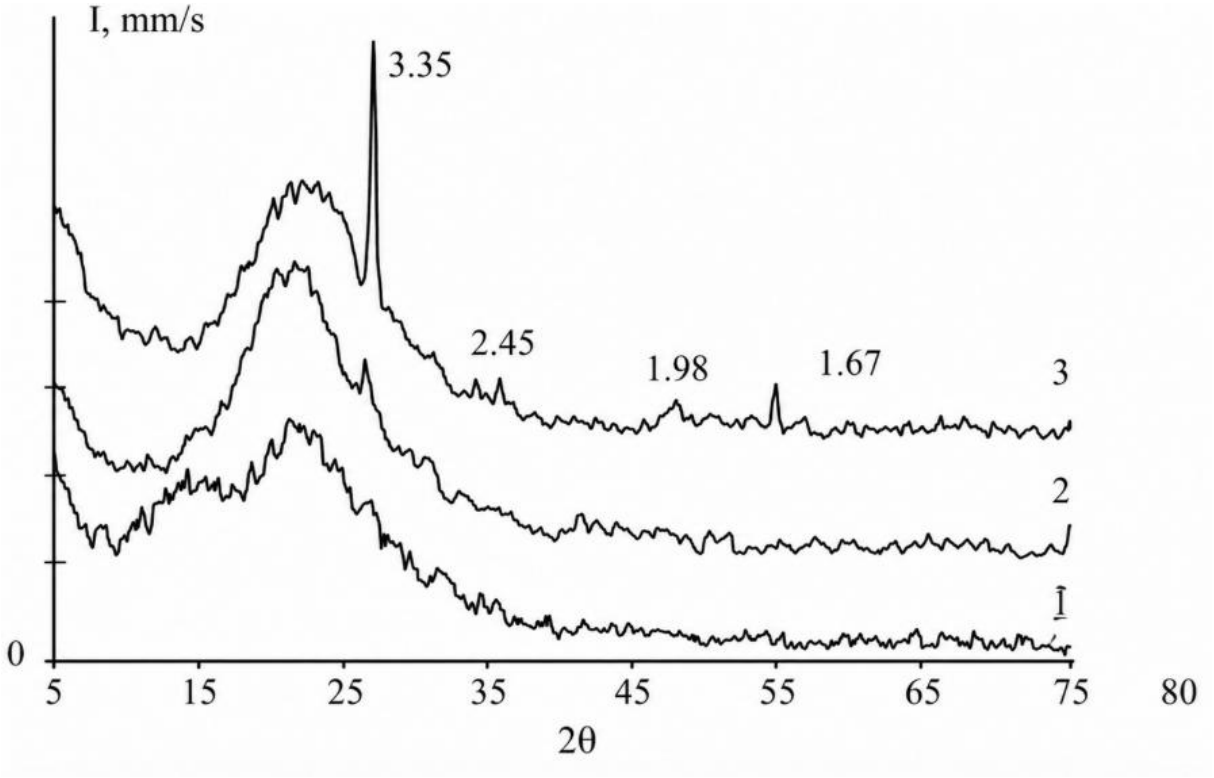

1 – 600°C; 2 – 700°C; 3 – 800°C

Figure 5.2. X-ray diffraction patterns of silicon (IV) oxide samples obtained after thermal treatment.

Source of the figure: author's development

Fig. 5.2 shows the X-ray diffraction patterns of silicon (IV) oxide samples obtained from rice husk (RH) after lignin extraction and subsequent thermal treatment in an air atmosphere at 600, 700, and 800°C.

As can be seen from Figure 5.2, diffraction pattern 3 exhibits characteristic diffraction peaks at d_{HKL} = 3.35, 2.45, 1.98, and 1.67 Å [56]. These values correspond to the interplanar spacings of crystalline silicon (IV) oxide, indicating the presence of a crystalline phase in the sample. Diffraction pattern 2, corresponding to thermal treatment at 700°C, also displays diffraction peaks characteristic of crystalline silicon

(IV) oxide; however, their intensities are considerably lower than those observed in pattern 3. In contrast, diffraction pattern 1, corresponding to the sample thermally treated at 600°C, shows no diffraction peaks associated with crystalline modifications of silicon (IV) oxide. This indicates that the sample is completely X-ray amorphous [15,16].

Thus, to obtain amorphous silicon (IV) oxide, the thermal treatment of the sample should be carried out at temperatures between 600 and 650°C.

The elemental composition of the solid residue after lignin extraction is presented in Table 5.1.

Table 5.1.

Proximate analysis and elemental composition of the rice husk (RH) sample after lignin extraction.

Indicator name	Analysis method	Symbol, unit of measurement	Actual value Initial sample
1	2	3	4
Ash content per dry matter	ISO 1171-97	A^d,%	31,8
Mass fraction of carbon	ISO 625-96	C^d,%	23,52
Mass fraction of hydrogen		H^d,%	4,694
Mass fraction of nitrogen	ISO 333-83	N^d,%	0,28
Mass fraction of oxygen	ISO 1994-76	O^dd,%	39,76

At approximately 102°C, the removal of crystallization water takes place, accompanied by the formation of the intermediate product $C_{196}H_{464}O_{248}N_2 \cdot 53SiO_2$. In the temperature range of 250-530°C, thermo-oxidative decomposition of cellulose occurs, resulting in the formation of the intermediate product $C_{94}H_{248}O_{188} \cdot 53SiO_2$. Subsequently, in the temperature range of 530-730°C, further thermal decomposition of the residual carbon-containing components takes place, leading to the formation of silicon (IV) oxide.

To determine the reaction mechanism, samples were collected at the temperatures corresponding to the extrema of the thermal effects (355 and 600°C). The carbon content was determined in accordance with using an AN7552 carbon analyzer, while the composition of the remaining components was established on the basis of stoichiometric calculations.

Based on the results of the thermogravimetric, chemical, and X-ray diffraction (XRD) analyses, three chemical reactions were proposed to describe the thermal decomposition of the solid residue after lignin extraction and its conversion into SiO_2 in an air atmosphere [27]. The reactions constituting the proposed mechanism of silicon (IV) oxide formation are presented below.

$$C_{196}H_{464}O_{248}N_2 \cdot 53\ SiO_2 \cdot 30\ H_2O \rightarrow C_{196}H_{464}O_{248}N_2 \cdot 53\ SiO_2 + 30H_2O \quad (5.16)$$

$$C_{196}H_{464}O_{248}N_2 \cdot 53SiO_2 + 124O_2 \rightarrow C_{94}H_{248}O_{188} \cdot 53SiO_2 + N_2 + 108H_2O + 102CO_2 \quad (5.17)$$

$$C_{94}H_{248}O_{188} \cdot 53SiO_2 + 62O_2 \rightarrow 53SiO_2 + 124H_2O + 94CO_2 \quad (5.18)$$

For calculations, we will use the component designations given in Table 5.2.

Seven components participate in chemical transformations, according to the proposed mechanism of SiO_2 release. The mathematical model corresponding to this process consists of three differential and four algebraic material balance equations.

Table 5.2.

Symbols of the amount of substance of components participating in the reactions of thermal treatment of the sample after lignin extraction

component	symbol
1	2
$C_{196}H_{464}O_{248}N_2 \cdot 53\ SiO_2 \cdot 30\ H_2O$	n_1
$C_{196}H_{464}O_{248}N_2 \cdot 53\ SiO_2$	n_2
$C_{94}H_{248}O_{188} \cdot 53SiO_2$	n_3
N_2	n_4
H_2O	n_5
CO_2	n_6
SiO_2	n_7

Since all model reactions are pseudo-first order, the system of equations in general form can be written as the following equations:

$$\frac{dn_1}{d\tau} = -k_1 n_1 \quad (5.19)$$

$$\frac{dn_2}{d\tau} = k_1 n_1 - k_2 n_2 \quad (5.20)$$

$$\frac{dn_3}{d\tau} = k_2 n_2 - k_3 n_3 \quad (5.21)$$

$$n_4 = n_1^0 - n_1 - n_2 \quad (5.22)$$

$$n_5 = 262n_1^0 - 262n_1 - 232n_2 - 124n_3 \quad (5.23)$$

$$n_6 = 196n_1^0 - 196n_1 - 196n_2 - 94n_3 \quad (5.24)$$

$$n_7 = 53(n_1^0 - n_1 - n_2 - n_3) \quad (5.25)$$

where $k_1 – k_3$ are the rate constants of the corresponding reactions, s^{-1},

τ – time, s,

n_1^0 – the initial number of moles,

$n_1 – n_7$ – the current number of moles of the corresponding components.

To determine the kinetic parameters of the thermal decomposition process after lignin removal, peaks corresponding to reactions (5.19 - 5.25) were determined on the thermogram (Fig. 5.1).

The reference temperatures are determined by the extremum point on the DTG curve and are: $Ts_1 = 375$ K, $Ts_2 = 628$ K, $Ts_3 = 823$ K. From the curve of sample mass

change (TG), the value of W was determined according to equation 5.11 at reference temperatures Ts_i.

To construct the dependence W*=f(θ), we divide the DTG curve on the derivative graph into n equal parts with parallel lines. The intersection points of these parallel lines with the thermogravimetric curve allow us to determine the mass of the sample at a given time. The value of Ts is determined by the extremum point on the DTG curve.

From the angle of inclination of the linear dependence $W^* = \ell n \frac{W_o - W_k}{W_o - W_\tau}$ on θ, the value of the activation energy of the thermal decomposition reaction of a substance can be determined by equation (5.12). The calculated values of E and k_0 are presented in Table. 5.3.

After substituting the kinetic constants into the differential equations and solving the system of equations (5.19-5.25) on a computer using the Runge-Kutta method [57], the spatiotemporal characteristics of the thermal decomposition process of samples after lignin removal were obtained (Fig. 5.2).

Table 5.3.

Kinetic parameters of the thermal decomposition process of RH after lignin removal

Chemical reaction	T, K	Pre-exponential factor, k_0, s^{-1}	Conditional activation energy of the reaction, E, J/mol
1	2	3	4
1	375	$0,69 \cdot 10^2$	$30,8 \cdot 10^3$
2	628	$1,23 \cdot 10^4$	$62,95 \cdot 10^3$
3	823	$1,00 \cdot 10^5$	$119 \cdot 10^3$

Analysis of calculated data on the ratio of product concentrations in the process of thermal decomposition of RH after lignin removal at a sample heating rate of 0.17 K/s made it possible to determine that 20 min are required for the release of silicon (IV) oxide at a sample heating rate of 0.17 K/s.

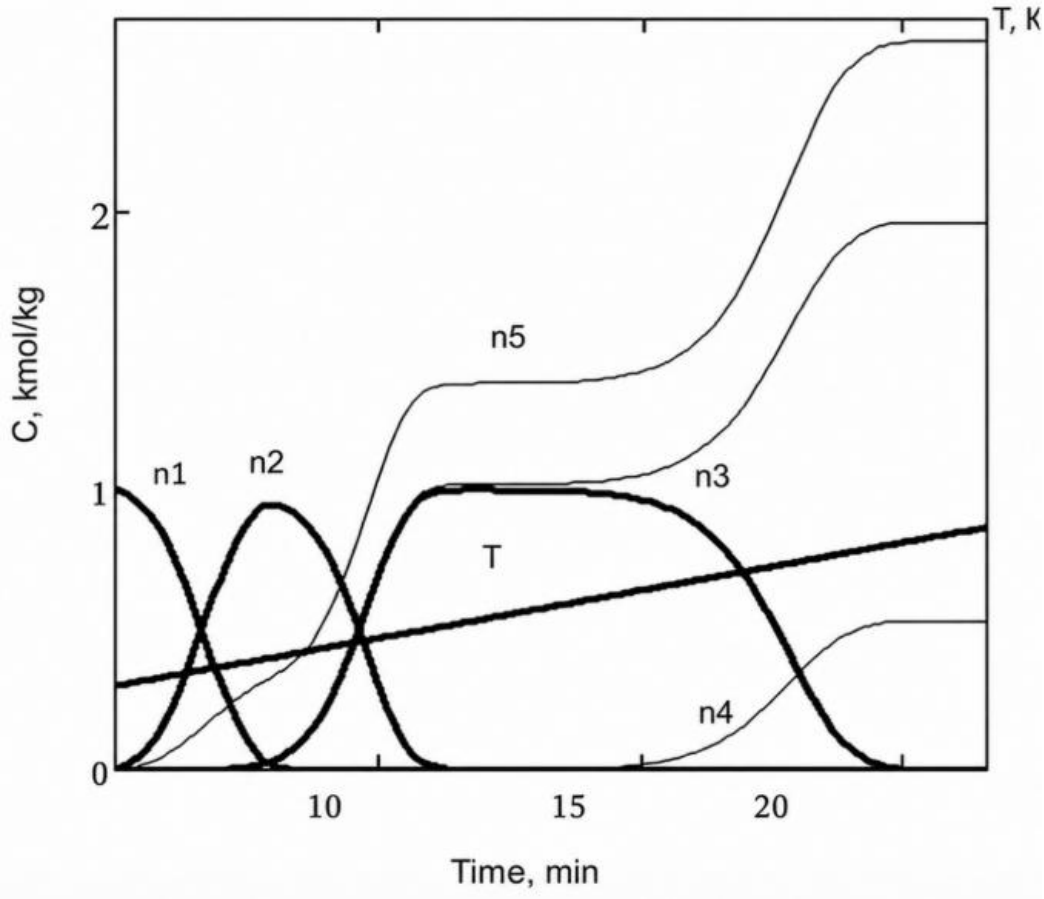

Figure 5.3. The ratio of product concentrations in the process of thermal decomposition of the sample after lignin extraction at a sample heating rate of 0.17 K/s

Source of the figure: author's development

In this case, the process of isolating silicon (IV) oxide takes place in three stages with the production of by-products and the final amorphous SiO_2 [15,16].

At the first stage of the thermal decomposition process in the air environment, the bound moisture is removed from the sample and at a temperature of 160°C it is completely removed and converted into $C_{196}H_{464}O_{248}N_2 \cdot 53\ SiO_2$.

At the second stage, the process of thermal decomposition of $C_{196}H_{464}O_{248}N_2 \cdot 53SiO_2$ occurs, during which gaseous products H_2O and CO_2 and a solid residue $C_{94}H_{248}O_{188} \cdot 53SiO_2$ are formed. With a further increase in temperature, its thermal decomposition occurs with the formation of gaseous H_2O and CO_2, as well as the target product SiO_2. This process is completed at a temperature of 680°C.

To determine the error in the calculations of E and k_0, a comparison of experimental and calculated data on the degree of conversion (α) of $C_{196}H_{464}O_{248}N_2 \cdot 53SiO_2 \cdot 30H_2O$ into SiO_2 was performed. The calculated data were obtained as a result of solving the system of equations (5.19-5.25), and the experimental data were calculated using the derivative data of the thermal treatment of the sample after extraction (Fig. 5.1).

The degree of conversion of $C_{196}H_{464}O_{248}N_2 \cdot 53SiO_2 \cdot 30H_2O$ into SiO_2 (Fig. 5.4) was calculated by the formula (5.7).

Comparison of experimental and calculated data on the degree of conversion of $C_{196}H_{464}O_{248}N_2 \cdot 53SiO_2 \cdot 30H_2O$ into SiO_2 (Fig. 5.4) showed that the deviation of the corresponding values does not exceed 5-7%.

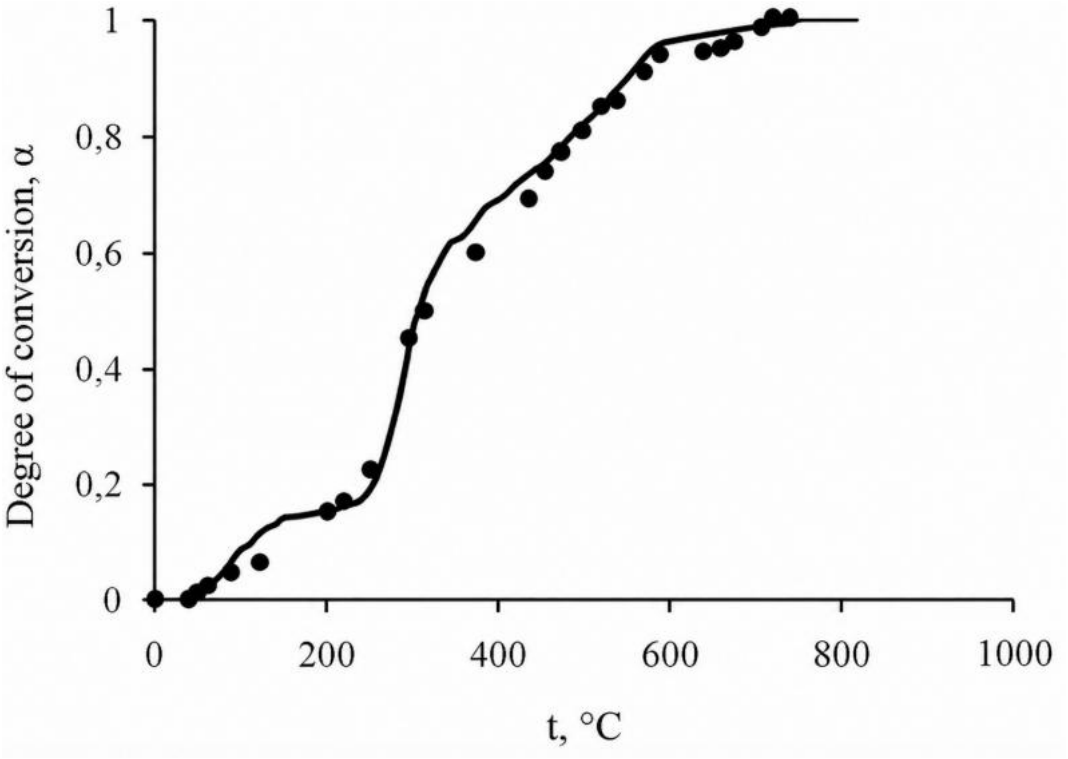

— – calculated curve;

● – experimental values.

Figure 5.4. Dependence of the degree of sample conversion after extraction on temperature

Source of the figure: author's development

This allows us to conclude that the obtained chemical reaction constants at the corresponding stages can be used to calculate the process of thermal decomposition of the sample after extraction to obtain silicon (IV) oxide as a whole.

Additionally, in order to determine the influence of the heating rate of the sample after extraction on the time of formation of silicon (IV) oxide, we studied the influence of the heating rate of the sample after extraction on the time of formation of silicon (IV) oxide. The results of the studies are shown in Fig. 5.5.

The curve shown in Fig. 5.5 can be divided into two sections. The first section of the curve, at heating rates after extraction (0.02÷0.2) K/s, corresponds to the diffusion region, since the time of the reactions of the thermal treatment of the sample after extraction depends on the intensity of heat supply to the sample.

In this region, the time required for the formation of the final product decreases sharply from 40 to 20 min with an increase in the sample heating rate from 0.02÷0.2 K/s. The second section of the curve corresponds to heating rates of the sample more than 0.2 K/s and belongs to the kinetic region.

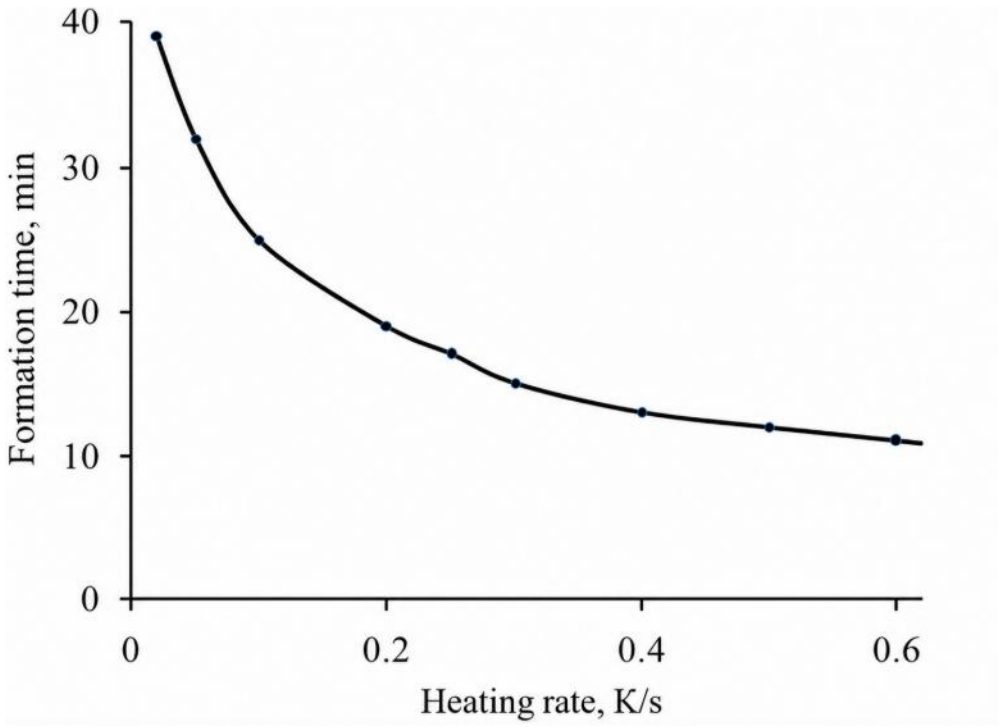

Figure 5.5. Dependence of the time τ (s) of complete conversion of the sample after extraction into SiO_2 on the sample heating rate y (K/s)

Source of the figure: author's development

In this region, increasing the heating rate of the sample does not significantly affect the time required to implement the final stage of the silicon (IV) oxide formation process. In this region, the time required to form the final product decreases from 20 to 10 min. with an increase in the heating rate from 0.2 to 0.6 K/s. Further, increasing the heating rate to 0.6 K/s does not significantly affect the time required to implement the final stage of the silicon (IV) oxide separation process.

5.2.2 Study of the kinetics of the thermal decomposition process of solid residues after two-stage extraction to obtain silicon (IV) oxide

When conducting kinetic studies, the method [55] was used, which is described in section 5.1.

Fig. 5.6 shows the derivative of the thermal decomposition of the sample after two-stage extraction in air.

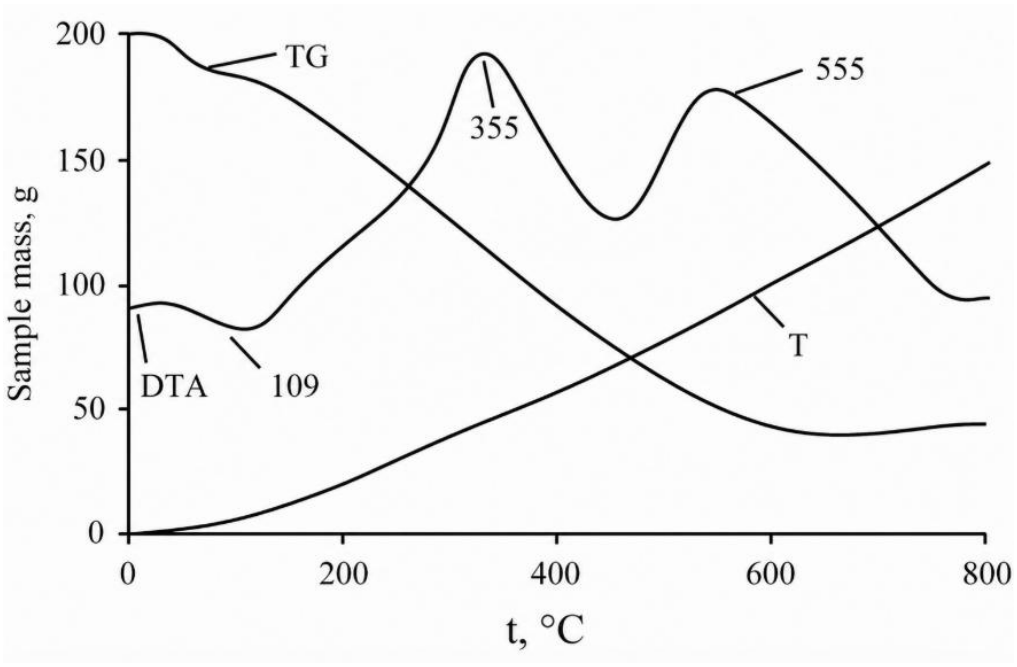

Figure 5.6. Derivative diagram of thermal decomposition of a two-stage extraction sample in air at a sample heating rate of 0.17 K·s-1

Source of the figure: author's development

As can be seen from the TG derivatogram curve, at 109°C, free and bound moisture is removed from rice husk, which is accompanied by a small endoeffect (DTA curve). Then, with an increase in the temperature of the sample, its thermal decomposition of RH occurs with the release of a large amount of heat. The temperature of the beginning of the thermal destruction of cellulose from RH is 210-220°C, and the end of the oxidative-thermal destruction of cellulose is achieved at 400-4200C. At a temperature of 420-700°C, oxidative-thermal destruction of lignin is observed with the subsequent formation of silicon (IV) oxide. The maximum speed of this process is observed in the temperature range of 450-700°C.

The residue after two-stage extraction has the following elemental composition, which is given in Table. 5.4.

Table 5.4.

Technical analysis and elemental composition of solid residues after two-stage extraction

Indicator name	Analysis method	Symbol, unit of measurement	Actual value
1	2	3	4
Ash content per dry matter	ISO 1171-97	A^d,%	42,98
Mass fraction of carbon	ISO 625-96	C^d,%	11,88
Mass fraction of hydrogen		H^d,%	3,90
Mass fraction of nitrogen	ISO 333-83	N^d,%	0,28
Mass fraction of oxygen	ISO 1994-76	O^dd,%	40,96

Based on data on the chemical composition of the solid residue after extraction, the results of thermodynamic calculations and derivatographic studies [55-57], and also on the condition that the process takes place in three stages, the following sequence of chemical reactions is proposed:

$$C_{99}H_{328}O_{234}\cdot N_2\cdot 72\ SiO_2\cdot 31H_2O \xrightarrow{air} C_{99}H_{328}O_{234}\cdot N_2\cdot 72SiO_2+31H_2O \quad (5.26)$$

$$C_{99}H_{328}O_{234}\cdot N_2\cdot 72SiO_2 \xrightarrow{air} C_{64}H_{180}O_{112}\cdot 72SiO_2+N_2+74H_2O+35CO_2 \quad (5.27)$$

$$C_{64}H_{180}O_{112}\cdot 72SiO_2+53O_2 \xrightarrow{air} 72SiO_2+90H_2O+64CO_2 \qquad (5.28)$$

For calculations, we will use the component designations given in Table 5.5.

Table 5.5.

Symbols of the amount of substance of components participating in the reactions of thermal treatment of solid residues after extraction

component	symbol
1	2
$C_{99}H_{328}O_{234}\cdot N_2 \cdot 72\ SiO_2\cdot 31\ H_2O$	n_1
$C_{99}H_{328}O_{234}\cdot N_2 \cdot 72\ SiO_2\cdot$	n_2
$C_{64}H_{180}O_{112}\cdot 72SiO_2$	n_3
N_2	n_4
H_2O	n_5
CO_2	n_6
SiO_2	n_7

According to the proposed mechanism, seven components participate in the chemical transformations that form silicon (IV) oxide from the solid residue after extraction. To determine the kinetic and time characteristics of the process, it is necessary to solve a system of seven equations. The mathematical model that corresponds to this process consists of seven equations. Three differential equations corresponding to the three reactions of the silicon (IV) oxide formation process and four algebraic equations based on material balance equations. If we assume that the above reactions are first-order reactions, according to the mechanism of the process and the accepted notations, then the system of equations describing the process of thermal decomposition of RH with the formation of silicon (IV) oxide will be written in general form as follows:

$$\frac{dn_1}{d\tau} = -k_1 n_1 \qquad (5.29)$$

$$\frac{dn_2}{d\tau} = k_1 n_1 - k_2 n_2 \qquad (5.30)$$

$$\frac{dn_3}{d\tau} = k_2 n_2 - k_3 n_3 \qquad (5.31)$$

$$n_4 = n_1^0 - n_1 - n_2 \quad (5.32)$$

$$n_5 = 195n_1^0 - 195n_1 - 164n_2 - 90n_3 \quad (5.33)$$

$$n_6 = 99n_1^0 - 99n_1 - 99n_2 - 64n_3 \quad (5.34)$$

$$n_8 = 72(n_1^0 - n_1 - n_2 - n_3) \quad (5.35)$$

where n_1^0 is the initial number of moles;

$n_1 \div n_7$ is the current number of moles.

To find the apparent activation energy and pre-exponential factor for reactions 5.29-5.35, peaks corresponding to the reactions occurring during the decomposition of the initial rice husk are identified on the differential enthalpy change (DTA) curve in Fig. 5.6. Extrema are found at the above peaks and, by lowering the vertical line onto the temperature curve (T), the corresponding reference temperatures (Ts) are determined, which correspond to the following temperatures: T_{S1}= 382 K, T_{S2}= 608 K, T_{S3}= 830 K.

From the curve of the change in the mass of the sample (TG), the value of W was determined according to equation 5.11 at the reference temperatures Ts. To construct the dependence W*=f(θ), the DTG curve on the derivative graph is divided by parallel lines into n equal parts. The intersection points of these parallel lines with the thermogravimetric curve allow us to determine the mass of the sample at a given time. The value Ts is determined by the extremum point on the DTG curve.

From the angle of inclination of the linear dependence $W^* = \ell n \frac{W_o - W_k}{W_o - W_\tau}$ on θ, we can determine the value of the activation energy of the thermal decomposition reaction of the substance of equation (5.12).

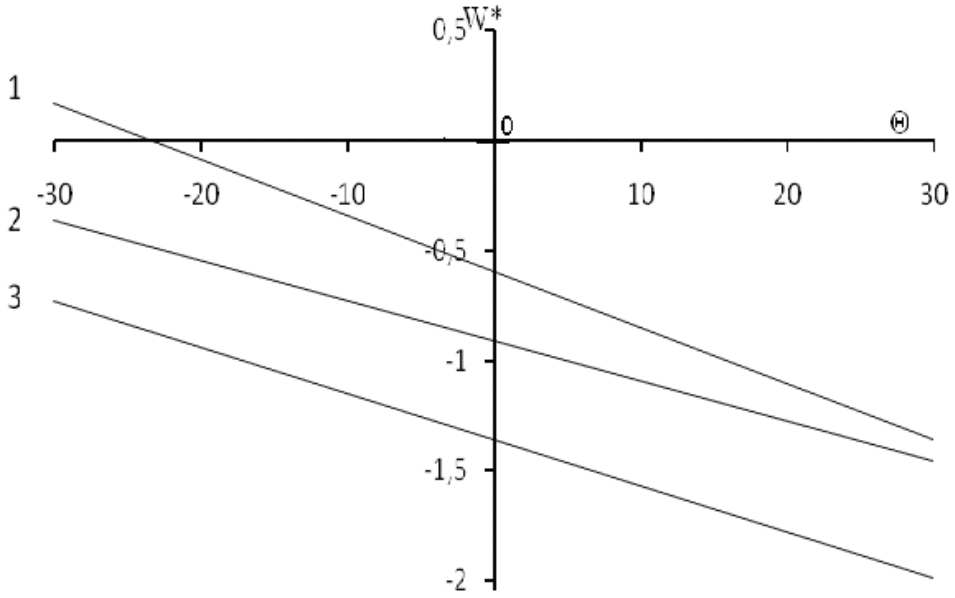

1 – at Ts_1 =382K, 2 – at Ts_2 =608K, 3 – at Ts_3 =830K.

Figure 5.7. Dependence of W* on the conditional temperature θ

Source of the figure: author's development

Mathematical processing (Fig. 5.7) gives the values of the apparent activation energy for the corresponding stages: $E_1 = 30.82 \cdot 10^3$J/mol; $E_2 = 64.54 \cdot 10^3$ J/mol, $E_3 = 118.56 \cdot 10^3$ J/mol.

The values of the pre-exponential factor according to formula (5.13) for the corresponding stages: $k_{01} = 6.94 \cdot 10^1 s^{-1}$; $k_{02} = 1.23 \cdot 10^3 s^{-1}$; $k_{03} = 1.00 \cdot 10^5 s^{-1}$.

The obtained kinetic characteristics of the successive stages of thermal treatment of the sample to obtain silicon (IV) oxide are used to determine the spatiotemporal characteristics of the process by solving the system of equations of the mathematical model (5.29) – (5.35). Thus, it is necessary to solve seven equations, which are equal to the number of components of the process being studied. Three of them are differential, the number of which is equal to the number of chemical reactions, and four algebraic, which are obtained from the material balance equation. The system of differential equations was solved by the Runge-Kutta numerical method using a computer.

The rate constants of chemical reactions described by the Arrhenius equation are determined by expression 5.11.

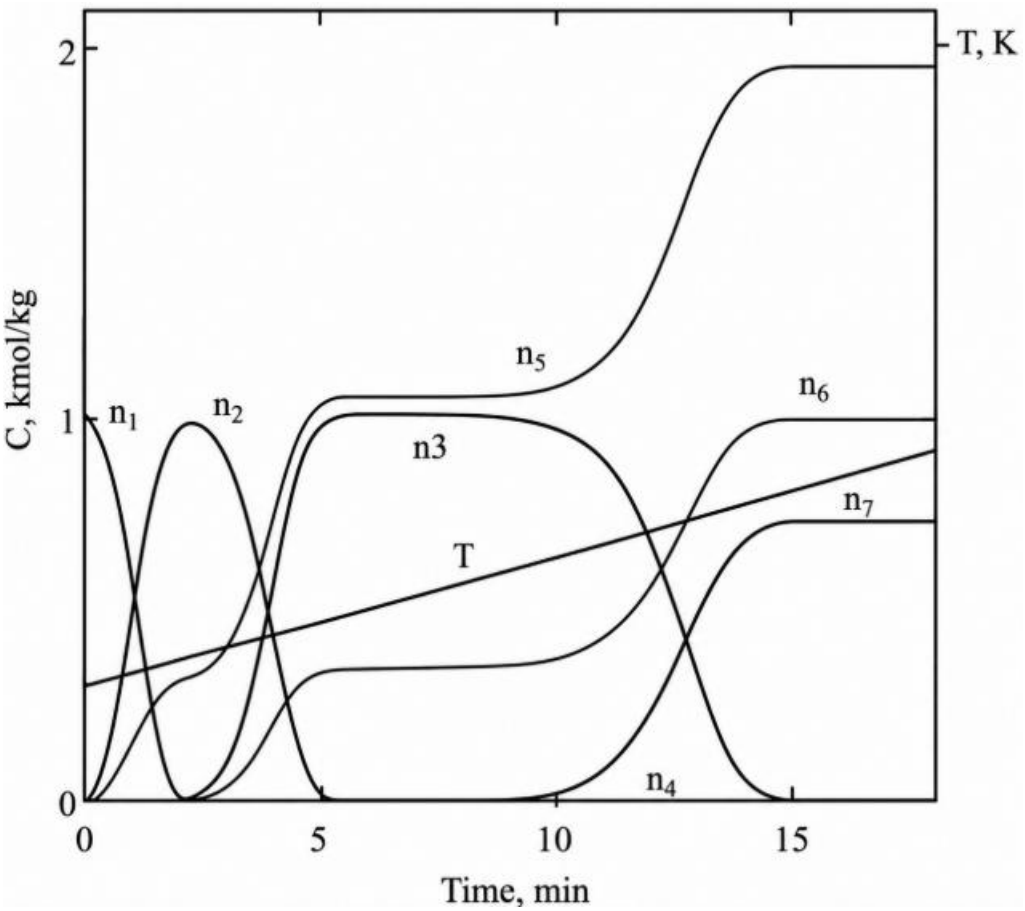

Figure 5.8. Ratio of product concentrations in the process of thermal decomposition after extraction at a sample heating rate of 0.17 K/s

Source of the figure: author's development

Analysis of the curves of the ratio of product concentrations in the process of thermal decomposition of solid residues after extraction in time depending on the temperature (Fig. 5.8) showed that the complete transformation of solid residues into silicon (IV) oxide occurs in 3 stages and ends at a temperature of 700 - 960 K, the total time of thermal decomposition at three successive stages of the process is 12-14 min., and the temperature is about 760 K.

At the first stage of the thermal decomposition process, in the air environment, the removal of bound moisture from component n_1 and the formation of component n_2 occurs. At the second stage, the decomposition process of component n_2 occurs with the formation of gaseous components n_4, n_5, n_6 and solid n_3. At the third stage, the

decomposition process of component n_3 occurs, with the formation of gaseous n_5, n_6 and the final product n_7 (Fig. 5.8).

The validity of the obtained theoretical results was verified by comparing them with experimental data [50,51,53].

As can be seen from Fig. 5.9, the deviation of the corresponding values of the degree of transformations at three stages does not exceed 5-7%.

This allows us to conclude that the obtained constants of chemical reactions at the corresponding stages can be used to calculate the process of thermal decomposition of RH to obtain silicon (IV) oxide as a whole.

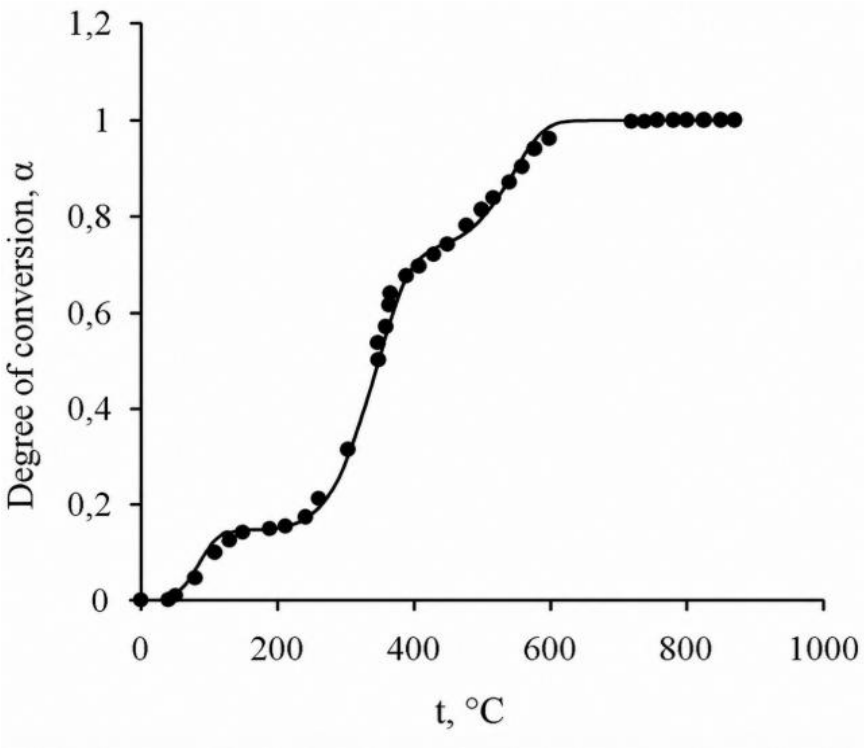

• • • – experimental data;

—— – calculated data.

Figure 5.9. Dependence of the degree of sample transformations after extraction on temperature

Source of the figure: author's development

Additionally, the influence of the heating rate of the initial RH on the time of formation of silicon (IV) oxide was studied. The results of the studies are shown in Fig. 5.10.

As can be seen from Fig. 5.10, the time required for the implementation of the final stage of the process of formation of silicon (IV) oxide is significantly affected by the heating rate of the RH, i.e. the intensity of heat supply. When carrying out the process of obtaining silicon (IV) oxide from RH, the raw material must be heated at a rate ranging from 0.3-1.5 K/s. The figure shows that an increase in the heating rate above 2.5 K/s does not significantly reduce the duration of the process. Therefore, based on the data in Fig. 5.10, it can be concluded that at a sample heating rate of 0.3-1.5 K/s, the process occurs in the diffusion region, and at rates greater than 1.5 K/s – in the kinetic region.

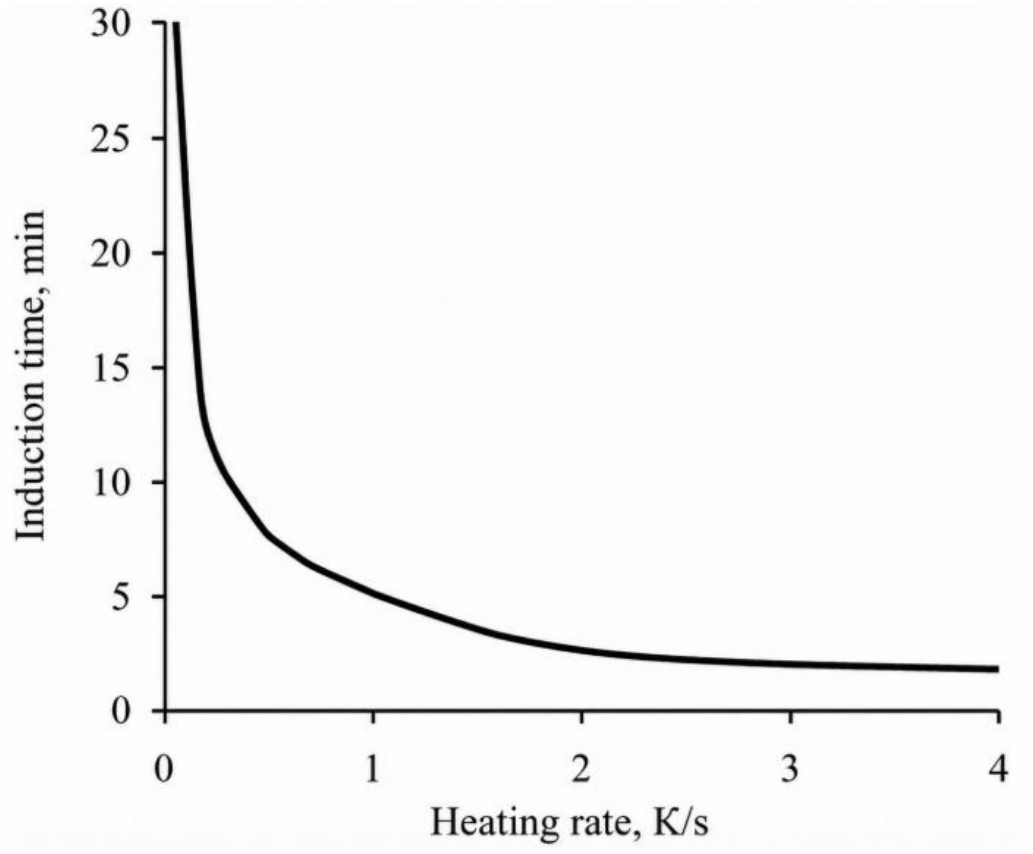

Figure 5.10. Dependence of the time of formation of silicon(IV) oxide on the rate of heating of the sample after extraction

Source of the figure: author's development

Thus, as a result of theoretical and experimental studies, the mechanism of thermochemical transformations in the process of obtaining silicon (IV) oxide from RL has been clarified. A mathematical model has been proposed that describes this process. Kinetic characteristics for three consecutive stages of thermochemical transformations have been determined.

5.3 Study of thermal treatment processes of solid residues after extraction to obtain amorphous silicon (IV) oxide

Obtaining amorphous silicon (IV) oxide of high purity (99.9%) is possible after removing the organic component [27, 53] (as a source of unwanted carbon) and metal compound impurities from the starting material.

The technology for obtaining high-purity amorphous silicon (IV) oxide should include three main stages: grinding of the RH, removing part of the organic component and inorganic impurities from it, and thermal treatment of the insoluble residue. The insoluble residue should have a maximum content of silicon (IV) oxide and a minimum of organic compounds [27,44,50,51].

5.3.1 Study of the chemical composition of rice husk and solid residues after extraction to obtain amorphous silicon (IV) oxide

We conducted studies of the chemical composition of rice husk and solid residues after extraction to obtain the final product of amorphous silicon (IV) oxide from them. Data on the elemental composition of rice husk samples and solid residues after extraction were given earlier in Table 5.4.

The chemical composition of the raw material and the finished product was determined by X-ray diffractometry, atomic absorption spectrometry, volumetric and gravimetric analysis methods [27,44,50,51].

Spectroscopic studies were carried out using the infrared spectroscopy (IR spectroscopy) method using an IR spectrometer "Specord M-80" in the optical range ν = 800-3500 cm^{-1}.

Phase identification was performed using X-ray catalogs and reference data [27,44.50,51].

IR spectra of X-ray samples and solid residues after extraction are shown in Fig. 5.11.

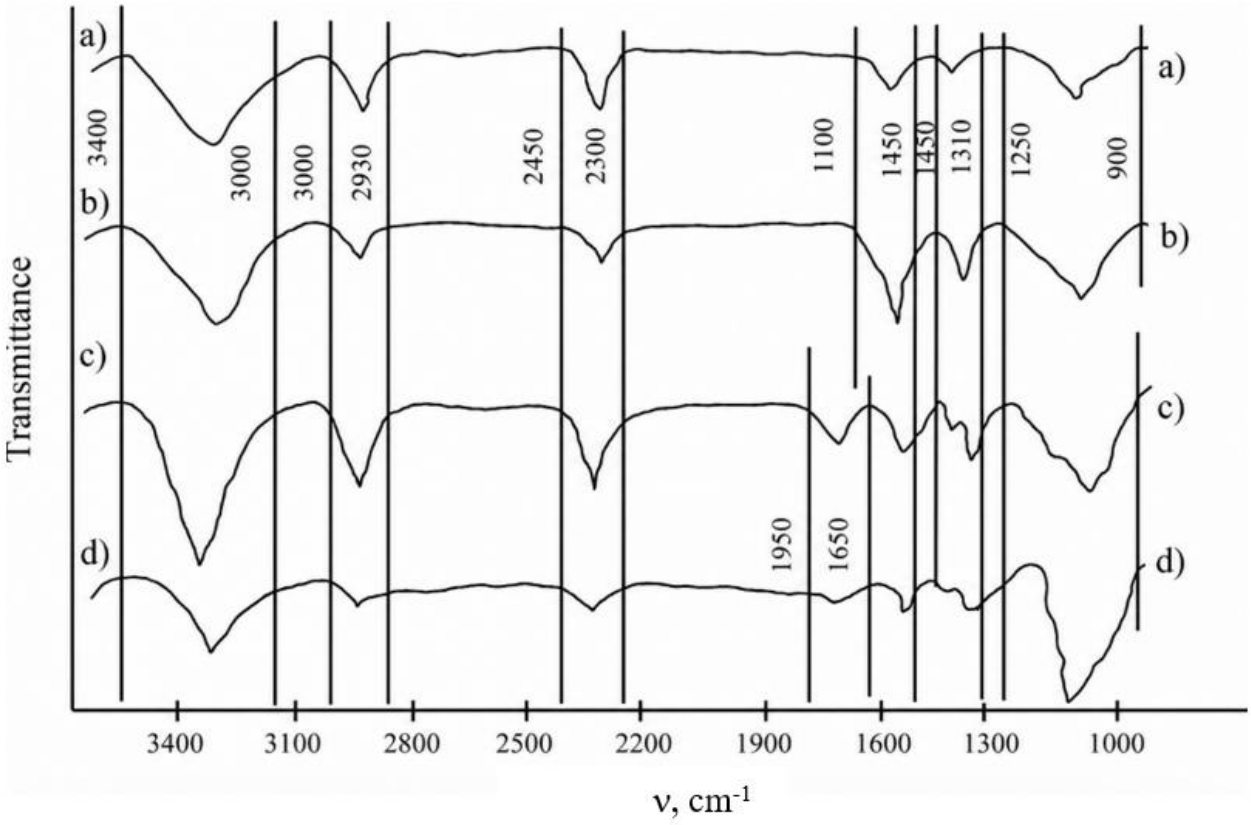

a) sample No. 1 of the original RH; b) sample No. 2 after lignin extraction; c) sample No. 3 after cellulose extraction; d) sample No. 4 after two-stage extraction.

Figure 5.11. IR spectra of samples

Source of the figure: author's development

Identification of absorption bands confirmed the presence of the following chemical bonds in the IR spectrum of sample No. 1 (Fig. 5.11a): O-H (ν=3450-

3100 cm^{-1}); C-H (ν=3000-2930 cm^{-1}); C C (ν=2450-2300 cm^{-1}); C-C (ν=1660-1590 cm^{-1}); C-O (ν=1490-1310 cm^{-1}) and Si–O; Si–O–Si; Si–O–C (ν=1300-850cm^{-1}).

In the IR spectrum of sample No. 2, obtained by lignin extraction, (Fig. 5.11 b) there are the same absorption bands that are characteristic of sample No. 1, but at the same time there is a decrease in the intensity of the bands at ν = 3000-2930 cm^{-1} (C–H bond) and at ν = 2450-2300 cm^{-1} (C–C bond), which are characteristic of the chemical composition of lignin. At the same time, the intensity of the absorption bands at ν = 1660-1590 cm^{-1} (simple C–C bond) increased; at ν = 1490-1310 cm^{-1} (C–O bond). But the intensity of the absorption band at ν = 1300-850 cm^{-1}, which is characteristic of oxygen compounds of silicon, increased the most. Such changes in the IR spectrum of sample No. 2 indicate a decrease in the lignin content and an increase in the silicon (IV) oxide content.

In the IR spectrum of sample No. 3, obtained during cellulose extraction, Fig. 5.11c, some differences from samples a and b are observed. In sample No. 3, the intensity of the absorption bands characteristic of O–H, C–C and C–H bonds increased. The intensity of the absorption band related to a simple C–C bond decreased. New absorption bands of low intensity appeared at ν =1790-1610 cm^{-1} and at ν =1450-1350 cm^{-1}, which can be identified for C=O and C–O bonds, respectively. The intensity of the absorption band characteristic of oxygen bonds of silicon (ν =1300-850 cm^{-1}) increased. Such changes can be explained by an increase in the concentration of the organic component of rice husk - lignin, as well as its partial condensation under the influence of mineral acid. The cellulose content is reduced due to the removal of its amorphous part of hemicellulose. In this case, oxygen compounds of silicon are formed more effectively than in the 1st method as a result of the rupture of Si–C bonds.

The IR spectrum of sample No. 4 (Fig. 5.11d), obtained after two-stage extraction of rice husk, is characterized by a low intensity of absorption bands corresponding to chemical bonds, both in lignin (ν =3000-2930 cm^{-1} and ν = 2450 - 2300 cm^{-1}) and in cellulose (ν =1660-1590 cm^{-1} and ν =1490-1310 cm^{-1}).

However, when compared with samples No. 2 and No. 3, the intensity of the absorption band corresponding to chemical bonds of silicon (IV) oxide (ν =1300-850

cm^{-1}) increased. Therefore, sample No. 4 has the lowest content of carbon-containing components and the highest concentration of silicon (IV) oxide.

In order to determine the impurities and the structure of silicon (IV) oxide, X-ray phase analysis was performed on a DRON-3 diffractometer in the range of reflection angles 2θ= 10-800 in Cu-Kα radiation according to standard methods.

To determine the optimal conditions for lignin extraction from X-rays, X-ray diffraction patterns of silicon (IV) oxide samples treated with 1.5% and 3%wt. alcohol-acid solution were recorded on the DRON-3.0 device and are shown in Fig. 5.12.

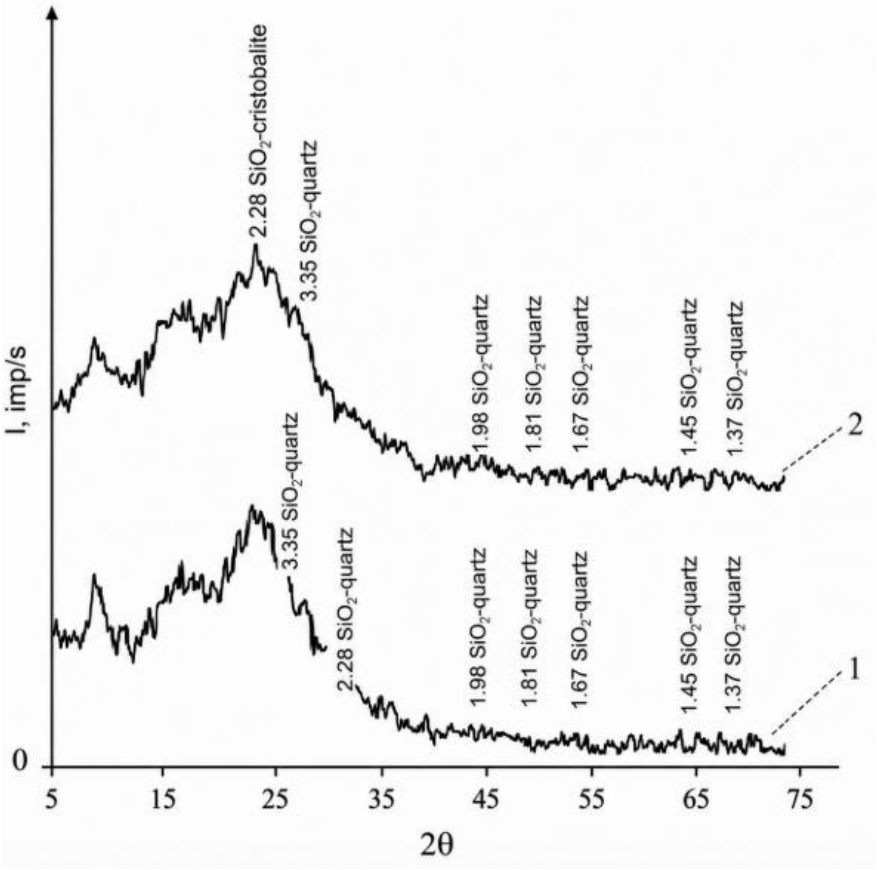

1 – ethyl alcohol with the addition of hydrochloric acid (1.5% by weight);

2 – ethyl alcohol with the addition of hydrochloric acid (3% by weight)

Figure 5.12. X-ray diffraction patterns of silicon(IV) oxide samples after extraction with an alcohol-acid solution and heat treatment at a temperature of 600°C

Source of the figure: author's development

As can be seen from Fig. 5.12, there are no clearly pronounced diffraction peaks in the diffractograms that are responsible for the presence of the crystalline form of silicon (IV) oxide. This indicates that the samples are X-ray amorphous.

Samples of silicon (IV) oxide, obtained after heat treatment in an oxygen environment at T=923 K and 1073 K of insoluble residues of RH of two-stage extraction, were analyzed for purity by the X-ray diffraction method (Fig. 5.13).

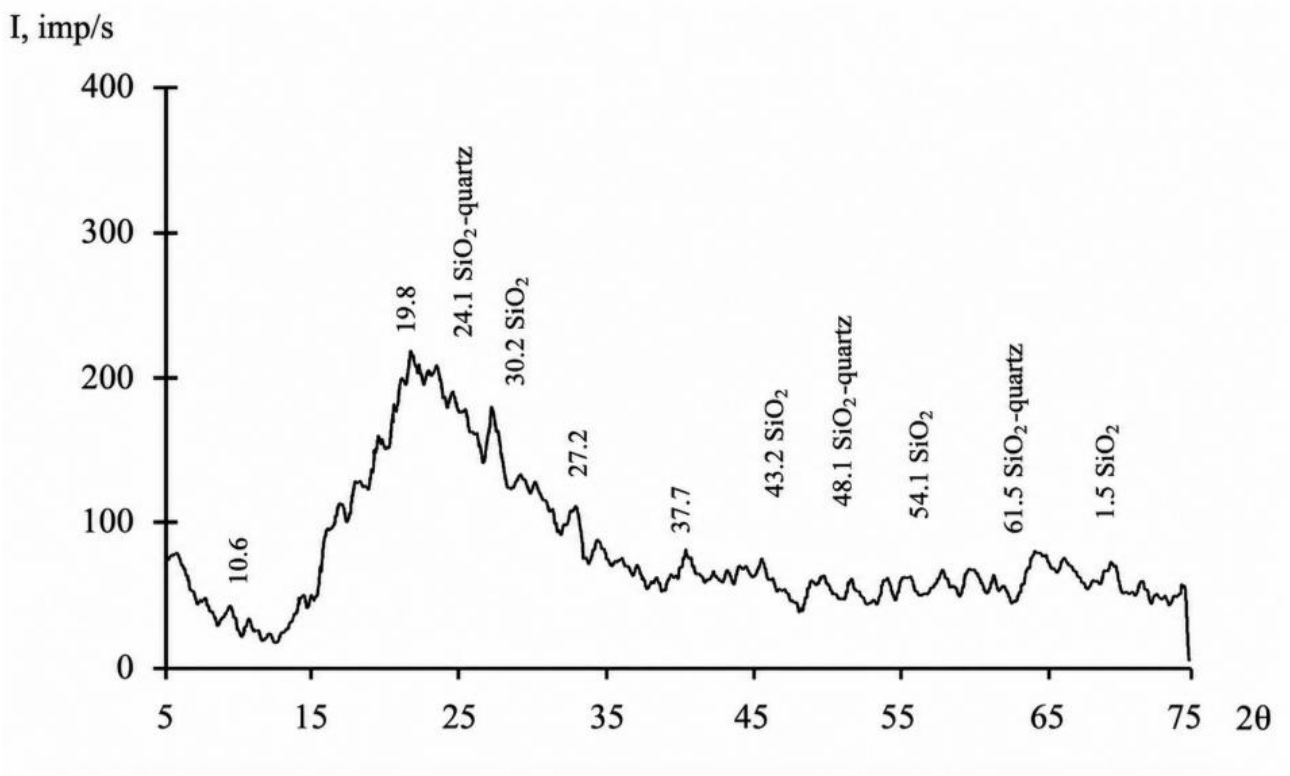

Figure 5.13. X-ray diffraction patterns of silicon(IV) oxide samples after two-stage extraction and heat treatment at a temperature of 600 °C

Source of the figure: author's development

As can be seen from Fig. 5.13, there are no clearly expressed diffraction maxima in the diffractograms, which are responsible for the presence of a crystalline form of silicon (IV) oxide. As the diffractogram showed, in the sample obtained at T = 923 K, silicon (IV) oxide had an amorphous structure. The answer to the question of the presence of undesirable impurities is given by the diffractogram of the sample obtained at T = 1073 K (Fig. 5.14).

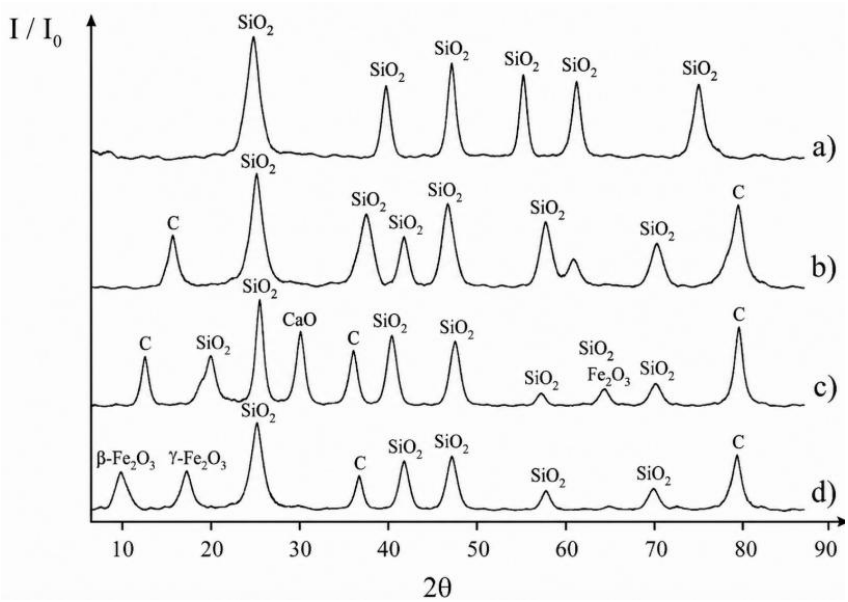

a) SiO_2 – from the original rice husk;

b) SiO_2 – from the sample after lignin extraction;

c) SiO_2 – from the sample after cellulose extraction;

d) SiO_2 – from the sample after two-stage extraction.

Figure 5.14. X-ray diffraction patterns of crystalline silicon (IV) oxide samples

Source of the figure: author's development

As can be seen from Fig. 5.14 a, crystalline silicon (IV) oxide, which was obtained from the initial RH (sample No. 1), contains impurities of γ-iron oxide, calcium oxide and carbon. These data are confirmed in Tables 2.2., 2.3.

Crystalline silicon (IV) oxide obtained from samples after extraction No. 2 and No. 3 (Fig. 5.14 b and 5.14 c, respectively) contains carbon impurities.

Pure silicon (IV) oxide without impurities (Fig. 5.14 d) was obtained only after two-stage treatment (sample No. 4).

5.3.2 Thermal treatment of solid residues after extraction to obtain amorphous silicon(IV) oxide.

The studies were carried out on a laboratory installation, which is shown in Fig. 5.15. The installation consists of two blocks - an oxygen (air) supply and purification unit and a carbon analysis unit.

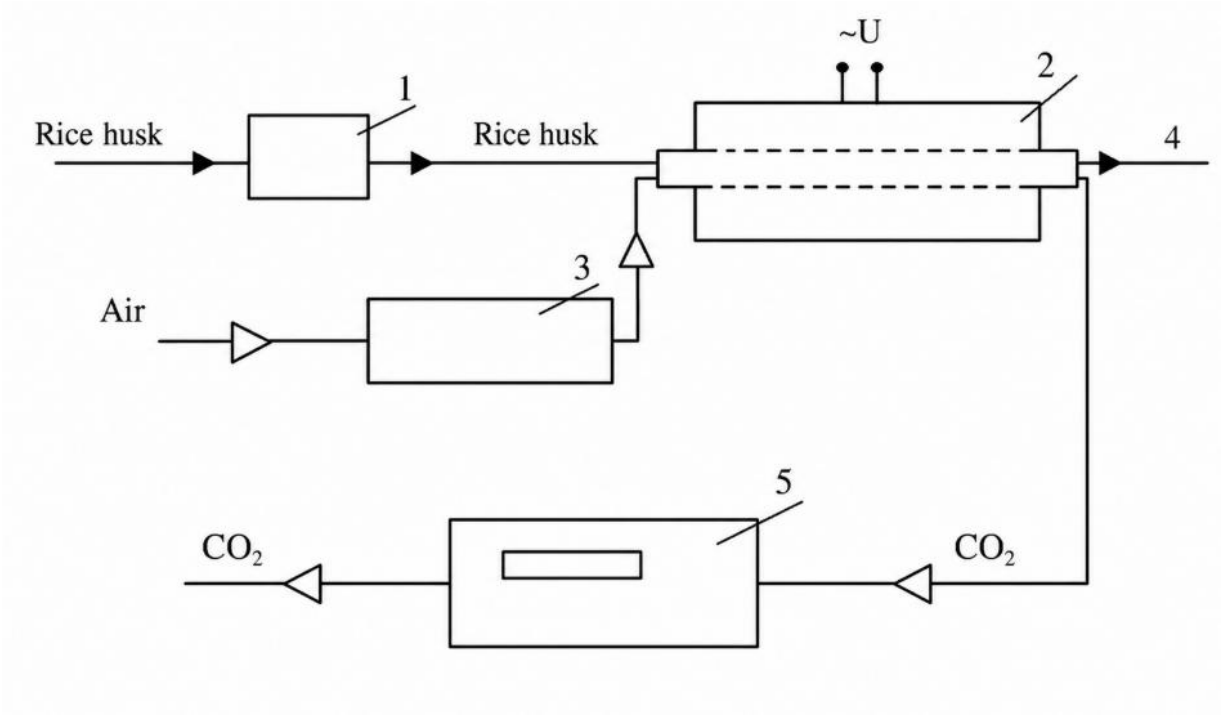

1 – analytical balance; 2 – furnace; 3 – air supply and purification unit; 4 – technical silicon(IV) oxide, 5 – carbon analysis unit.

Figure 5.15. Schematic diagram of the laboratory setup

Source of the figure: author's development

The studies were carried out as follows. Solid residues are weighed on an analytical balance 1 in an amount of 0.3 ± 0.01 g in a porcelain boat. The boat is placed in a reaction tube of an electric furnace 2 heated to the required temperature. The reaction tube is closed on one side with a cork with a fitting, through which air is pumped into the tube using a microcompressor through a rotameter in an amount sufficient for complete combustion of the carbon contained in the RH. The temperature in the furnace is regulated using an autotransformer by changing the voltage supplied

to the furnace. During the heating process in the air environment, carbon burns out of the RH. The boat is kept in such conditions for a certain period of time, after which, using the AN-7529 express carbon analyzer, the amount of carbon remaining in the product is determined.

The basis of the AN-7529 express analyzer is the method of automatic titration by pH. Formed during the combustion of carbon contained in the RH, carbon (IV) oxide is carried by a flow of oxygen into the electrolytic cell of the sensor and is absorbed in it by the solution, causing its acidification. Acidification of the solution leads to a change in the electromotive force of the electrode system, which is then converted by a series of converters into current pulses that cause the reduction of hydrogen ions at the cathode, neutralizing the acid formed during the absorption of carbon (IV) oxide. The amount of electricity required for neutralization is recorded by the current integrator in percent of the mass fraction of carbon.

As a result of the heat treatment of the RH in furnace 2, the amount of carbon contained in the RH sample is read in percent by mass on the indicator board of the current integrator.

As shown by previous studies of extraction kinetics [53,54], the amorphous components of RH are best dissolved - amorphous cellulose (hemicellulose) and lignin, which is not bound to cellulose.

Cellulose and cellolignin (a compound of lignin with cellulose) have a stable crystalline structure, so they can only be partially removed from the derived raw material. This is evidenced by the data of thermal-deposition destruction of samples obtained on the basis of derivatograms. The samples that were studied had different thermal characteristics and differed from the original RH. Thus, the most heat-resistant was the insoluble residue after treatment of RH with mineral acid. For it, the stages of thermal-deposition destruction of cellulose and lignin occurred in the temperature range of 475-845 K and 845-1065 K, respectively. While for the insoluble residue after alcohol treatment the temperature ranges are 581-607 K and 607-1033 K.

The insoluble residue of the two-stage treatment turned out to be less heat-resistant. Thermal-degradation destruction of cellulose for this sample occurred at T =

484-688 K, and lignin at T = 688-973 K. At the same time, the nature of the DTA (differential thermal analysis) curves for all samples is different, which indicates differences in their chemical composition.

After the primary treatment of RH with mineral acids, the content of crystalline cellulose and lignin in the insoluble residue increases, which are more heat-resistant.

The insoluble residue obtained after the primary treatment of RH in alcohol has a lower content of lignin, but a higher content of cellulose. Therefore, its heat resistance decreases compared to the previous sample.

The sample after two-stage treatment has the lowest heat resistance, because cellolignin and crystalline cellulose were partially extracted.

The stage of heat treatment of the insoluble residue after two-stage extraction (three-stage process) must be carried out in the temperature range of 690-920 K.

With increasing temperatures, amorphous silicon (IV) oxide changes its structure to crystalline. This is evidenced by the endoeffect on the DTA curve at a temperature of 983 K.

Based on the analysis of derivatographic studies, it can be concluded that the insoluble residue after double extraction of RH is the best starting material for obtaining amorphous silicon (IV) oxide of high purity. The optimal temperature of the heat treatment stage is 923-928 K.

In order to establish the duration of the heat treatment of the solid residue after extraction, kinetic studies of this stage of the process were conducted in a certain temperature range (isothermal mode) in an air environment (T_{opt} = 913-923 K).

As a result of the studies, the dependence of the content of solid residues after extraction and the initial RH during thermal decomposition (γ, %) on the duration of the process was obtained, Fig. 5.16.

During the thermal treatment of RH in an air or oxygen environment, the process of decomposition of organic compounds (cellulose and lignin) occurs. The unburned residue is amorphous silicon (IV) oxide.

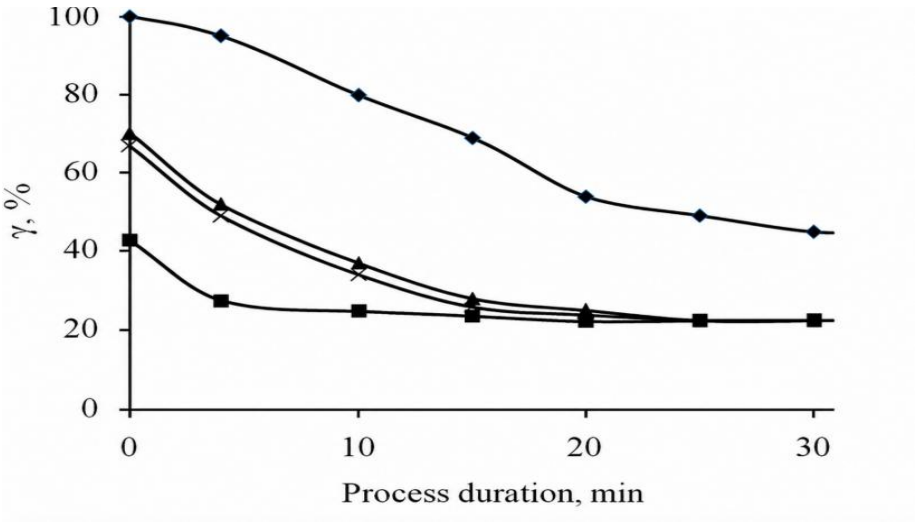

♦ – sample of the initial RH; ▲ – sample after lignin extraction; x– sample after cellulose extraction; ■ – sample after two-stage extraction

Figure 5.16. Dependence of the solid residue content (γ, %) during thermal decomposition on the duration of the process in air, T=923 K

Source of the figure: author's development

As can be seen from Fig. 5.16, the kinetic curves of thermal decomposition of the initial RH and samples of the solid residue after extraction are of different nature, the thermal decomposition of the initial RH ends at 35 minutes.

The curves of thermal decomposition of the initial RH and samples of the solid residue after extraction (Fig. 5.16) are of different nature, the thermal decomposition of the initial RH ends at 35 minutes. The unburned residue is amorphous silicon (IV) oxide and carbon. The curves after the removal of lignin and cellulose are similar to each other, the thermal decomposition of the solid residues after the extraction of lignin and cellulose is completed in 13-17 minutes. The duration of thermal treatment of the solid residue after 2-stage extraction is reduced to 7-10 minutes. For the solid residue after 2-stage extraction, the unburned residue is amorphous silicon (IV) oxide.

This allows us to significantly reduce energy consumption for the heat treatment process and conduct it in one stage at T=885-913 K without prior combustion in air.

5.4. Investigation of the dispersion composition and basic properties of amorphous silicon (IV) oxide

The basic properties of silicon (IV) oxide were determined [4,14,24,28], which are given in Tables 5.6 and 5.7.

Table 5.6.

Properties of silicon(IV) oxide powders

Physicochemical properties of silicon(IV) oxide	Technical silicon(IV) oxide	Silicon(IV) oxide obtained after two-stage extraction
1	2	3
Appearance	Gray powder	White powder
Mass fraction of moisture, %	1,2 – 1,5	0,9 – 1,2
pH of aqueous extract	7,0	6,5 – 6,8
Specific surface area by BET method, m^2/g	30 – 35	35 – 40
Bulk density (uncompacted), kg/m^3	235 – 257	217 – 230

Table 5.7.

Content of components included in the mineral part (ash) after two-stage extraction

component	% wt.
1	2
silicon(IV) oxide	99.99
magnesium oxide	0.005
sulfur (VI) oxide	0.005

The appearance of the powders indicates the presence of impurities. The powder obtained from RH is gray, which indicates the presence of residual carbon and inorganic metal impurities. Silicon (IV) oxide obtained after double extraction is white, which indicates the purity of the obtained product. The mass fraction of moisture in the samples is in the range from 0.9 to 1.5%, the pH of the aqueous extract is 6.5–7.0 [58].

The bulk density for technical silicon (IV) oxide is 235-257 kg/m^3, and for samples after double extraction – 217-230 kg/m^3.

The specific surface area of the powders was determined by the nitrogen thermal desorption (BET) method. For technical silicon (IV) oxide it is 30-35 m^2/g, and for samples after double extraction – 35-40 m^2/m.

The mass fraction of moisture in the samples is in the range from 0.9 to 1.5%, the pH of the aqueous extract is 6.5-7.0.

The image of the studied sample of amorphous silicon (IV) oxide is shown in Fig. 5.17.

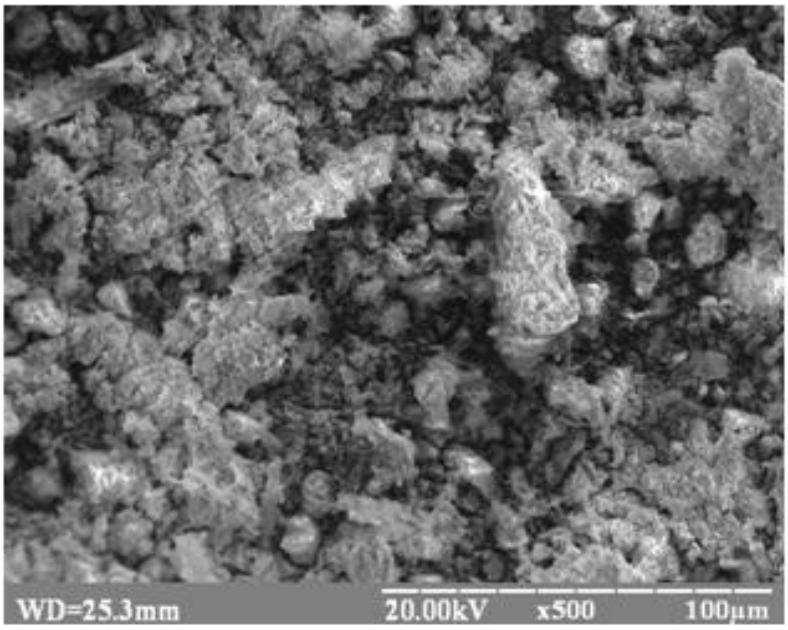

Figure 5.17. Micrograph of silicon (IV) oxide powder

Source of the figure: author's development

The surface of the studied sample was magnified 120 and 500 times. The sizes of the particles examined under the microscope were determined by comparing them with the scale applied to the photograph. The value of one scale division is 100 microns.

To assess the degree of dispersion, the smallest and largest particle size, the difference between the largest and smallest sizes, the average particle size, etc. were used. However, the most complete dispersion is characterized by the dispersed (granulometric, grain) composition [57,58]. With such a characteristic, not only the

parameters listed above were established, but also the percentage content of particles of each size.

The calculation of the numerical content of particles of each fraction was carried out by the formula:

$$Ni = ni / \sum ni \cdot 100\%, \quad (5.36)$$

where ni is the number of particles (δ, μm) of the same size fraction,

∑ni is the total number of counted particles.

As can be seen from Fig. 5.18, the largest number is made up of particles with sizes of 1 - 14 microns, the numerical content of which is 55% of the total number of counted particles in the experimental sample of silicon (IV) oxide powder.

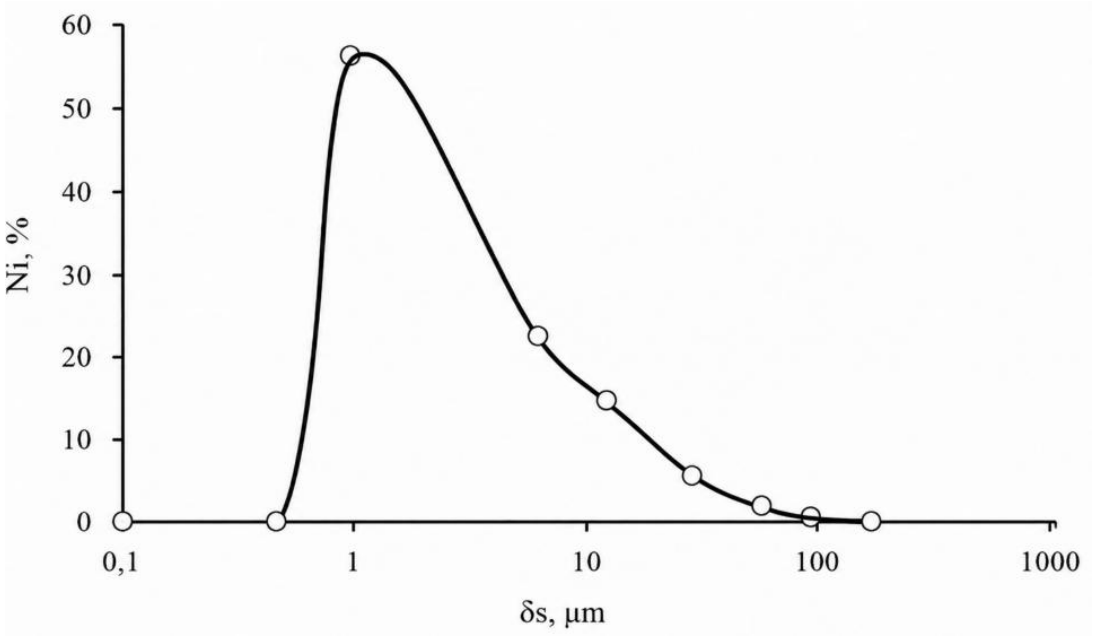

Figure 5.18. Numerical particle content of each fraction

Source of the figure: author's development

It can also be concluded that silicon (IV) oxide particles vary in size in the range from 1 to 100 microns. This fact can be explained by the fact that silicon (IV) oxide powder obtained from RH is a multicomponent system consisting of a large number of particles that differ in shape and size due to different degrees of grinding in the process of preliminary preparation of RH.

The size of the powder is characterized by the diameter of the particles. For powder products that have a regular spherical shape, the diameter accurately

characterizes all the remaining parameters: volume, surface, specific surface. Due to the irregular geometric shape, the size of the particles is difficult to determine by measurements. For a combined characteristic of the size and shape of the particles, the concept of equivalent diameter is adopted. Due to the fact that the silicon (IV) oxide powder obtained from the RH has a fairly wide size distribution, the average particle size was determined.

The results of measuring the number of silicon (IV) oxide powder particles and their size were expressed as an average value, as such the arithmetic mean diameter was used:

$$\overline{\delta_i} = \frac{\sum n_i \delta_i}{\sum n_i}, \quad (5.37)$$

where δ_i is the average particle diameter of silicon (IV) oxide powder, μm;

ni is the number of particles of the same size fraction.

The resulting silicon (IV) oxide powder, in terms of its dispersed composition, is similar to a multicomponent aggregate with a predominant content of particles with a size of 2.18 μm.

The properties of silicon (IV) oxide powder were described by the distribution function D (δ) of the number of particles by their diameters. The function D (δ) is equal to the ratio of the number of all particles with a diameter less than δ to the total number of counted particles, expressed as a percentage [58].

The distribution function was graphically depicted as an integral distribution curve (Fig. 5.19).

For such an image, the abscissa axis plotted the value of the particle diameter δ at the selected scale, and the ordinate axis plotted the percentage of all particles with a diameter smaller than δ, i.e., the value of the functions D (δ).

The distribution function D (δ) is a continuous monotonic function of the quantity δ, which is differentiable everywhere and has a continuous derivative. This means that there is a function φ (δ) that can be obtained by differentiating the distribution function D (δ) and which is continuous (in the interval δmin – δmax).

$$\int_{\delta_{min}}^{\delta_{max}} \varphi(\delta)\, d\delta = D(\delta_{max}) - D(\delta_{min}), \quad (5.38)$$

$$\varphi(\delta) = dD(\delta)/d\delta. \quad (5.39)$$

According to formula (5.38), the ordinates of the integral distribution function at points δi are equal to the areas deposited between the curve φ (δ) and the abscissa axis in the region δi – δmin.

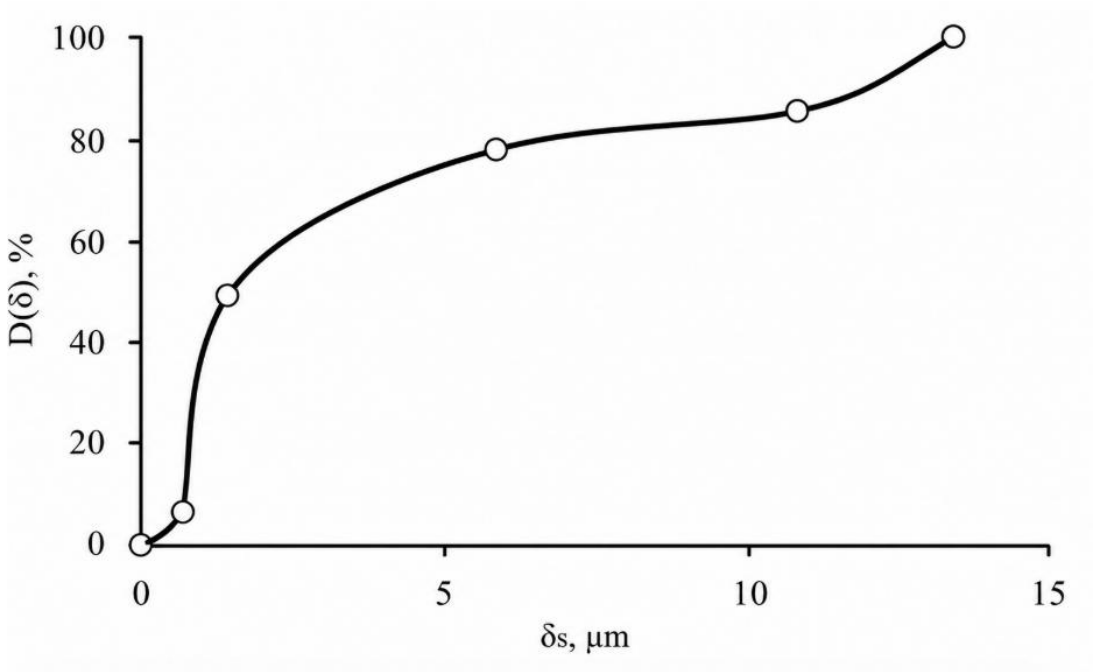

Figure 5.19. Integral curve of the distribution of the number of particles (D (δ)) by their size

Source of the figure: author's development

The percentage content of individual fractions obtained as a result of the analysis of the dispersed composition was depicted in the form of a step graph (histogram) (Fig. 5.20).

The abscissa axis plotted the particle sizes, and the ordinate axis plotted the relative fraction content, which was determined by the ratio of the percentage content of each fraction to the difference in their limiting sizes, due to the fact that the ranges of individual fractions were assumed to be unequal.

The histogram (Fig. 5.20) gives a visual representation of the dispersed composition of silicon (IV) oxide powder. The density distribution curve (Fig. 5.20) was obtained by combining the midpoints of the segments of each step of the

histogram. The resulting curve reflects the actual density distribution of particles with a maximum that corresponds to their most probable size.

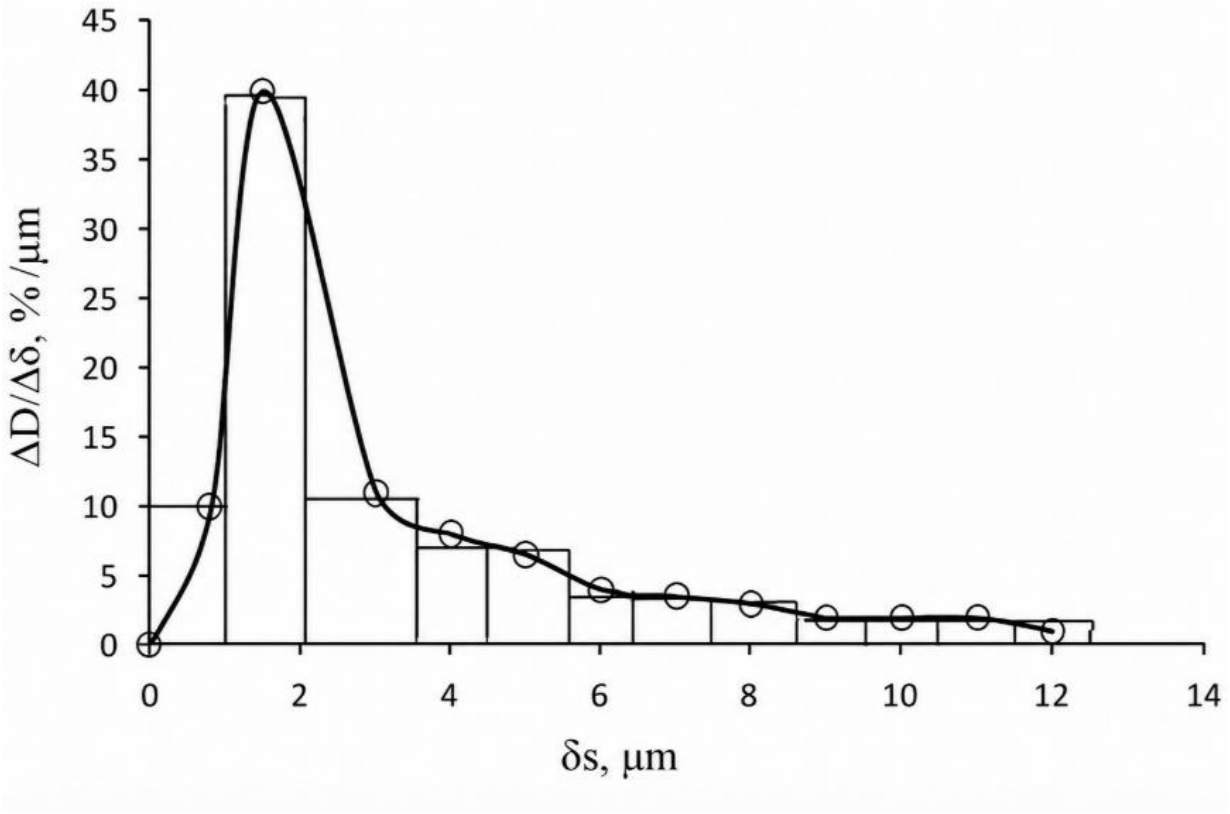

Figure 5.20. Differential density distribution curve of particles (ΔD/Δδ) by their size

Source of the figure: author's development

From Fig. 5.20, we can conclude that the obtained sample of silicon (IV) oxide powder, according to the particle size distribution, belongs to a monodisperse system with a minimum particle size of 0.2 μm, a maximum of 12 μm, and most likely 2 μm.

CONCLUSIONS

1. The heterogeneous system Si–O–C–H–N–S was studied in the temperature range of 300–2000 K at a pressure of 0.1-1 MPa during pyrolysis and steam-water conversion of rice husk

2. Thermodynamic studies have shown that as a result of pyrolysis, a high amount of carbon is retained in the solid residue, which does not allow us to count on obtaining pure silicon (IV) oxide.

3. The influence of pressure and temperature on the gasification of carbon and thus on the residual content of silicon (IV) oxide was determined. It was shown that the gasification reactions due to water vapor and silicon (IV) oxide intensify with increasing temperature, however, they are slowed down by pressure, which increases with increasing temperature.

4. Based on the results of the thermodynamic analysis of the RH thermolysis process, a list of probable carbon gasification reactions during steam-water conversion of RH substances was compiled. For each reaction, thermodynamic characteristics were calculated, which are the Gibbs energy (DG), enthalpy change (DH), equilibrium constant Kp and degree of conversion Xj.

5. It was established that carbon gasification reactions and accompanying RL decomposition reactions become thermodynamically plausible only after 973K. As a result, the pressure, which increases due to the increase in temperature, reduces the equilibrium degree of conversion for all cases. In this regard, the use of steam-water conversion was recognized as inexpedient, especially since it is accompanied by large energy consumption.

6. A hypothesis was formulated about the mechanism of the process of obtaining amorphous silicon (IV) oxide by extraction of carbon-containing components (lignin and cellulose) from rice husk. On this basis, an equation was derived that relates the concentration of the extractant to the degree of extraction of carbon-containing components, and the requirements for extractants and experimental conditions were also determined.

7. An experiment was planned and implemented to investigate the effect of the concentration of extractants (hydrochloric acid in ethyl alcohol and an aqueous solution of sulfuric acid), temperature, and duration of the process on the degree of extraction of lignin and cellulose from rice husk.

8. It is shown that the equation of the form $y = \frac{a}{1+b \cdot e^{-cx^2}}$, which relates the degree of extraction to the concentration of the extractant, adequately describes the experimental data at any ratios of temperature and process duration in the intervals, respectively, 20°C≤ t ≤100°C and 0.5 hours ≤ 6 hours.

9. The study of the obtained model showed that when using a fraction of RH with a size of 40-150 microns

- and extraction of lignin with a mixture of ethyl alcohol and hydrochloric acid, the maximum degree of extraction of lignin (33% wt.) is achieved at a temperature of 80°C for 6 hours and the addition of 3% wt. HCl;

- and extraction of cellulose with a 15% aqueous solution of sulfuric acid, the maximum degree of extraction (29.9% wt.) is achieved at a temperature of 100°C for 6 hours.

10. Sequential implementation of these stages allows to increase the degree of extraction of carbon-containing components to 57%, which will allow to increase the content of amorphous silicon (IV) oxide in the solid residue of RH from 20.90 to 42.98% by mass.

11. The process of thermal treatment of RH after lignin removal and two-stage treatment under non-isothermal conditions was investigated, the mechanisms of chemical reactions and mathematical models of the process of obtaining SiO_2 with the production of silicon (IV) oxide were proposed. The kinetic parameters of each stage of the process were calculated.

12. Unlike existing methods of obtaining amorphous silicon (IV) oxide, this thermal process can be carried out in one stage at T = 923 K without prior combustion in air. The content of silicon (IV) oxide is 33-42.98 wt %.

13. It was established that amorphous silicon (IV) oxide of high purity (99.99%) was obtained from RH after a two-stage extraction of carbon-containing compounds and subsequent heat treatment in one stage in air at T = 885-913 K.

14. The duration of heat treatment is reduced to 10 minutes. This allows to significantly reduce the energy consumption of the process.

15. The physicochemical properties and dispersion composition of silicon (IV) oxide powder obtained by different process implementation schemes were investigated. It was established that the particle size distribution of most of the system is in the range of 0.2-12 μm.

REFERENCES

1. Tolba, G. M. K., Bastaweesy, A.M., Ashour, E.A., Abdelmoez, W., Khalil, K. A., Barakat, N.A.M. (2016). Effective and highly recyclable ceramic membrane based on amorphous nanosilica for dye removal from the aqueous solutions. *Arabian Journal of Chemistry*, 9, 287–296.

2. Ghorbani, F., Sanati, A. M., Maleki, M. (2015). Production of Silica Nanoparticles from Rice Husk as Agricultural Waste by Environmental Friendly Technique. *Environmental Studies of Persian Gulf*, 2(1), 56–65.

3. Pode, R. (2016). Potential applications of rice husk ash waste from rice husk biomass power plant. *Renew Sustain Energy Rev*, 53(14), 68–85.

4. Babaso, PN., Sharanagouda, H. (2017). Rice husk and its applications: Review. *Int J Curr Microbiol Appl Sci*, 6(11), 44–56.

5. Adam, F., Appaturi, JN., Iqbal, A. (2012). The utilization of rice husk silica as a catalyst: review and recent progress. *Catal Today*, 190, 2–14.

6. Lovell, EC., Scott, J., Amal, R. (2015). Ni-SiO_2 catalysts for the carbon dioxide reforming of methane: varying support properties by flame spray pyrolysis. *Molecules*, 20(4), 594–609.

7. Terzieva, V., Fransaer, J., Celis, J.-P. (2000). Codeposition of Hydrophilic and Hydrophobic Silica with Copper from Acid Copper Sulfate Baths. *Journal of The Electrochemical Society*, 147 (1) 198-202.

8. Mehdinia, S. M. (2014). Rice husk silica adsorbent for removal of hexavalent chromium pollution from aquatic solutions. *Iran J Energy Environ*, 5, 2–8.

9. Zhang, Y., Zhang, H. (2008). Study on preparation of a novel silica adsorbent and its selective separation applied to genistein. *Braz J Chem Eng*, 25(20), 1–6.

10. Bernardos, A., Kourimsk´a, L. (2013). Applications of mesoporous silica materials in food - a review. *Czech J Food Sci*, 31, 99–107.

11. Tertyshnyi, O.A., Ovcharov, V.I., Sukhyy, K.M., Sokolova, L.A., Kalinyuk, V.L. (2018). The use of the heat-treated rise husk as elastomeric compositions fillers. *Voprosy khimii i khimicheskoi technologii*, (3), 79–89.

12. Hossain, S.K.S., Mathur, L., Roy, P.K. (2018). Rice husk/rice husk ash as an alternative source of silica in ceramics: A review. *Journal of Asian Ceramic Societies*, 6(4), 299–313.

13. Lee, T., Othman, R., Yeoh, FY. (2013). Development of photoluminescent glass derived from rice husk. *Biomass Bioenergy*, 59, 380-392.

14. Liou, T.-H. (2004). Preparation and characterization of nano-structured silica from rice husk. *Materials Science and Engineering*, A364, 313–323.

15. Costa, J. A. S., Paranhos, C. M. (2018). Systematic evaluation of amorphous silica production from rice husk ashes. *J Clean Prod.*, 192, 688–697.

16. Bakara, R. Abu., Yahyaa, R., Gana, S. N. (2016). Production of high purity amorphous silica from rice husk. *Procedia Chemistry*, 19, 189 – 195.

17. Umeda, J., Kondoh, K. (2010). High-purification of amorphous silica originated from rice husks by combination of polysaccharide hydrolysis and metallic impurities removal. *Industrial Crops and Products*, 32, 539–544.

18. Ghorbani, F., Younesi, H., Mehraban, Z., Celik, M.S., Ghoreyshi, A.A., Anbia, M. (2013). Preparation and characterization of highly pure silica from sedge as agricultural waste and its utilization in the synthesis of mesoporous silica MCM-41. *Journal of the Taiwan Institute of Chemical Engineers*, 44(822), 821–828.

19. Azat, S., Sartova, Z., Bekseitova, K., Askaruly, K. (2019). Extraction of high-purity silica from rice husk via hydrochloric acid leaching treatment. *Turkish J Chem*, 43(12), 58–69.

20. Kalapathy, U., Proctor, A., Shultz, J. (2000). A simple method for production of pure silica from rice hull ash. *Bioresource Technology*, 73, 257–262.

21. Soltani, N., Bahrami, A., Pech-Canul, M.I., Gonzalez, L.A. (2015). Review on the physicochemical treatments of rice husk for production of advanced materials. *Chemical Engineering Journal*, 264, 899–935.

22. Affandi, S., Setyawan, H., Winardi, S., Purwanto, A., Balgis, R. (2009). A facile method for production of high-purity silica xerogels from bagasse ash. *Advanced Powder Technology*, 20, 468–472.

23. Liou, T.-H., Yang, C-C. (2011). Synthesis and surface characteristics of nanosilica produced from alkali-extracted rice husk ash. *Materials Science and Engineering B*, 176, 521–529.

24. Dizaji, H.B., Zeng, T., Hartmann, I., Enke, D., Schliermann, T., Lenz, V., Bidabadi, M. (2019). Generation of high quality biogenic silica by combustion of rice husk and rice straw combined with pre- and post-treatment strategies–a review. *Apll. Sci.*, 9 (1083), 1–27.

25. Zako, J., Arzt, H. E. (1974). Kinetic Analysis of TG-data. Thermal decomposition of calcium carbonate. *Ibid.*, (6), 651−656.

26. Steven, S., Restiawaty, E., Pasymi, P., Bindar, Y. (2021). An appropriate acid leaching sequence in rice husk ash extraction to enhance the produced green silica quality for sustainable industrial silica gel purpose. *J Taiwan Inst Chem Eng*, 122C(5), 1–7.

27. Hrydnieva, T.V., Soroka, P.I., Tertyshnyi, O.A., Smirnova, H.S., Riabyk, P.V. (2007). Investigation of the lignin extraction process with an alcohol extractant. *Voprosy khimii i khimicheskoi technologii,* (6), 212–214.

28. Fernandesa, I. J., Calheiroa, D., Sanchezb, F. A. L., Camachob, A. L. D., Avila de Campos Rochac, T. L., Moraesd, C. A. M., Caldas de Sousa, V. (2017). Characterization of Silica Produced from Rice Husk Ash: Comparison of Purification and Processing Methods. *Materials Research*, 20(2), 512–518.

29. Yuvakkumar, R., Elango, V., Rajendran, V., Kannan, N. (2014). High-purity nano silica powder from rice husk using a simple chemical method. *Journal of Experimental Nanoscience*, 9(3), 272–281.

30. Hura, D.V. Soroka, P.I., Cheremysinova, A.A. (2014). Integrated process of obtaining heat and silicon (IV) oxide from siliceous plant materials. *Chemical and materials engineering*, 2(3), 72 – 78.

31. Madrid, R., Margarido, F., Nogueira, CA. (2011). Valorisation of rice husk by chemical and thermal treatments. *In: Advanced Materials Forum VI; Guimarães, Portugal*, 659-664.

32. Todkar, B.S., Deorukhkar, On. A., Deshmukh, Sat.M. (2016). Extraction of silica from rice husk. *Int. Journal of Engineering Research and Development,* 12(3), 69–74.

33. Real, C., Alcala, Maria D., Criado, Jose M. (1996). Preparation of silica from rice husks. *J. Am. Ceram. Soc.,* 79(8) 2012–2016.

34. Steven, S., Restiawaty, E., Bindar, Y. (2021). Routes for energy and bio-silica production from rice husk: A comprehensive review and emerging prospect. *Renewable and Sustainable Energy Reviews,* 149, 111329.

35. Carmona, V.B., Oliveira, R.M., Silva, W.T.L., Mattoso, L.H.C., Marconcini, J.M. (2013). Nanosilica from rice husk: Extraction and characterization. *Industrial Crops and Products,* 43, 291–296.

36. Mor, S., Manchanda, C. K., Kansal, S. K., Ravindra, K. (2016). Nanosilica extraction from processed agricultural residue using green technology. *Journal of Cleaner Production*, 1–23.

37. Setyawan, N., Hoerudin Wulanawati, A. (2019). Simple extraction of silica nanoparticles from rice husk using technical grade solvent: effect of volume and concentration. *IOP Conf Ser Earth Environ Sci*, 309.

38. Z. Luo, X. Cai, R.Y. Hong, L.S. Wang, W.G. Feng. (2012). Preparation of silica nanoparticles using silicon tetrachloride for reinforcement of PU. *Chemical Engineering Journal*, 187, 357-366.

39. Xu W., Zhang X., Huang W., Luan Y., Yang Y., Zhu M., Yang W. (2017). Synthesis of surface molecular imprinted polymers based on carboxyl-modified silica nanoparticles with the selective detection of dibutyl phthalate from tap water samples. *Applied Surface Science,* 426, 1075-1083.

40. Fernandes, I.J., Calheiro, D., Kieling, A. G., Moraes, C. A.M., Rocha, T. L.A.C., Brehm, F. A., Modolo, R.C.E. (2016). Characterization of rice husk ash produced using different biomass combustion techniques for energy. *Fuel*, 165, 351–359.

41. Shen, Y. (2017). Rice husk silica derived nanomaterials for sustainable applications. *Renewable and Sustainable Energy Reviews*, 80, 453–466.

42. Beidaghy Dizaji, H., Zeng, T., Hartmann, I., Enke, D., Schliermann, T., Lenz, V., Bidabadi, M. (2019). Generation of High Quality Biogenic Silica by Combustion of Rice Husk and Rice Straw Combined with Pre- and Post-Treatment Strategies—A Review. *Applied Sciences*, 9(1083), 1–27.

43. Sknar, Y., Hrydnieva, T., Sknar, I., Riabik, P., Demchyshyna, O. (2022). Characteristics of silicon dioxide produced from rice husk. *Journal of Chemistry and Technologies*, 30(1), 103–109.

44. Gridneva, T.V., Kravchenko, A.V., Barsky, V.D., Gurevina, N.A. (2016). Obtaining of high purity amorphous silicon dioxide from rice husk. *Chem. and Chem. Techn.* 10(4), 499–505.

45. Abu Bakar, R., Yahya, R., Gan, S. N. (2016). Production of High Purity Amorphous Silica from Rice Husk. *Procedia Chemistry*, 19, 189–195.

46. Kablanbekov, A., Yefremova, S., Berdikulova, F., Satbaev, S., Yermishin, S., Shalabaev, N., Satbaev, B., Terlikbayeva, A., Zharmenov, A. (2023). Rice Husk Cellulose-Based Adsorbent to Extract Rare Metals: Preparing and Properties. *Materials, 16*(18), 6277.

47. Yalcain, N., Sevinc, V. (2001). Studies on silica obtained from rice husk. *Ceramics International*, 27, 219–224.

48. Wolff, E. T. (1871). Aschen-Analysen von landwirthschaftlichen Producten, Fabrik-*Abfällen* und wildwachsenden Pflanzen. *Berlin: Wiegandt & Hempel, Bd 1*, P. 39.

49. Bash, A., Lewi, M. (1973) The influence of fine structureon on the pyrolysis of polymer scince. *Pol. Chem. Ed.* (11), 3071-3093.

50. Sknar, Yuri E., Hrydnieva, Tatyana V., Liashenko, Anna O., Riabik, Pavel V., Sknar, Irina V., Hrydniev, Yehor A. (2021). Study of kinetics of thermal decomposition of the rice husk, purified from cellulose. *Journal of chemistry and technologies*, 29 (1–2), 128–136.

51. Hrydnieva, T., Sknar, Y., Riabik, P., Liashenko, A., Demchyshyna, O. (2019). A study of lignin-free rice husk decomposition kinetics. *Journal of Chemistry and Technologies*, 27(2), 255–263.

52. Neish, A. C. (1965) *Coumarins, phenylpropanes and lignin. Plant biochemistry* In J. Bonner, J. E. Varner(Eds.). New York, USA: Academic Press.

53. Liashenko, A., Sknar, Y., Hrydnieva, T., Riabik, P., Demchyshyna, O., Plyasovskaya, K. (2020). Studying the kinetics of extraction treatment of rice husk when obtaining silicon carbide. *Eastern-European Journal of Enterprise Technologies*, 103, 25–31.

54. Gu, S., Zhou, J., Luo, Z., Wang, Q., Shi, Z. (2015). Kinetic study on the preparation of silica from rice husk under various pretreatments. *Journal Therm Anal Calorim*, 119, 2159–2169.

55. Sestak, J., Satavo, V., Wendlandt, W.W. (1973). The studies of heterogeneous processes by thermal analysis. *Thermochim. acta.*, 7(5), 333−356.

56. Brebu, M., Tamminen, T., Spiridon, I. (2013). Thermal degradation of various lignins by TG-MS/FTIR and Py-GC-MS. *Journal of Analytical and Applied Pyrolysis*, 104, 531-539.

57. Butcher, J.C. Numerical Methods for Ordinary Differential Equations, *2nd edn. Wiley, New York* (2008), 463.

58. Duncan J. Shaw. Introduction to Colloid and Surface Chemistry. *Book • Fourth Edition* (1992).